Academic Year: 2025–2026

SCHOOL OF ENGINEERING — MECHANICAL TECHNOLOGY COURSE

NMRV WORM GEAR REDUCER

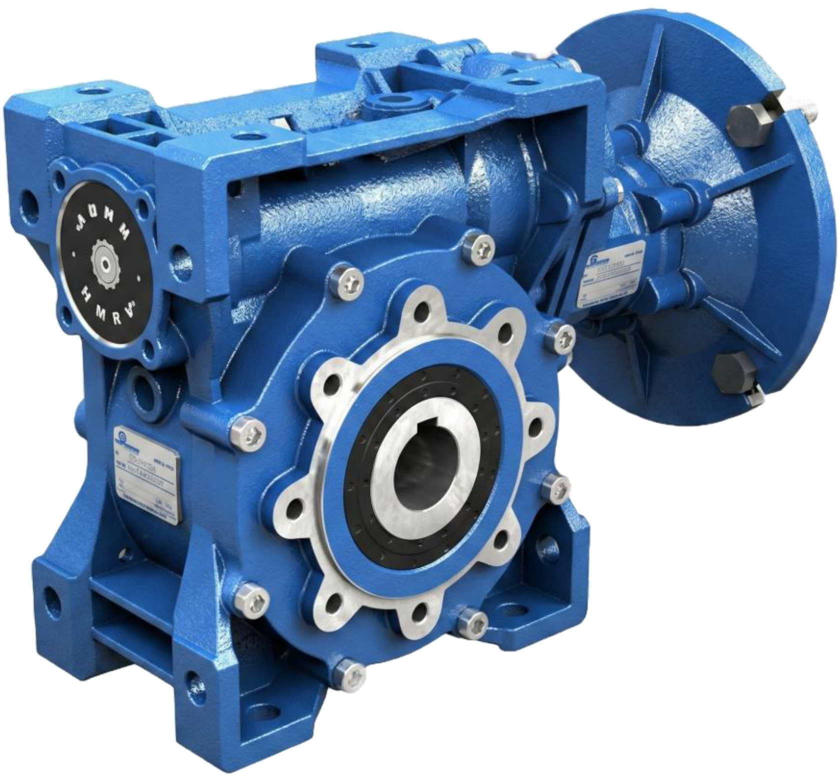

Project carried out by: Riccardo Pantani, Matteo Fornasiero
Tutors: Michele Lanzetta

CONTENTS

1. INTRODUCTION

1.1 Project objectives and client requirements

This thesis sets out the production process planning for the mechanical components of a selected assembly, simulating the management of an industrial order. The work documents the entire operational cycle through the drafting of a technical report.

Once the reference assembly had been defined, 3D models were developed using CAD software, along with the relevant manufacturing drawings, replicating the workflow of a technical department. The work also included estimating processing times and costs for each cycle analysed.

The project simulates the supply of 500 gear motors with the primary constraint of minimising costs. The analysis explores the main processes covered in the Mechanical Technologies course: casting, machining, plastic deformation, welding, assembly and 3D printing.

1.2 General Information

Worm gear motors transmit motion from an electric motor by reducing its angular velocity and increasing the torque available at the output shaft.

Dimensions and reduction ratios depend on the application requirements. Classification is based primarily on the centre distance and the coupling methods, such as output flanges, reaction arms or hollow shafts, designed to directly accommodate the user's driven shaft.

The internal kinematics consist of an induction-hardened and tempered carbon steel worm gear meshing at 90° with a helical ring gear made of bronze alloy; this orthogonal configuration gives the unit considerable geometric compactness and quiet operation.

1.3 Components of the assembly

The technical drawing of the assembly, shown below, has been produced to illustrate the main dimensions (the specific dimensions will be provided in the technical drawings of the components analysed) and the names and quantities of all components.

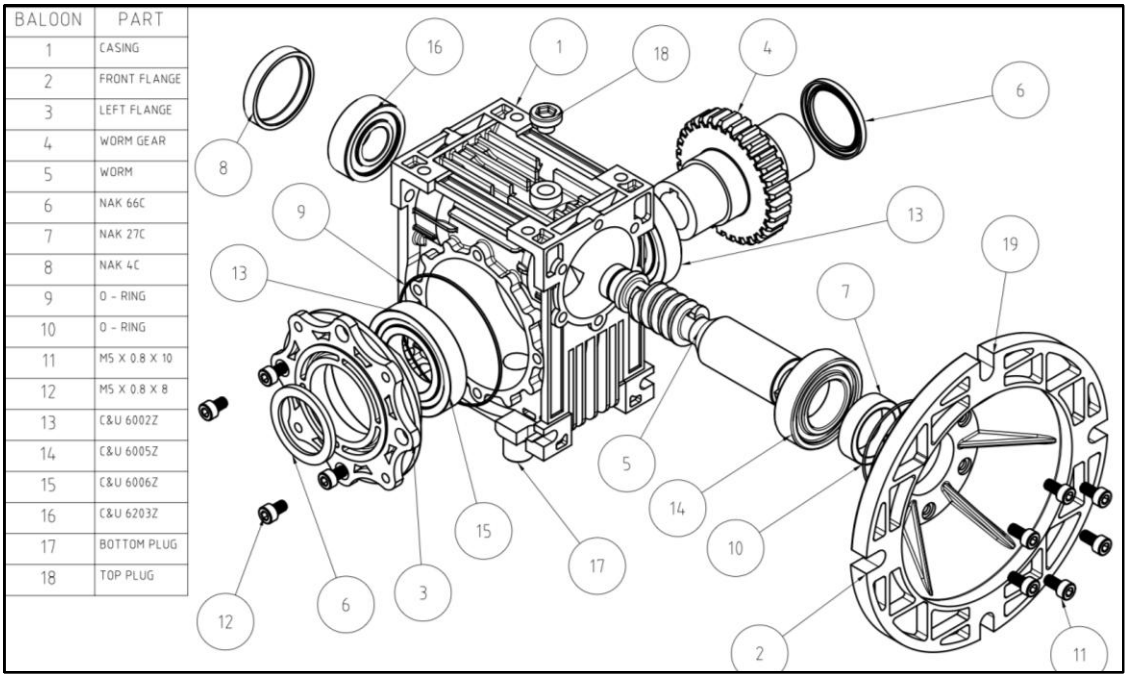

Figure 1 – Technical drawing

1.4 Exploded and sectional view

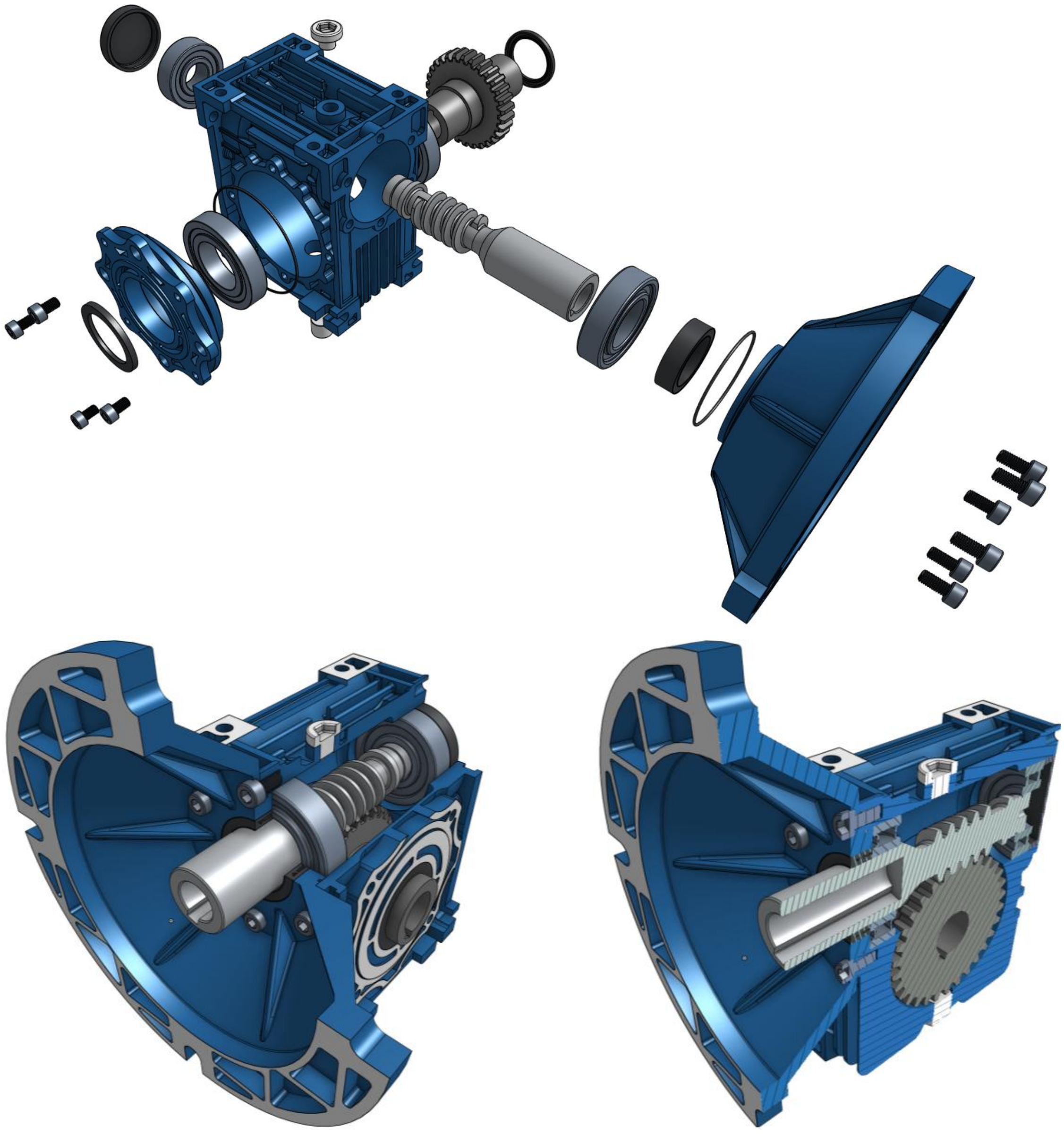

Figure 2 – Exploded view

1.5 Selection of machining operations and renderings of components

The components of the assembly analysed in detail in this report are the housing (part no. 1), the worm shaft (part no. 5), the output flange (part no. 2), the reaction arm (structural restraint component) and the oil filler cap (part no. 18). Each component has been matched with the most suitable manufacturing technology in relation to its geometry, order quantities (500 units) and functional requirements:

Housing (Carter, No. 1):

given its complex box-like geometry and the presence of orthogonal internal cavities to support the bearings, it is produced using shell moulding (moulding in a pre-coated sand shell on a metal pattern plate), ensuring an excellent balance between rough dimensional accuracy and tooling wear.

Worm Shaft (No. 5):

a primary kinematic component operating at high speed, it is manufactured by machining from a solid rolled bar of C45 steel. The manufacturing process includes turning in two set-ups, axial drilling and boring, helical thread milling using a universal milling machine and a mechanical divider, vertical slotting of the tongue seat, high-frequency induction hardening with stress relief on the tooth flanks and bearing seat, and finally external cylindrical grinding.

Output flange (2 pcs):

a sealing component and structural interface, it is produced by plastic deformation via hot forging with flash on a hydraulic press from an EN AW-6082 aluminium alloy billet, ensuring the continuity of the metal grain flow lines and the absence of porosity.

Reaction arm (auxiliary component):

designed to absorb the reaction torque and transfer it to the frame, it is manufactured by continuous arc MIG/MAG (GMAW) welding, joining a shaped plate made of S235JR structural steel to a cylindrical bushing via a T-joint with a fillet weld.

Upper oil filler cap (no. 18):

a sealing component designed to withstand low mechanical stress; it is produced using 3D printing with FDM technology (Bambu Lab P1S), utilising PETG filament with high chemical inertness towards lubricating oils, thereby minimising set-up times and fixed costs.

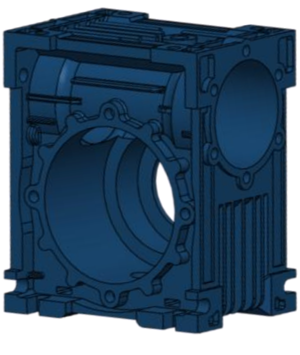

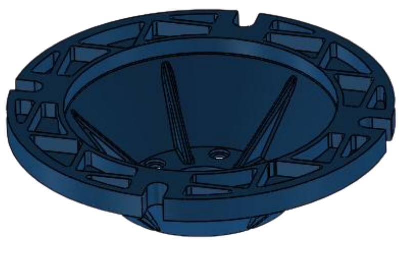

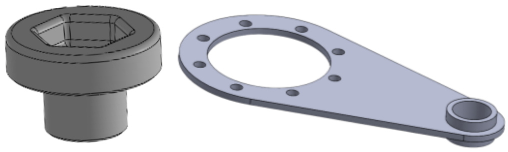

Figure 3 – Project components

1.6 Client's requirements

We assume a request from a company in the logistics sector for 500 gearmotors. As this is a small to medium-sized order, it requires a careful balance between quality, dimensional accuracy and production costs.

In terms of performance, the client requires a reliable gearbox suitable for continuous operation, with particular emphasis on minimising vibration, noise and wear. A long service life and maintenance requirements reduced to a minimum are key requirements of the contract.

From an economic perspective, the aim is to keep costs down without compromising product quality. This constraint has guided the choice of technologies and materials, favouring solutions designed to maximise the performance-to-cost ratio.

2. CASTING

2.1 Component overview and choice of material

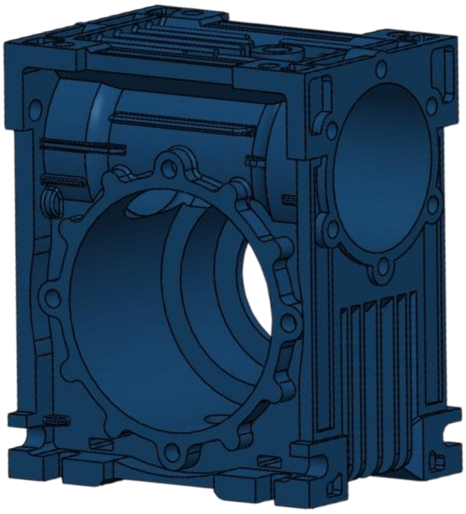

The housing (component no. 1) forms the structural body of the gearmotor, serving to house and protect the internal mechanism. It fulfils a dual role: it provides mechanical support for the internal components (shafts, bearings and connecting elements), ensuring their correct relative positioning, and facilitates the dissipation of heat generated during operation.

The material chosen was the EN AC-43000 aluminium alloy [AlSi10Mg], selected for its combination of lightness and high thermal conductivity – a critical requirement in a worm gearbox, where sliding friction generates significant heat.

This alloy was preferred to the Al-Si-Cu series alloys (e.g. 46000), typically used in the production of Motovario gearmotors, due to its superior ability to fill complex geometries and the excellent structural integrity it imparts to the casting. The absence of copper also increases resistance to atmospheric corrosion and reduces susceptibility to hot cracking, ensuring the lubricant remains sealed and providing a reliable basis for subsequent precision machining of the bearing seats.

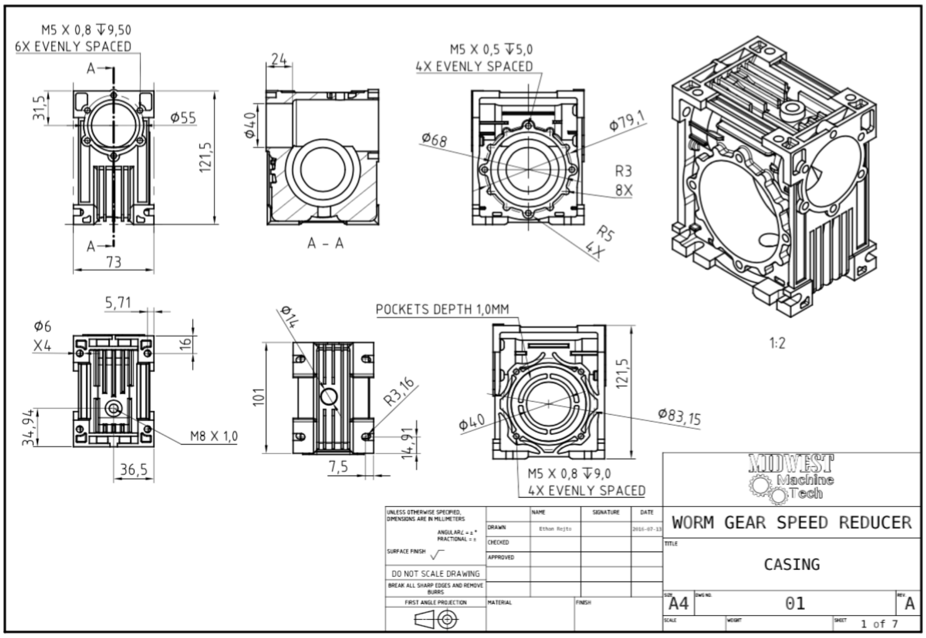

Figure 4 – Technical drawing

BAYRAM METAL

Continuous casting aluminium alloys.

Standard: **UNI EN 1676 and 1706**

Alloy group: **Al Si 10 Mg**

Alloy designation: **EN AB and AC 43000 Al Si 10 Mg (a)**

Replaces: **DIN 239 A Al Si 10 Mg**

CHEMICAL COMPOSITION %

ALLOY		ELEMENTS												
		Si	Fe	Cu	Mn	Mg	Cr	Ni	Zn	Pb	Sn	Ti	Individual impurities	Global impurities
EN AB 43000	min	9,0				0,25								
	max	11,0	0,40	0,03	0,45	0,45	-	0,05	0,10	0,05	0,05	0,15	0,05	0,15
DIN 239 A - Al Si 10 Mg	min	9,0				0,20								
	max	11,0	0,50	0,05	0,4	0,50	-	0,05	0,10	0,05	0,05	0,15	0,05	0,15

MECHANICAL FEATURES DETECTED FROM SEPARATE CASTING TEST SPECIMENS

Casting process	Temper designations	Rm Tensile strenght		Sp 0,2 Yield strenght		A Elongation		HB Brinell hardness	
		EN 1706	DIN 1725	EN 1706	DIN 1725	EN 1706	DIN 1725	EN 1706	DIN 1725
		Mpa	N/mm2	Mpa	N/mm2	%	%	HBW	HB
SAND (as cast)	F	150	160 - 210	80	80 - 110	2	2 - 6	50	50 - 60
Hardened and Aged artif.	T6	220	220 - 320	180	180 - 260	1	1 - 4	75	80 - 110
SHELL (as cast)	F	180	180 - 240	90	90 - 120	2,5	2 - 6	55	60 - 80
Hardened and Aged artif.	T6	260	240 - 320	220	210 - 280	1	1 - 4	90	85 - 115
Hardened and Sub-aged artif.	T64	240		200		2		80	
PRESSURE DIE (as cast)									

PHYSICAL PROPERTIES (indicative values subject to the UNI EN and ex DIN Standards)

DENSITY	2.68 Kg/dm³
MELTING RANGE or MELTING POINT	550 ℃ 600 ℃
SPECIFIC HEAT (at 100)°	0.91 J/Gk
LINEAR SHRINKAGE IN SAND PROCESS	1.0 - 1.2 %
LINEAR SHRINKAGE IN SHELL PROCESS	0.5 - 0.8 %
ELECTRIC CONDUCTIVITY	18 - 25 MS/m
MODULUS OF ELASTICITY	7400 Kg/mm²

THERMAL CONDUCTIVITY at 20°C	140 - 170 W/(m K)
LINEAR THERMAL EXPANSION from 20 t 100°C	21 10-6/°K
LINEAR THERMAL EXPANSION from 20 t 200°C	22.0-10-6/K
LINEAR THERMAL EXPANSION from 20 t 300°C	-
SUGGESTED MAXIMUM TEMPERATURE	770 ℃
SUGGESTED CASTING TEMPERATURE	
°in sand	680 - 750 ℃
°in shell	680 - 750 ℃
°in pressure die	-

TECHNOLOGICAL FEATURES, QUALITATIVE INDICATIONS

STRENGTH AT ELEVATED TEMPERATURE(to 200°C)	SUFFICIENT
GENERAL RESISTANCE TO CORROSION	GOOD
MACHINABILITY	GOOD
CASTABILITY	GOOD
POLISHING	MEDIUM

RESISTANCE TO HOT TEARING	SMALL
PRESSURE TIGHTNESS	GOOD
WELDABILITY	EXCELLENT
DECORATIVE ANODISING	LOW
PROTECTIVE ANODISING	SUFFICIENT

Address: Veliköy Sanayi Bölgesi 1. Kısım Osman Uzun Cad. No: 2/1 Çerkezköy / Tekirdağ / TURKEY
Email: info@bayrammetal.com.tr - **Phone:** +90 282 746 10 41 (Pbx) - **Web:** bayrammetal.com.tr

Figure 5 – AC 43000 properties

2.2 Choice of forming process

In selecting the forming process best suited to the client's requirements, a number of criteria were taken into account: the component's geometry, the required dimensional accuracy, the production volume and production costs.

Based on these parameters, three casting processes were compared: sand casting, shell moulding and die casting.

For a small to medium-sized batch such as ours, the choice comes down to a trade-off between the investment in equipment – which must be amortised over the batch – and the dimensional accuracy achievable on the rough-cast part, which determines the extent of subsequent machining operations.

The tolerance grades assigned to each process (Table 2.2) illustrate the relationships: hand-moulded sand casting falls within the DCTG 9–12 range; shell moulding, being a higher-precision form of sand casting, falls within the DCTG 7–9 range; whilst die casting, using a permanent mould, achieves the DCTG 5–7 range.

Sand casting has the lowest tooling cost, but its poor dimensional accuracy (DCTG 11) necessitates substantial allowances, resulting in increased machining times.

Die-casting, at the opposite end of the spectrum, requires a permanent steel mould, the high cost of which is justified only for production volumes greater than ours.

Shell moulding occupies a favourable middle ground: the metal pattern plate entails a tooling cost higher than that of sand casting but lower than that of die-casting, and can be amortised over 500 parts, whilst the greater dimensional accuracy (DCTG 8, Table 2.2) reduces material allowances and the need for subsequent machining operations.

Linear Dimensional Casting Tolerance Grades (DCTG)

Nominal Dimension related to the Moulded part, mm		DCTG5	DCTG6	DCTG7 (Pattern)	DCTG8 (Pattern Core Complex)	DCTG9 (Sand Printed)	DCTG10	DCTG11	DCTG12	DCTG13
-	≤ 10	0.36	0.52	0.74	1.00	1.50	2.00	2.80	4.20	-
> 10	≤ 16	0.38	0.54	0.78	1.10	1.60	2.20	3.00	4.40	-
> 16	≤ 25	0.42	0.58	0.82	1.20	1.70	2.40	3.20	4.60	6.00
> 25	≤ 40	0.46	0.64	0.90	1.30	1.80	2.60	3.60	5.00	7.00
> 40	≤ 63	0.50	0.70	1.00	1.40	2.00	2.80	4.00	5.60	8.00
> 63	≤ 100	0.56	0.78	1.10	1.60	2.20	3.20	4.40	6.00	9.00
> 100	≤ 160	0.62	0.88	1.20	1.80	2.50	3.60	5.00	7.00	10.00
> 160	≤ 250	0.70	1.00	1.40	2.00	2.80	4.00	5.60	8.00	11.00
> 250	≤ 400	0.78	1.10	1.60	2.20	3.20	4.40	6.20	9.00	12.00
> 400	≤ 630	0.90	1.20	1.80	2.60	3.60	5.00	7.00	10.00	14.00
> 630	≤ 1000	1.00	1.40	2.00	2.80	4.00	6.00	8.00	11.00	16.00
> 1000	≤ 1600	-	1.60	2.20	3.20	4.60	7.00	9.00	13.00	18.00

DCTG 9 – 12 Sand Casting, Hand Moulding

DCTG 7 – 9 Sand Casting and Sand Printed Moulding

DCTG 6 – 8 Permanent mould casting. Gravity and Low Pressure Die casting

DCTG 5 – 7 Pressure Die casting: Use of tight tolerance grade (DCTG 5) to be agreed by case. Note 4

Note 1: The tolerance grades indicated are those which can normally be held for castings produced for long series and if production factors influencing the dimensional accuracy of the casting have been fully developed.

Note 2: For complex castings, one grade coarser is recommended

Note 3: For wall thickness, one grade coarser applies

Note 4: Differs. from original standard text.

Table - 'Linear Dimensional Casting Tolerance Grades (DCTG)'

2.3 Design modifications and material allowances

The original geometry of the casing is excessively complex for the casting design process. For this reason, the 3D model was reworked to produce a simplified rough casting. Specifically, the cooling fins on the outer faces of the component were omitted. The walls have been converted into smooth, continuous surfaces, which will subsequently be achieved through machining processes (milling).

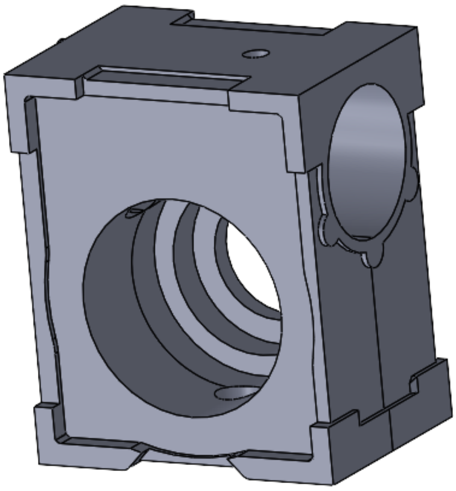

Figure 6 - Simplified casing

When defining the foundry mould, the decision was taken to close off small holes such as threaded fixing holes (of small diameter and shallow depth) or oil fill/drain/level holes. Machining these holes directly into the casting would require a greater expenditure of resources than can be achieved by creating them through subsequent machining operations. Subsequent machining ensures superior dimensional accuracy and surface finish, whilst simultaneously optimising and simplifying the entire casting process.

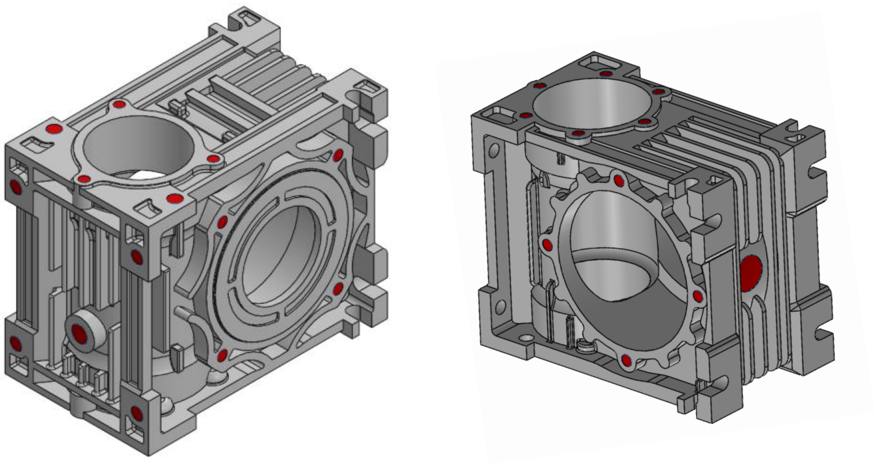

Figure 7 - Original casing with closed holes

The functional surfaces of the casing, such as the bearing seats, flange mating surfaces and fastening areas, require mechanical finishing operations to ensure the tight tolerances and geometric accuracy specified in the design. As the as-cast part obtained by casting does not directly meet these requirements, it is essential to allow for excess material to be removed by machine tools.

With reference to the technical manuals for shell moulding, the tabulated values for aluminium alloys in this size range indicate a material allowance of between 0.5 mm and 1.0 mm. An operational value of 0.8 mm was therefore established for the design.

Dimensioni nominali (mm)	Sovrametalli di lavorazione (mm)	Tolleranze (mm)
≤ 50	0,5 ÷ 1	± 0,1 ÷ 0,25
50 ÷ 175	0,5 ÷ 1	± 0,16 ÷ 0,42
175 ÷ 300	1 ÷ 2	± 0,29 ÷ 0,67
300 ÷ 450	1,3 ÷ 2,5	± 0,71 ÷ 0,83

Tab. 4-16 Valori medi indicativi dei sovrametalli di lavorazione e delle tolleranze realizzabili su getti in leghe di rame, di alluminio, di magnesio, di zinco, col procedimento shell molding.

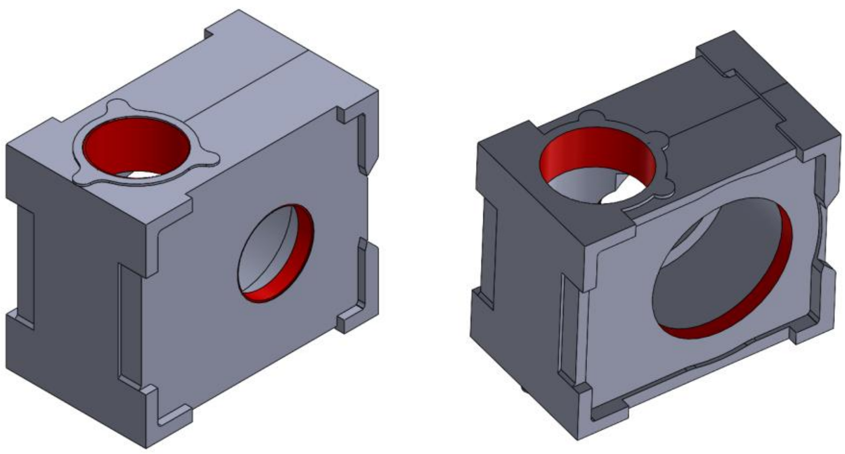

Figure 8 - Simplified casing with excess material

2.4 Parting line

The main criterion for selecting the parting line is to minimise undercuts, in order to simplify demoulding and reduce the complexity of the mould. The final parting line runs through the centreline of the casing, parallel to the longest side of the component. This configuration optimises the symmetry of the two mould halves and ensures the correct ejection of the casting.

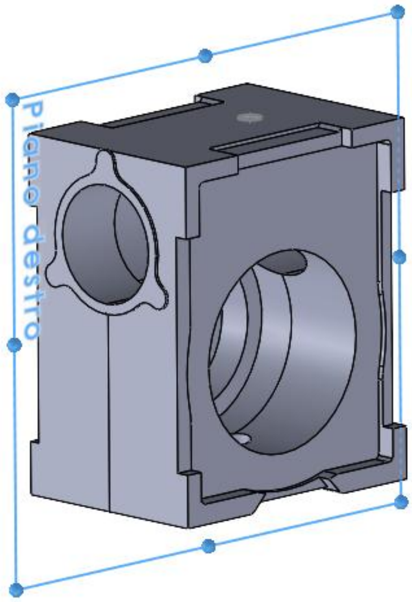

Figure 9 - Parting line

2.5 Draft angle

For all surfaces perpendicular to the parting line, a single draft angle of 30' (half a degree) has been adopted. This decision is dictated by the need to ensure easy and clean separation of the mould from the pre-coated sand shell, avoiding abrasions or micro-cracks in the mould walls during removal.

Valori indicativi dell'angolo di sformo	
Modelli in legno	1°-2°
Modelli metallici	30'
Portate d'anima verticali	10°-12°
Nervature sottili	1'-2'

Figure 10 - Guide values for draft angles according to 'Santochi'

2.6 Fillet radii

With regard to corner fillets, a single dimension of 3 mm is adopted. This prevents the concentration of residual stresses during the solidification phase of the alloy and facilitates the proper flow of molten metal within the mould.

Furthermore, the removal of sharp corners is crucial to prevent the initiation of cracks caused by material shrinkage and to avoid localised erosion of the sand shell during casting.

2.7 Shrinkage

To compensate for the volumetric contraction of the metal during cooling, the mould must be oversized in advance.

The average linear shrinkage coefficient for aluminium alloy castings produced in temporary moulds is conventionally taken as 1.6 per cent. However, for the component in question, this value is overestimated for two main reasons:

Material: the EN AC-43000 (AlSi10Mg) alloy has a high silicon content (~10%), which reduces its contraction compared to alloys with lower silicon content. Indeed, the material's technical data sheet itself states a nominal shrinkage of 0.8 per cent.

Process: the shell moulding process offers greater structural rigidity than green sand moulding, thereby limiting the shrinkage of the casting.

By balancing the characteristics of the material and the process with the literature data, the actual shrinkage is estimated to be between 1.0% and 1.3%. For design purposes, a linear shrinkage coefficient of 1.2% is adopted.

The model will therefore be oversized by applying the following equation:

$$Lmodello = Lnominale \times (1 + 0,012)$$

MATERIALI	RITIRO %(2)		
	Getti piccoli(1)	Getti medi(1)	Getti grandi(1)
Ghise grige	1	0,85	0,7
Ghise malleabili	1,4	1	0,75
Ghise legate	1,3	1,05	0,35
Acciaio	2	1,5	1,2
Alluminio e leghe	1,6	1,4	1,3
Bronzi	1,4	1,2	1,2
Ottoni	1,8	1,6	1,4
Leghe di magnesio	1,4	1,3	1,1

(1) I «getti piccoli» comprendono getti con una dimensione max < 500 mm; i «getti medi» comprendono getti con una dimensione massima compresa tra 500 e 1000 mm; i «getti grandi» comprendono getti con una dimensione massima < 1000 mm.
(2) Il ritiro delle cavità è in genere un po' minore (5–10%) rispetto a quello delle superfici esterne a causa della resistenza che oppongono le anime alla libera contrazione del metallo.

Tab. 4-1 Ritiri lineari per getti colati in sabbia (valori medi indicativi).

Figure 11 - Indicative values for shrinkage angles according to 'Santochi'

2.8 Design of cores

The through-holes in the casing are formed using two cores: one for the hole intended for the worm screw and one for the gear support hole.

For a batch of 500 parts, in order to ensure dimensional accuracy and cost-effectiveness, the cores are produced using the same process as for the housing, namely shell moulding.

The material used is quartz sand pre-coated with thermosetting phenolic resin, blown into the preheated core box.

2.8.1 Dimensioning criteria

The core diameter is defined by the following formula:

$$\text{Core diameter} = (D_{finished} - \text{excessmaterial}_{Total}) \times (1.011)$$

The factor 1.011 applies a shrinkage correction of 1.1 per cent.

As the core is a rigid, non-deformable body, it partially hinders the contraction of the metal towards the centre of the cavity during cooling. This value is derived from the 'Santochi' text, specifically Table 2.8, according to which the shrinkage of cavities is on average 5–10 per cent lower than that of external surfaces.

2.8.2 Draft angles

On the cylindrical bodies of both cores, a draft angle of 30’ has been applied across the entire surface parallel to the direction of extraction, to ensure design consistency.

2.8.3 Fillet radii

Fillet radii have been incorporated to increase the mechanical strength of the core, minimising the risk of breakage during handling, assembly and casting.

2.8.4 Core positioning and core runner design

The correct positioning of the cores within the mould is ensured by specific core runners. These form an extension of the core body and, as these are through-cavities, both cores rest on both sides of the mould.

The core for the worm gear, having an axis parallel to the parting line, requires cylindrical core runners. Their length is proportional to the diameter and weight of the core, extending 20 mm on each side.

The core for the gear wheel, on the other hand, having its axis perpendicular to the parting line, requires truncated conical support surfaces.

In accordance with the rules for clay moulding, cores positioned with their axis perpendicular to the parting line must have truncated-conical flanges with a wide draft angle ($\delta = 10°$). This geometry ensures self-centring and facilitates the guided descent of the core during the slipping and closing of the mould.

Consequently, the ends have been shaped as truncated cones by applying a draft angle of $\delta = 10°$.

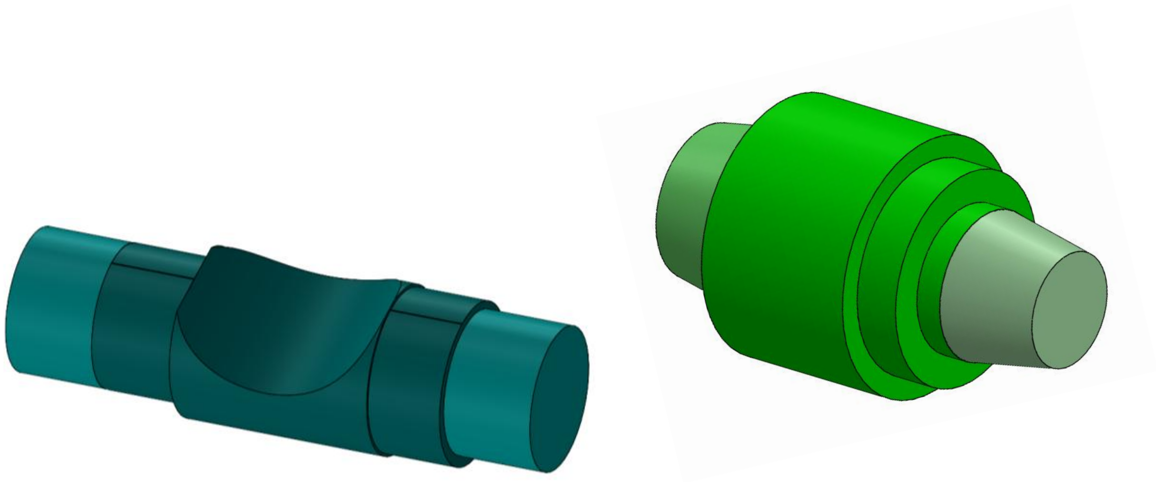

Figure 12 - Shafts with bore, for gear wheel bore (right) and worm screw bore (left)

2.8.5 Core boxes

The cores are produced using a dedicated core box, made from hot-work steel (X40CrMoV5-1).

The two half-moulds are fitted with reference pins for centring, ensuring coaxiality and repeatability in every production cycle.

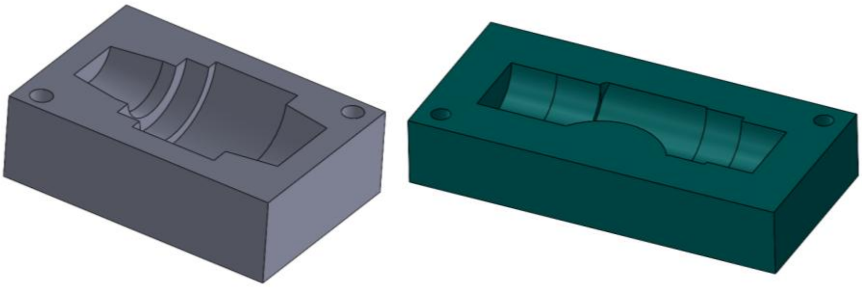

Figure 13 - Cores with bore, for gear wheel bore (right-hand) and worm screw bore (left-hand)

Qualità materiale	**X40CrMoV5-1**	Stato di fornitura:	*Scheda Dati*
Norma di riferimento	**UNI EN ISO 4957: 2002**	Ricotto	*Lucefin Group*
Numero	**1.2344**		

Composizione chimica

C%	Si%	Mn%	P% max	S% max	Cr%	Mo%	V%
0,35-0,42	0,80-1,20	0,25-0,50	0,030	0,020	4,80-5,50	1,20-1,50	0,85-1,15
± 0.02	± 0.05	± 0.04	+ 0.005	+ 0.005	± 0.10	± 0.05	± 0.05

Scostamenti ammessi per analisi di **prodotto**

Temperature in °C

Deformazione a caldo	**Tempra**	**Rinvenimento** vedere tabella	**Ricottura di distensione**	La ricottura di distensione va eseguita dopo lavorazione meccanica e prima della tempra
1050-900	preriscaldo 800 sosta poi 1020-1080 olio, polimero o b.t.	immediato dopo tempra almeno **2 cicli**	600-650 raffredd. In forno a 350 poi aria	

Ricottura di lavorabilità	**Ricottura isotermica**	**Preriscaldo per saldatura**	**Distensione dopo saldatura**
820 raffreddamento in forno (HB max 229)	880 raffreddamento in forno fino a 780 sosta, poi raffreddamento in forno fino a a 750 poi aria	350	650 raffreddamento forno

Ac1	**Ac3**	**Ms**	**Mf**
830	915	300	80

b.t. = bagno di sali o termale (450-500 °C)

Proprietà meccaniche

Tabella di rinvenimento tempra a 1040 °C in olio. Valori su Ø 20 mm

HB	560	543	525	512	504	512	525	543	577	577	512	455	390	301
HRC	55	54	53	52	51.5	52	53	54	56	56	52	48	42	32
N/mm^2	2070	2010	1950	1880	1850	1880	1950	2010	2160	2160	1880	1640	1340	1010
Rinvenimento a **°C**	**50**	**100**	**150**	**200**	**250**	**300**	**350**	**400**	**450**	**500**	**550**	**600**	**650**	**700**

Espansione termica	$10^{-6} \cdot K^{-1}$	10.0	10.7	10.8	11.3	11.8	12.3	12.7	13.0	13.2
Modulo elastico	long. GPa			210	205	198	191	182000	173	
Calore specifico	J/(Kg•K)			461	479	499	517	536	558	587
Conducibilità termica	W/(m•K)			19.2	20.1	22.4	24.0	25.1	25.8	26.1
Densità	Kg/dm^3			7.74						
Resistività Elettrica	$Ohm \cdot mm^2/m$			0.543	0.638	0.705	0.782	0.868	0.96	1.06
R materiale bonificato per	N/mm^2			**1600**			1400	1300	1100	800
Rp 0.2	N/mm^2			1460			1200	1100	900	600
R materiale bonificato per	N/mm^2			**1200**			1120	1000	850	580
Rp 0.2	N/mm^2			1060			900	800	650	420
Prove a	**°C**	**-100**	**0**	**20**	**100**	**200**	**300**	**400**	**500**	**600**

Nitrurazione in ammoniaca gassosa. Materiale temprato e rinvenuto a min. 580 °C prima della nitrurazione.

Temperatura **°C**	Tempo **h**	Profondità di indurimento **mm**	Durezza strato indurito **HV**
525	10	0,125	1000 - 1250
525	20	0,180	1000 - 1250
525	40	0,250	1000 - 1250
525	60	0,300	1000 - 1250

Acciaio da utensili per impieghi ad alte temperature

- buona resistenza agli shock termici ed alla criccatura a caldo
- ottime caratteristiche meccaniche e tenacità a caldo
- costanza di durezza durante tutto il ciclo produttivo e ottima lavorabilità
- l'elevato grado di micropurezza conferisce buone caratteristiche di lucidatura e fotoincidibilità
- possibilità di intervenire sugli stampi con tecniche di saldatura TIG (Tungsten Inert Gas) o MMA (Manual Metal Arc)
- possibilità di rivestimento con processi PVD o PA/CVD, indurimenti alla fiamma/induzione e nitrurazione
- applicazioni: *stampi per pressocolata alluminio, stampi per bassa pressione, conchiglie per fusioni in gravità, contenitori per presse presso colata, matrici estrusione alluminio, tacchi pressatori, camicie per estrusione e stampi ad iniezione*

Figure 14 - Specification sheet for X40CrMoV5-1 steel

2.9 Study of the casting's solidification

To analyse the solidification process and determine the correct positioning of the sprue, it is essential to calculate the cooling coefficients of the casting.

Given the complex geometry of the component, it was broken down into simpler volumes. The volume and surface area measurements for each section were obtained using the 'Mass Properties' and 'Measure' functions of the SolidWorks CAD software.

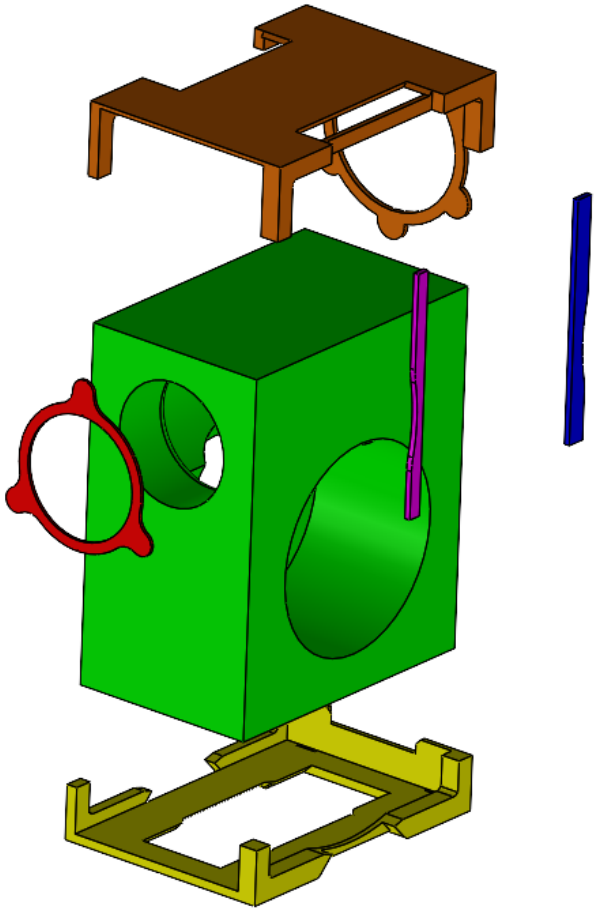

Figure 15 - Division of cooling modules

The cooling modulus was calculated using the equation: $M = V/ S$st, where V represents the volume of the area under consideration and Sst the heat transfer surface area facing the mould.
This was derived from the difference between the total surface area Stot and the common surface area Scom, i.e. the area that does not directly contact the mould and therefore does not undergo heat exchange.

The calculations for the cooling modules are set out below:

- **M1 (green area):**
  V = 389,979.17 mm³
  Stotal = 66,161.47 mm²
  Scomune = 14,714 mm²
  Sst = Stotal – Scommon = 51,447.47 mm²
  M1 = V/Sst = 7.58 mm

- **M2 (orange area)**:
  V = 15,843.82 mm³
  Total = 19,086.94 mm²
  Common area = 7,773 mm²
  Sst = Total area – Common area = 11,313.94 mm²
  M2 = V/Sst = 1.4 mm

- **M3 (yellow area):**
  V = 16,424.02 mm³
  Total = 14,298.80 mm²
  Common area = 5,283 mm²
  Sst = Total area – Common area = 9,015.8 mm²
  M3 = V/Sst = 1.8 mm

- **M4 (red area):**
  V = 680.93 mm³
  Total = 1,668.21 mm²
  Common area = 680 mm²
  Sst = Total area – Common area = 988.21 mm²
  M4 = V/Sst = 0.6 mm

- **M5 (blue area):**
  V = 882.37 mm³
  Stotale = 1254.35 mm²
  Common area = 489 mm²
  Sst = Total – Common = 765.35 mm²
  M5 = V/Sst = 1.15 mm

- **M6 (pink area)** ≤ M5 = 1.15 mm

In ascending order: M4 < M6 < M5 < M2 < M3 < M1

Component	Cooling module (mm)
1 (green area)	7.58
3 (yellow area)	1.8

2 (orange area)	1.4
5 (blue zone)	1.15
6 (pink zone)	≤1.15
4 (red zone)	0.6

Table – Cooling modules (in descending order)

2.9.1 Heuvers' circles method

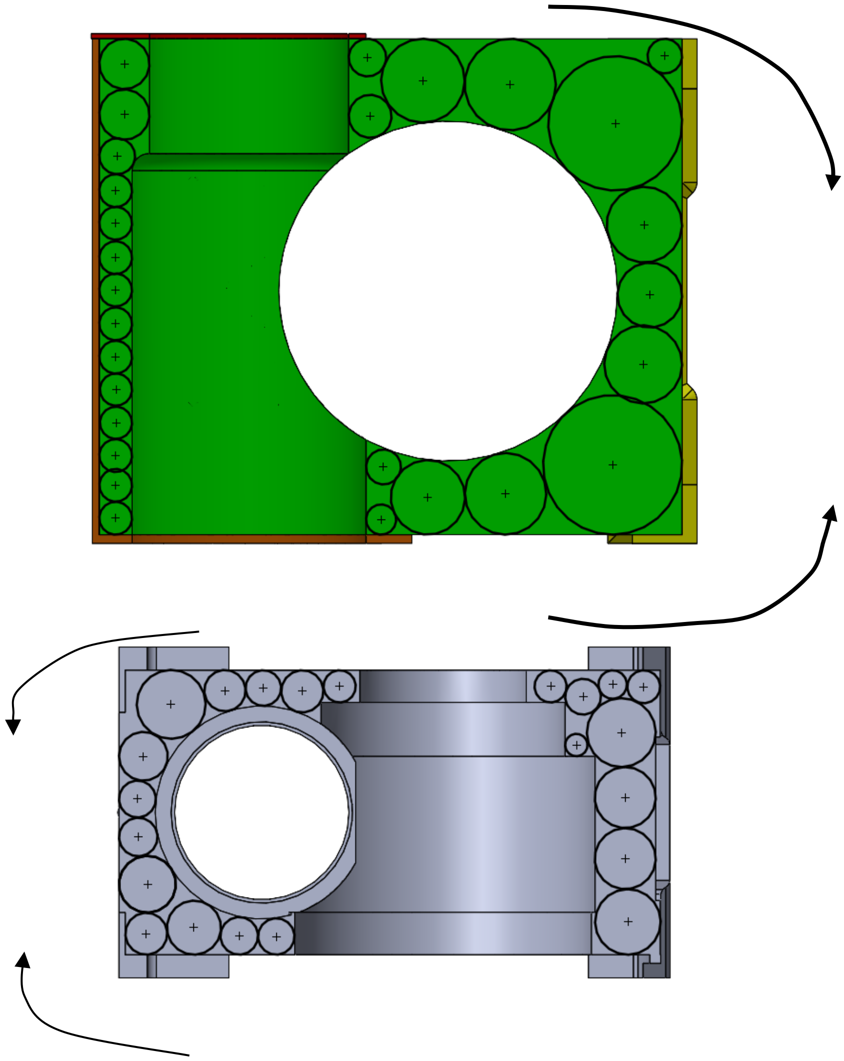

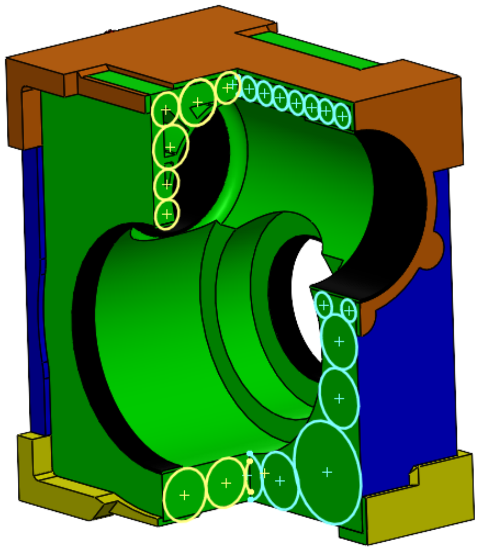

Figure 16 - The three views relating to the Heuvers circle method

Analysis of the cross-sections shows that the previous subdivision into sub-volumes was based solely on geometric criteria, whereas the study of Heuvers' inscribed circles qualitatively maps the actual thermal nodes.

The critical areas are mainly concentrated in module M_1 and, to a lesser extent, in M_2 and M_3 .

- **Section 1 (Division Plane):** Around the through-hole in the gear wheel, in the area extending to the worm screw hole and the base of the casing, the inscribed circles reveal massive volumes at the corners. These thermal nodes result in a longer cooling time and a high risk of shrinkage porosity or hot cracks if not adequately fed.

- **Section 2 (Perpendicular Plane):** A section perpendicular to the parting plane is essential for assessing the volumetric distribution along the Z-axis, which is not visible in the first analysis. This view reveals further critical thermal nodes requiring attention, located at the upper corners (worm screw hole) and the lower right-hand corner.

- **Section 3 (Mixed View):** Shows the overall progression of the solidification front.

2.9.2 Simulation with InspireCast

To validate the analytical and geometric results, a simulation of the casting process was carried out using the 'Altair Inspire Cast' software. The CAD model was imported, defining the following process parameters:

- **Cast material:** EN AC-43000 aluminium alloy.
- **Mould and core material:** Silica sand (silica sand bonded with synthetic resin).
- **Mould geometry:** Shell with a uniform thickness of 20 mm.
- **Initial mould temperature:** 423.15 K (150 °C).
- **Temperature of the casting upon mould opening (end of analysis):** 610.04 K (approximately 337 °C).

The solidification analysis made it possible to monitor the evolution of the solid fraction. The results of the simulation are shown in the figures below.

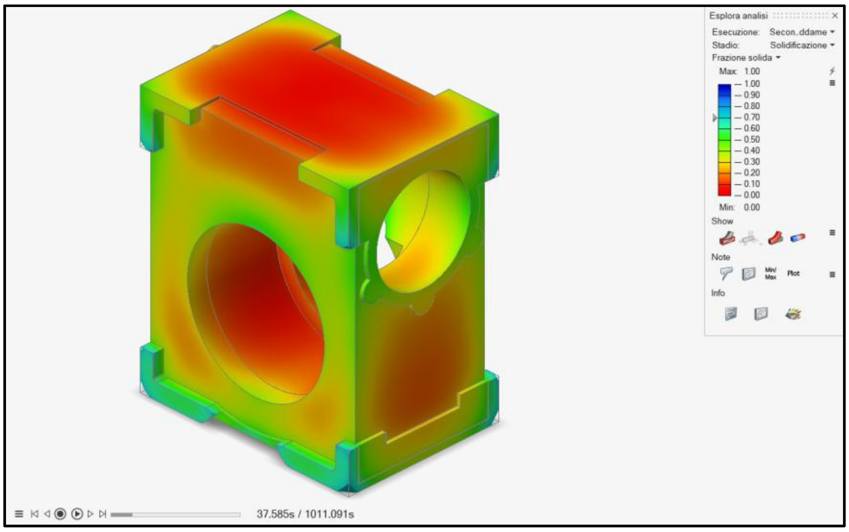

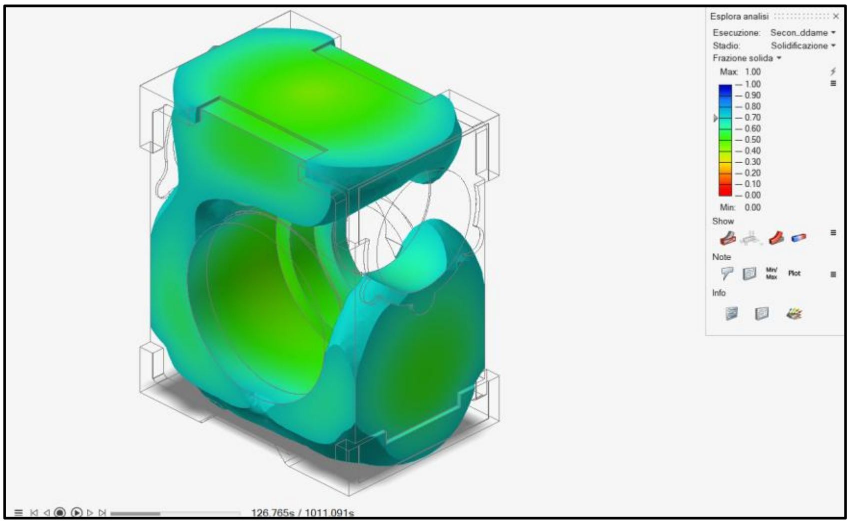

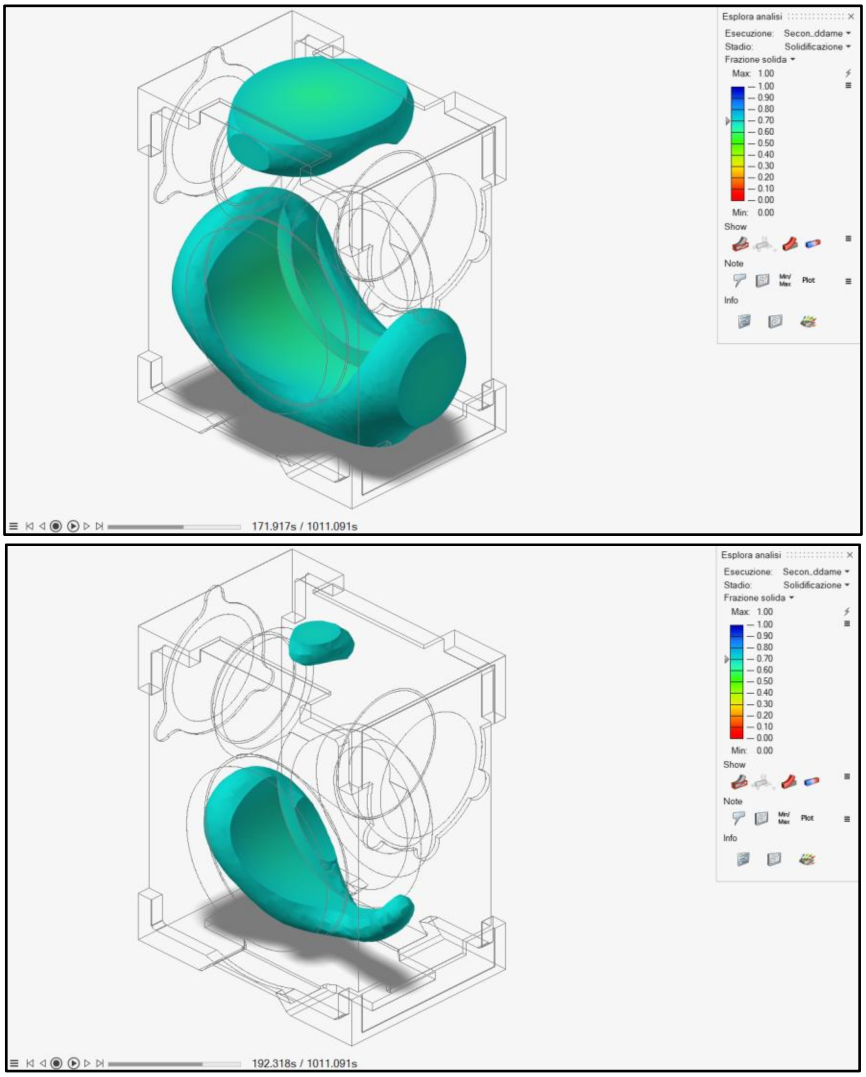

Figure 17 - Solidification simulation – Solid fraction

The images highlight (in light blue) the last regions to solidify. These areas constitute the hot spots of the component where volumetric shrinkage is concentrated, causing non-uniform solidification and promoting the formation of defects.

This trend is confirmed by the specific study of porosity, shown in the next image.

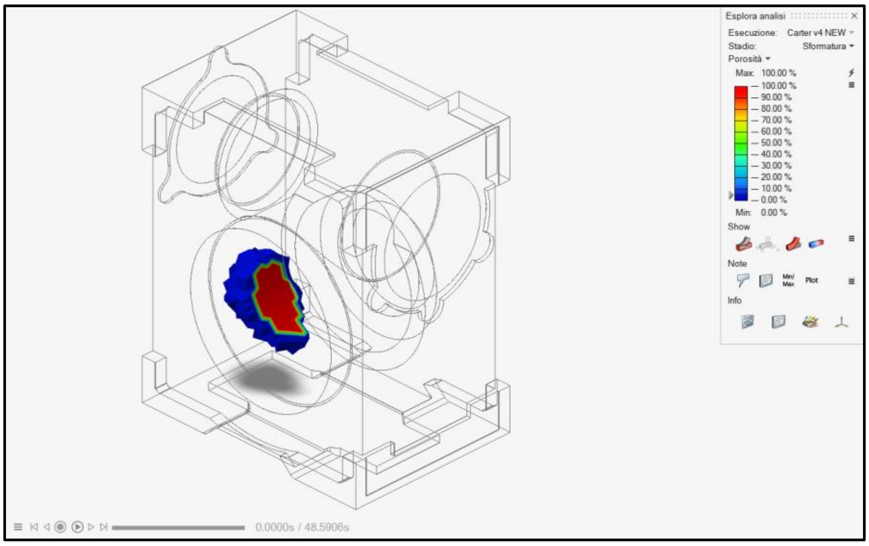

Figure 18 - Demoulding simulation – Porosity

The software has also calculated the component's actual thermal moduli, validating the approximation made in section 2.10 and the qualitative analysis of the Heuvres circles in 2.10.1: the main geometry (rectangular structure) has the highest thermal modulus.

The precise measurements of the cooling moduli extracted from the simulator are shown below.

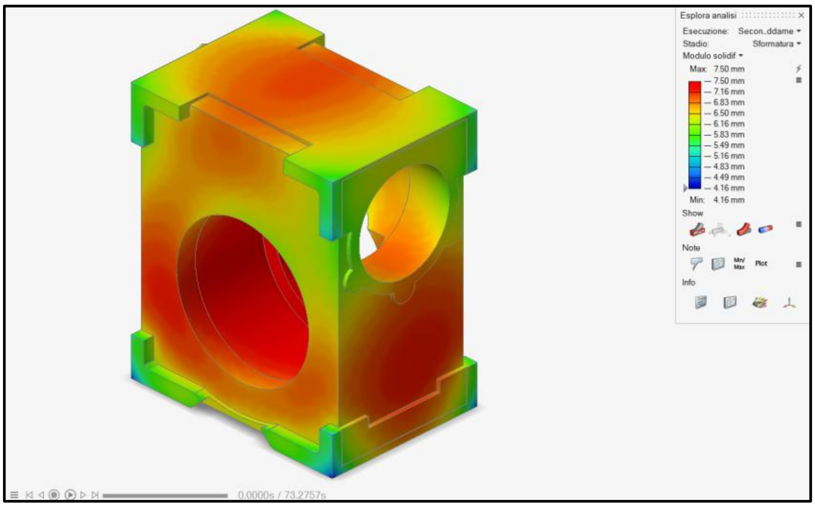

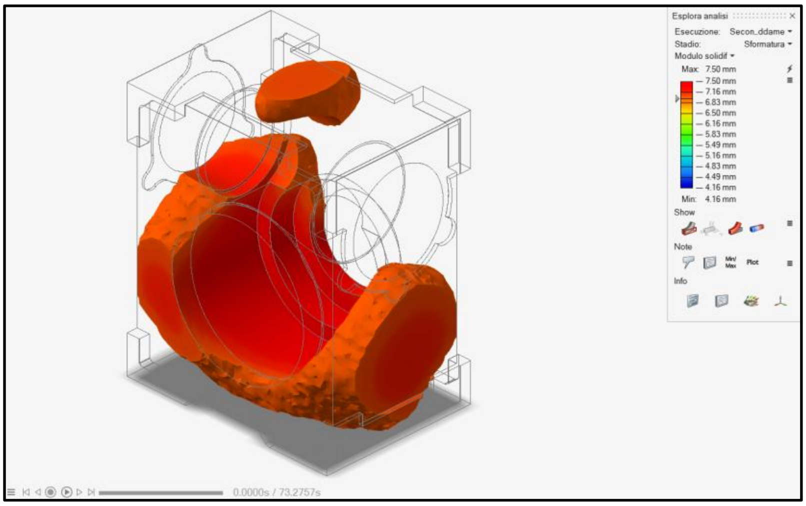

Figure 19 - Demoulding simulation – Solidification modulus

2.10 Design of the sprue and the connecting collar

The sprue is connected directly to the section of the ingot with the highest modulus, which must be adequately fed in order to compensate for volumetric shrinkage in the final stage of solidification.

A sprue with dimensions equal to $M_{sprue} = 1.2 \cdot M_{zone}$ is positioned in contact with the wall adjacent to the critical section of the ingot.

A cylindrical geometry is adopted, with height H and diameter D, and it is blind, as it is positioned to the side of the ingot; this is because an open-top sprue would have even more exposed surface area, thereby increasing heat loss.

For a cylindrical blind sprue, the text by 'Santochi-Giusti' gives the following relationship:

$$\mathbf{M_{sprue}} = 0.19 \cdot D$$

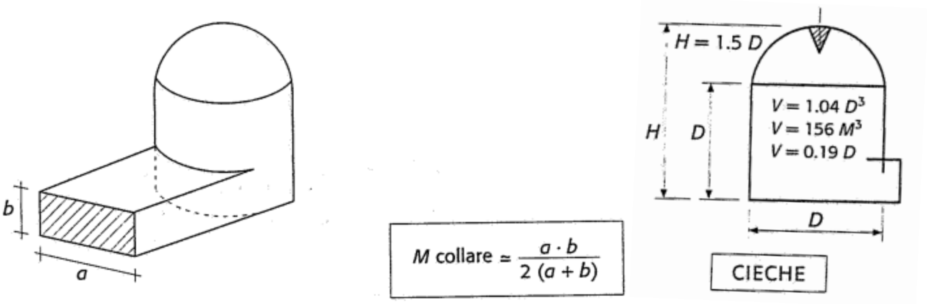

Figure 20 - Images from the Santochi text

2.10.1 Preliminary sizing and simulation

Taking the maximum modulus identified analytically (M_1 = 7.58 mm) as a reference, we obtain:

M_{sprue} = 1.2 × 7.58 ≈ 9.1 mm → D = 9.1 / 0.19 ≈ 47.9 mm

For safety and consistency, D = 48 mm is adopted, from which:

H = 1.5 × D = 72 mm → V_{sprue} = 1.04 × D^3 ≈ 115,015 mm^3

With regard to the dimensioning of the connecting collar:
M_{collar} = (1.1 / 1.2) · M_{sprue}

Substituting the previously calculated parameters, we obtain a value equal to:
M_{collar} = (1.1 / 1.2) · (1.2 · 7.58) = 1.1 · 7.58 = 8.338 mm.

However, the simulation carried out in Inspire Cast refutes the effectiveness of this configuration (D = 48 mm, H = 72 mm, M_{collar} ≈ 8.34 mm).
With the sprue connected laterally to the main body of the casting, at the M_1section, proper thermal control is observed in the attachment region; however, porosity and significant pipe shrinkage persist in the upper part of the casting, near the M_2section, which is not served by the sprue in this configuration.
Although alternative configurations were tested, varying only the connection position whilst keeping the geometry the same, no positioning was identified that could eliminate both critical issues simultaneously.
This result confirms the need to use two separate risers, each dedicated to one of the two critical zones.

2.10.2 Identification of critical zones and recalibration of modules

Since each sprue must be verified in relation to the portion of the casting for which it is responsible, and not in relation to the entire component, the two volume portions affected by the residual defects highlighted by the simulations in section 2.10 were qualitatively isolated using the 'Mass Properties' command in SolidWorks

- **Zone A (lateral):**

  V_A = 239,281.75 mm^3 → S_A = 37,545.90 mm^2 → M_A ≈ 6.37 mm

- **Zone B (top):**

  V_B = 129,953.96 mm^3 → S_B = 28,379.64 mm^2 → M_B ≈ 4.58 mm

Applying the standard criterion $M_{sprue} = 1.2 \cdot M_{zone}$ yields theoretical moduli of 7.65 mm (zone A) and 5.50 mm (zone B).

An initial simulation carried out using these values produced a positive result.

2.10.3 Sizing of the two risers and the collar using the thermal method

Applying $M = 0.19 \cdot D$ once again to the recalibrated moduli:

Parameter	Sprue A (lateral)	Spout B (top)
M_{sprue}	7.65 mm	5.5 mm
D = M / 0.19	40.2 mm	29.0 → 30 mm
H = 1.5 × D	60.4 mm	45 mm
$V_{sprue} = 1.04 \times D^3$	≈ 67,563 mm^3	≈ 25.365 mm^3

Figure 21 - Parameter table

According to the exact formula given in the text, for blind risers the ratio between the cooling coefficients must comply with the following proportion:

$$M_{sprue} : M_{collar} : M_{workpiece} = 1.2 : 1.1 : 1$$

I calculate M for the collar solely using the ratio for the sprue:

$$M_{collar} = 1.1 / 1.2 * M_{sprue}$$

Sprue A (Side):
The required collar module is 7.01 mm.
For a square cross-section, this gives a side length $a = 4 \times 7.01 = 28.04$ *mm*.
A 28 x 28 mm element can be fitted onto a 40.2 mm cylinder without any external protrusions.

Spigot B (Top):
The diameter of the sprue has been set at 30 mm. The required collar module is calculated as 5.04 mm. For a square cross-section, the side length *a is* $4 \times 5.04 = 20.16$ *mm*.

In this case too, a 20 x 20 mm component can be fitted to a 30 mm cylinder.

2.10.4 Cross-check using Caine's method

The criterion used in the previous paragraph ($M_{sprue} = 1.2 \cdot M_{zone}$) verifies only a thermal requirement, namely that the sprue cools more slowly than the portion of the casting to be fed. This approach, however, addresses the problem in an approximate manner.

To complete the dimensional verification, the Caine method was therefore applied as a cross-check; this method incorporates the specific volumetric shrinkage coefficient of the alloy used in addition to the thermal criterion. The method is based on the following dimensionless ratios:

$$X = M_m / M_p \qquad Y = V_m / V_p$$

where M_p and V_p are, respectively, the modulus and volume of the portion of the casting to be fed, whilst M_m and V_m are the modulus and volume of the sprue. The sprue is correctly dimensioned when the point (X, Y) lies above and to the right of the limit curve defined by the equation:

$$X = a / (Y - b) + c$$

The parameters used for the calculation are summarised in the following table:

Parameter	Value	Info
a	0.1	experimental constant
b	0.035 (3.5%)	Santochi table, aluminium-silicon alloy
c	1	uninsulated sprue (no sleeve)
K_1 ($V_m = K_1 \cdot D^3$)	1.04	blind geometry: cylinder + dome
K_2 ($M_m = K_2 \cdot D$)	0.19	blind geometry: cylinder + dome

Parameter	Value	Info
$V_{p,A}$ / $M_{p,A}$	239,281.75 mm³ / 6.37 mm	(Zone A)
$V_{p,B}$ / $M_{p,B}$	129,953.96 mm³ / 4.58 mm	(Zone B)

Figure 21 - Table of parameters for the Caine method

Starting with an initial volume $V_m = (0.1 + STEP) \cdot V_p$, the diameter D is derived and, consequently, the modulus $M_m = K_2 \cdot D$. The values of X and Y are then calculated to check that the inequality $X > a / (Y - b) + c$ holds.

If the condition is not met, STEP is increased by 0.05 and the iteration is repeated until the condition is satisfied.

Applying this procedure to the two critical zones previously identified, the condition is satisfied at the 7th and 5th increments respectively:

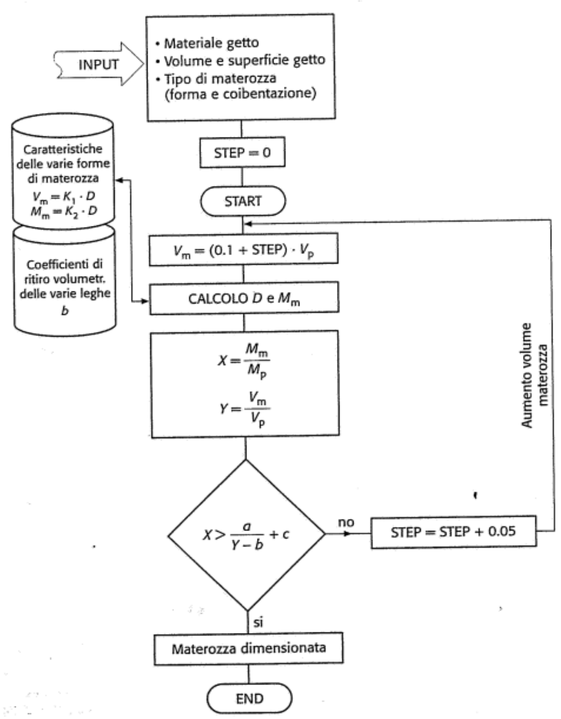

Figure 22 - Diagram relating to the Iter, from Santochi's text

Materozza A (lateral):

STEP	Y	D (mm)	M_m (mm)	X	a / (Y – b) + c
0.00 – 0.25	0.10 – 0.35	28.4 – 43.2	5.40 – 8.21	0.85 – 1.29	2.54 – 1.32 (*unverified*)
0.30	0.40	45.15	8.58	1.35	1.27 (*verified*)

Figure 23 - Sprue A table

Sprue B (upper)

STEP	Y	D (mm)	M_m (mm)	X	a / (Y – b) + c
0.00 – 0.15	0.10 – 0.25	23.2 – 31.5	4.41 – 5.98	0.96 – 1.31	2.54 – 1.47 (*unverified*)
0.20	0.30	33.47	6.36	1.39	1.38 (*verified*)

Figure 24 - Spud table B

2.10.5 Summary table

Below is a summary comparison of the results of sprue sizing obtained using the thermal method and the Caine method.

The calculation of the dimensions of the attachment collar follows the same procedure for the Caine method as well:

Parameter	Thermal method	Caine's method
Slag A (lateral)		
Diameter D_A	40.2 mm	45.2 mm
Height H_A (= 1.5 × D)	60.4 mm	67.7 mm
Volume V_A	67,563 mm^3	≈ 95,713 mm^3
Sprue module $M_{m, A}$	7.65 mm	8.58 mm
Collar module $M_{c,A}$ (= 1.1 / 1.2 · M_m)	7.01 mm	7.86 mm
Square collar a = 4 · M_c	28 × 28 mm	≈ 31.5 × 31.5 mm
Sprue B (upper)		
Diameter D_B	30 mm	33.5 mm
Height H_B (= 1.5 × D)	45 mm	50.2 mm
Volume V_B	≈ 28,080 mm^3	≈ 38,986 mm^3
Sprue module $M_{m,B}$	5.5 mm	6.36 mm
$M_{c,B}$collar module	5.04 mm	5.83 mm
Square collar a = 4 · M_c	20 × 20 mm	≈ 23.3 × 23.3 mm

Figure 25 - Summary table

Below is a comparison of the porosity and pipe shrinkage simulations for the two sprue measurements using the two methods:

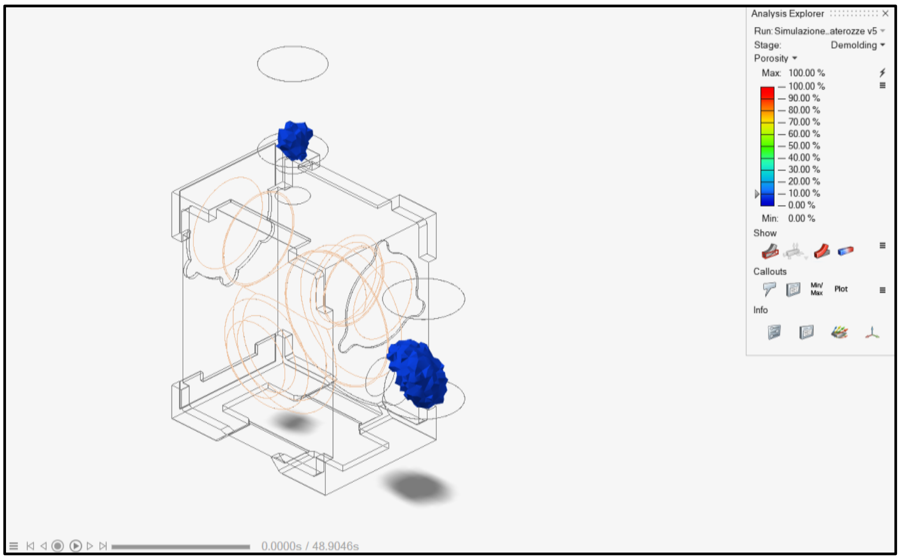

Figure 26 – Porosity simulation (thermal method)

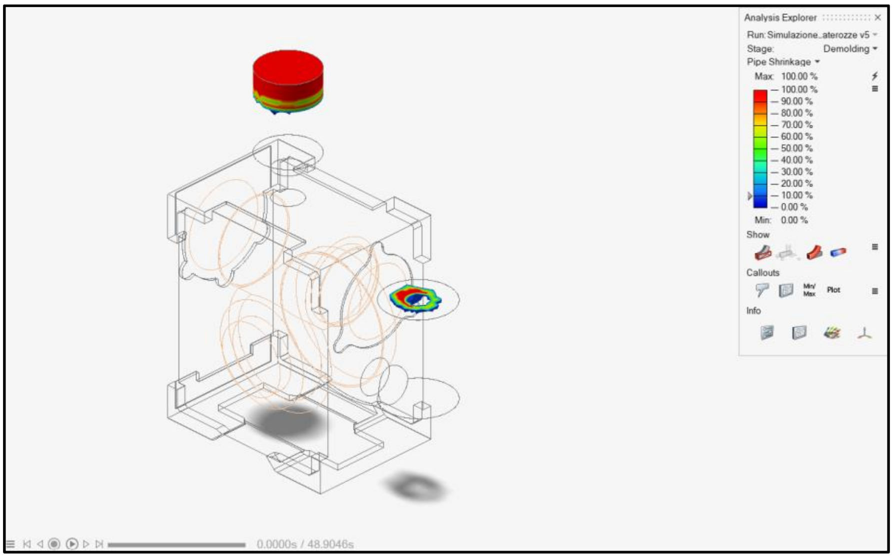

Figure 27 – Pipe shrinkage simulation (thermal method)

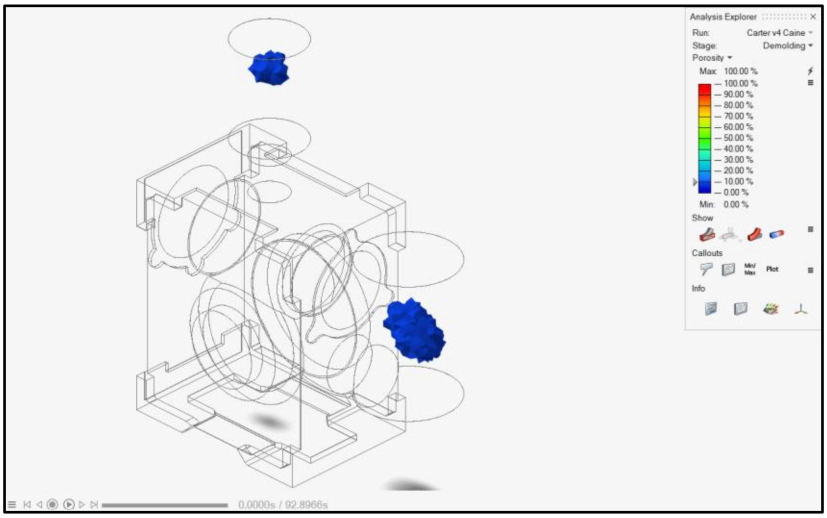

Figure 28 – Porosity simulation (Caine method)

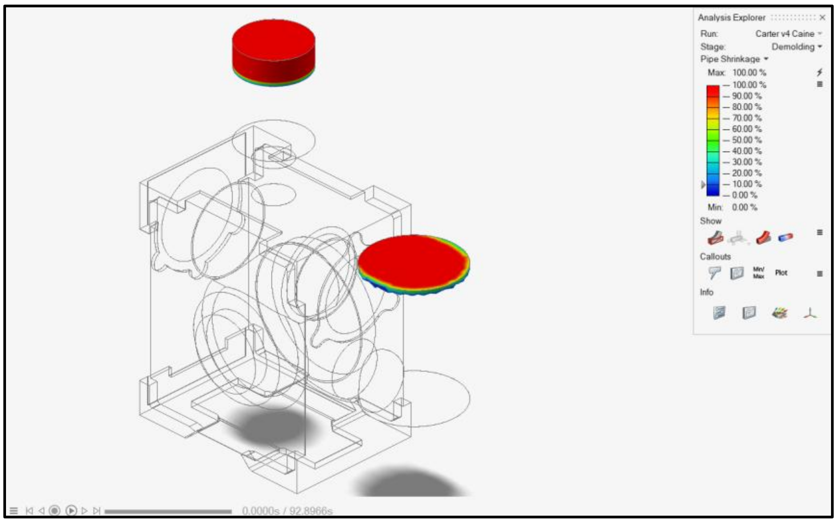

Figure 29 – Pipe shrinkage simulation (Caine method)

A compromise solution between the two approaches was adopted. The aim is to ensure that critical thermal areas are adequately supplied without resulting in excessive oversizing of the risers, which would lead to an unjustified waste of material and increased costs relating to labour and subsequent finishing operations.

2.11 Design of the casting system

Once the casting configuration has been defined, the feeding system is designed; its main components are the pouring basin, the pouring channel, the distributor channel and the pouring spout.

2.11.1 Geometric and weight data

The total volume of the casting (including the net part, risers, collars and flash) was calculated using the 'Altair Inspire Cast' software:

- Total volume (V): 581,716 mm^3 = 0.582 dm^3
- Alloy density (ρ): 2.68 kg/dm^3 (equivalent to 2.68×10^{-6} kg/mm^3)
- Total mass (G): $G = \rho \times V \approx 1.56$ kg

2.11.2 Casting parameters

- Static metal head (h): h is assumed to be 100 mm (measured between the free surface of the ladle and the pouring spout). This height keeps the ladle below the upper sprue, limiting the size of the mould shell whilst ensuring adequate hydrostatic pressure for small castings.
- Pouring time (T): Calculated using an empirical formula for light castings:

  $T = 3.2 \cdot \sqrt{G} = 3.2 \cdot \sqrt{1.23} \approx 3.55$ s

- Inlet velocity (v): Derived from Torricelli's theorem (neglecting pressure losses):

  $v = \sqrt{(2 \cdot g \cdot h)} = \sqrt{(2 \cdot 9810 \cdot 100)} = \sqrt{1{,}962{,}000} \approx 1{,}400.7$ mm/s

- Mass flow rate (K):

  $K = G / T = 1.18 / 3.55 \approx 0.33$ kg/s

- Cross-sectional area of the connection (S_a): Derived from the mass flow rate balance:

  $S_a = K / (v \cdot \rho) = 0.33 / (1400.7 \cdot 2.68 \cdot 10^{-6}) \approx 90.3$ mm^2

2.11.3 Channel sizing and positioning

According to the reference text, selecting a pressurised pouring ratio ensures that the channels remain constantly filled with molten metal along the entire feed path, thereby preventing air suction.

Applying a ratio of 1 : 0.5 : 0.5 to the theoretical cross-sections, we obtain:

- $S_{inlet} \approx 90$ mm^2

- $S_{distributor}$ ≈ 90 mm²
- $S_{casting}$ = 2 × $S_{connection}$ ≈ 180 mm²

Regarding their geometry and positioning:

- Gating: A rectangular cross-section of 15 × 6 mm (≈ 90 mm²) has been chosen. The length of the mould is the minimum required to allow the gate to reach the designated green shot area without coming dangerously close to the core channels.
- Gating channel: circular in cross-section with a diameter of 15 mm (area ≈ 176.7 mm², consistent with the required 180 mm²) and height h = 100 mm. The junction with the sprue is tangential.
- Casting basin: designed as a stepped tank with a rectangular base. Given the alloy's high susceptibility to oxidation, the molten metal strikes a blind area to dampen turbulence. The depth ensures immediate filling, guaranteeing that the system operates under constant pressure.
- Fittings: fitted throughout the system to eliminate sharp edges and avoid obstructing the flow of metal.
- Positioning: In accordance with the 'Santochi' guidelines, the channels are connected to the parting line of the ingot at a distance from the risers, in order to promote the generation of a continuous, uninterrupted thermal gradient.

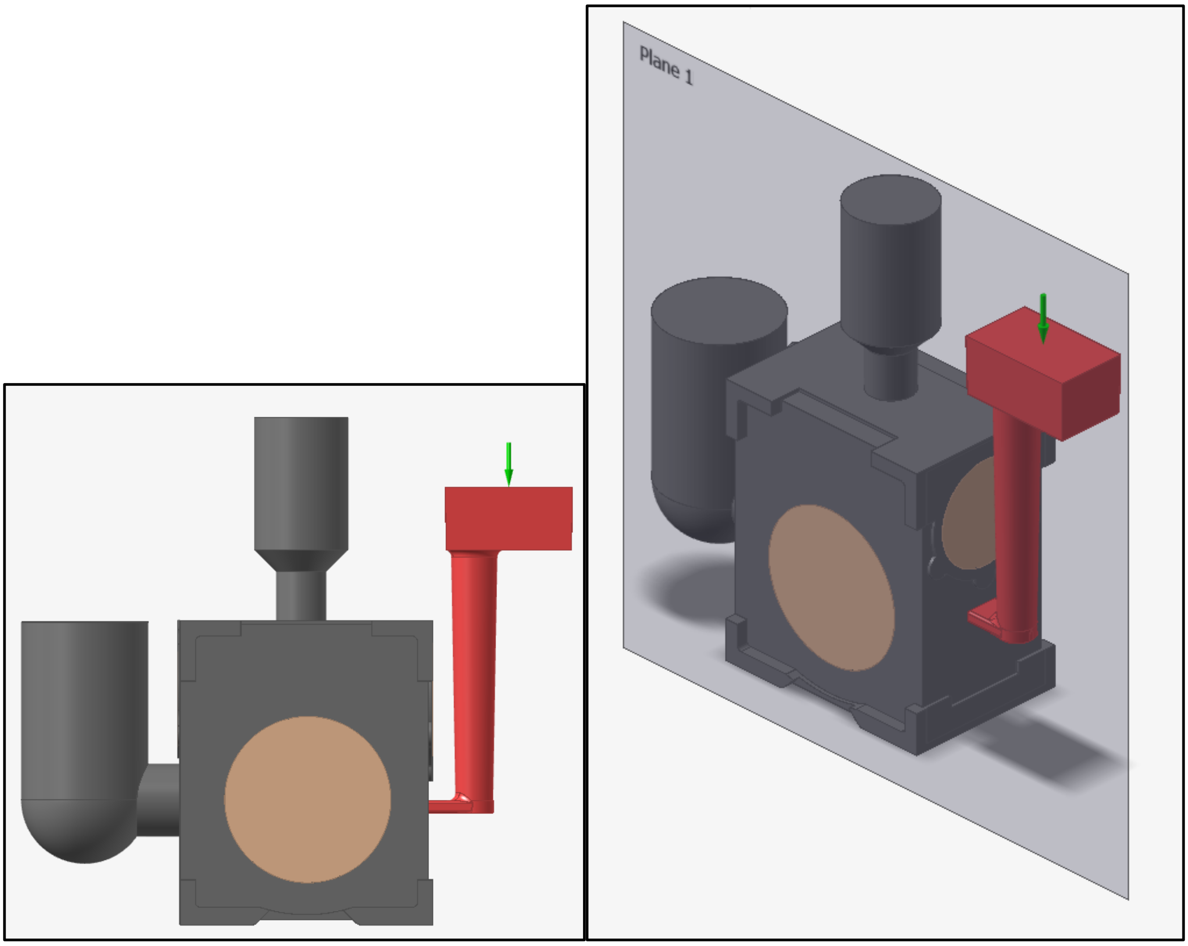

Figure 30 – Ingot with riser and casting system, set up for Inspire Cast simulation

2.12 Software-based analysis of the casting process

The dimensioned geometries were subjected to a simulation using the ‘Altair Inspire Cast’ software.

The operating parameters set for the analysis are as follows:

- Alloy (Cast): Aluminium EN AC-43000 with an initial temperature of 668.7 °C (961.8 K).
- Mould (Shell): Silica sand preheated to 150 °C (423 K).
- Core material: Silica sand at room temperature of 20 °C (293 K).

To ensure that certain software limitations in the processing of more complex geometries could be overcome, it was necessary to introduce some simplifications to the model. These measures should not affect the validity of the analysis. Specifically, the following geometric compromises were adopted:

- The sprue heads and their connecting collars were modelled as simple cylindrical geometries.
- The cores were inserted without modelling the core passages.
- The geometric distances between the sprue, the gates and the risers have been reduced.

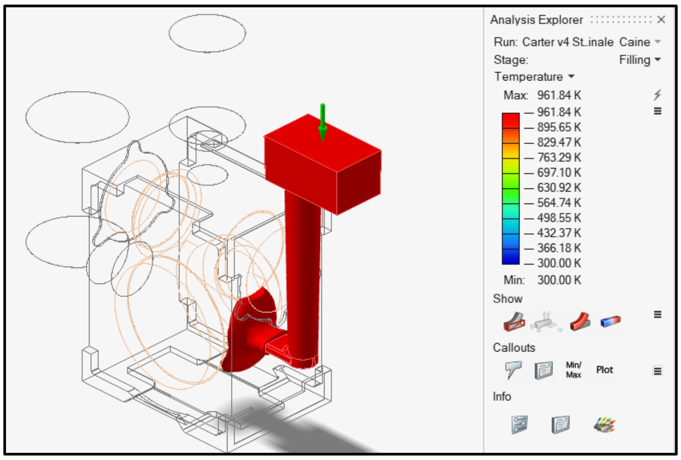

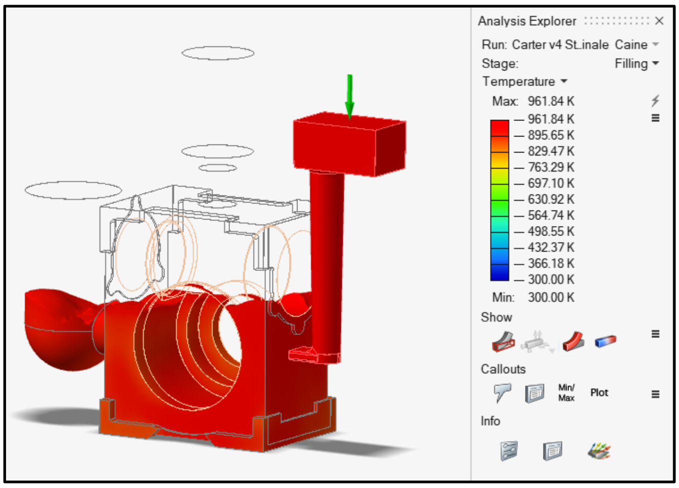

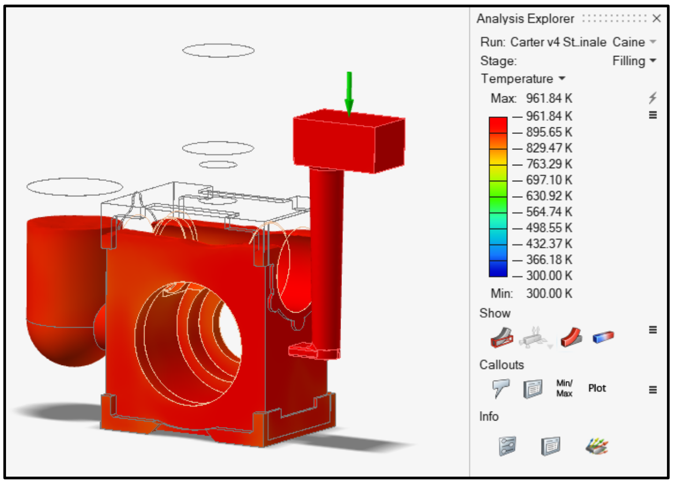

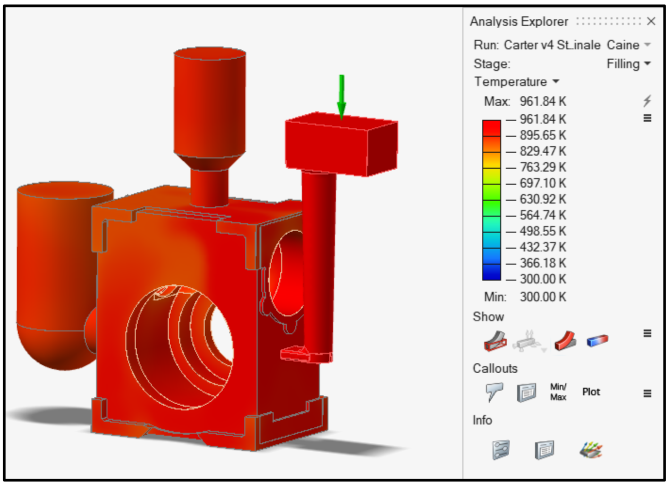

Figure 31 – Temperature during filling

The filling analysis shows a steady advance of the molten metal within the cavity.

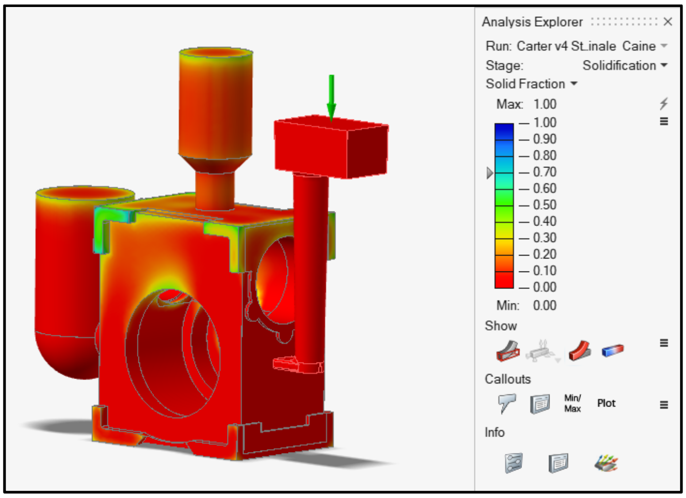

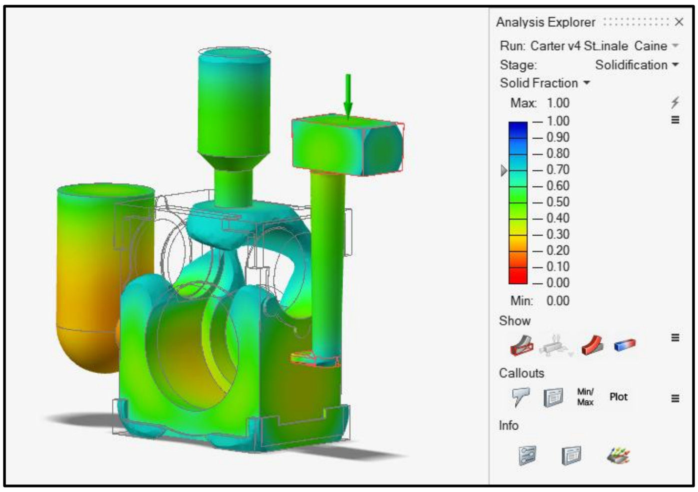

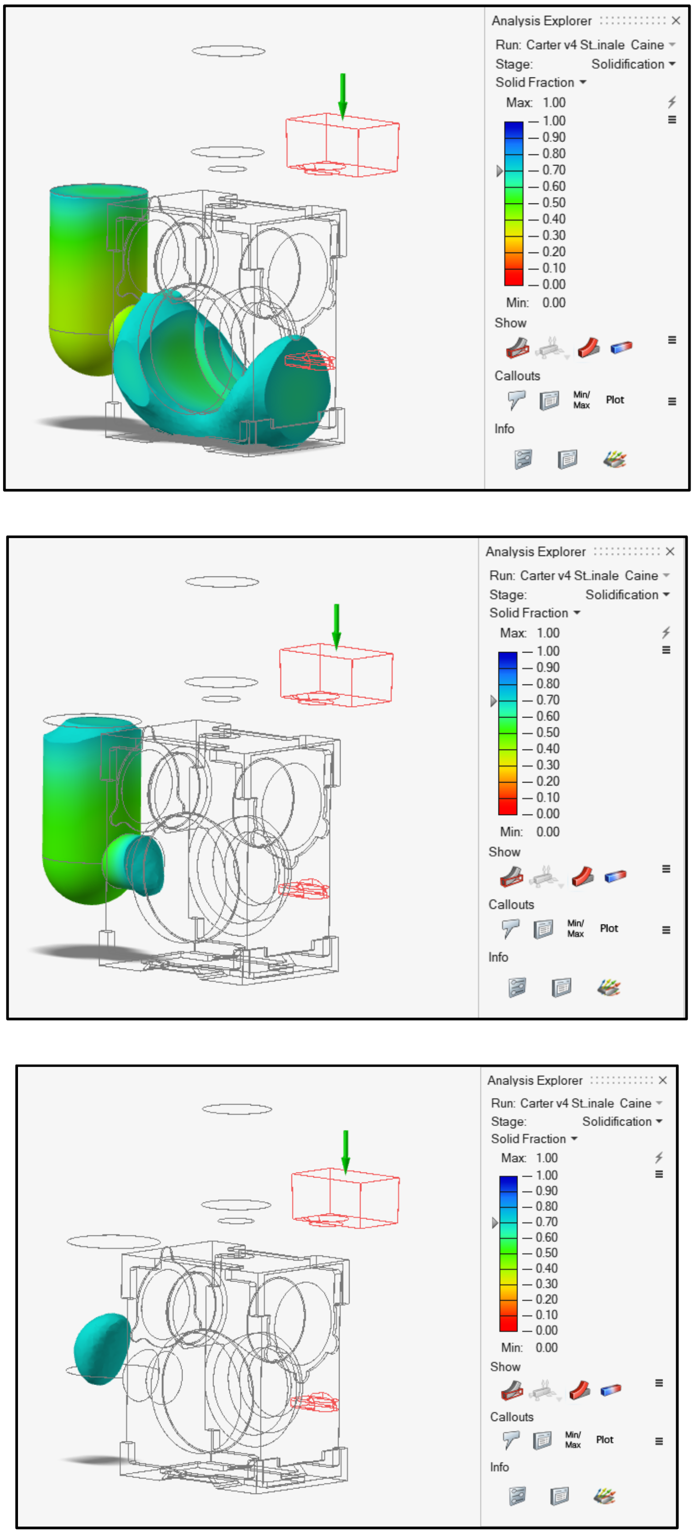

Figure 32 – Solid fraction during solidification

The evolution of the solid fraction shows that solidification begins at the surfaces in contact with the mould and progresses gradually towards the areas characterised by a higher thermal modulus.

It appears that the portions of molten metal cool progressively in those areas where the highest thermal modulus had previously been confirmed, and where the risers were therefore placed (first in the upper zone and then in the lateral zone, where, indeed, there is a higher cooling modulus).

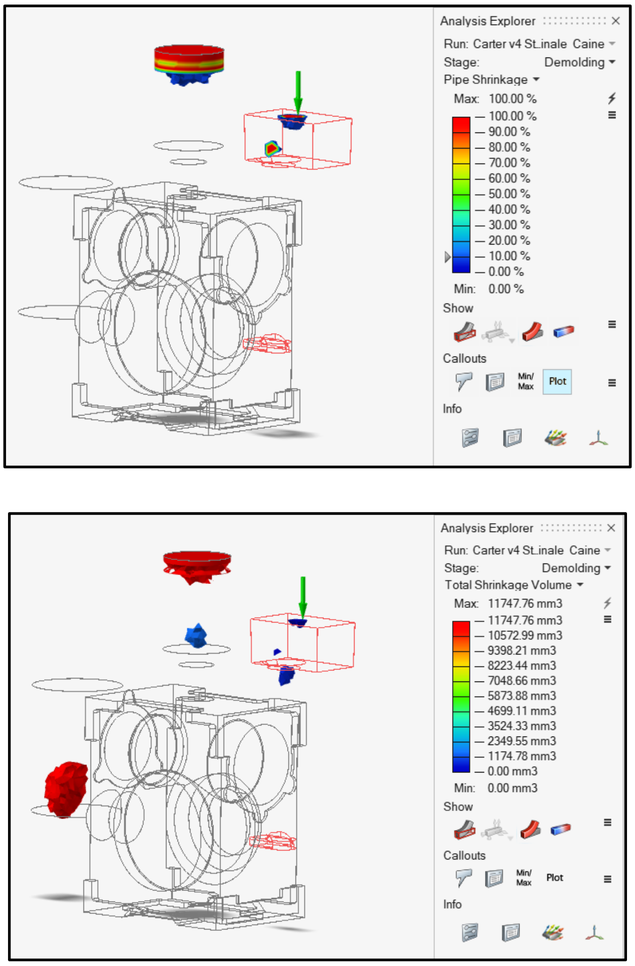

Figure 33 – Analysis of the total shrinkage volume

The analysis of the total shrinkage volume shows that shrinkage phenomena are concentrated exclusively within the sprue, whilst the casting is free from defects related to solidification.

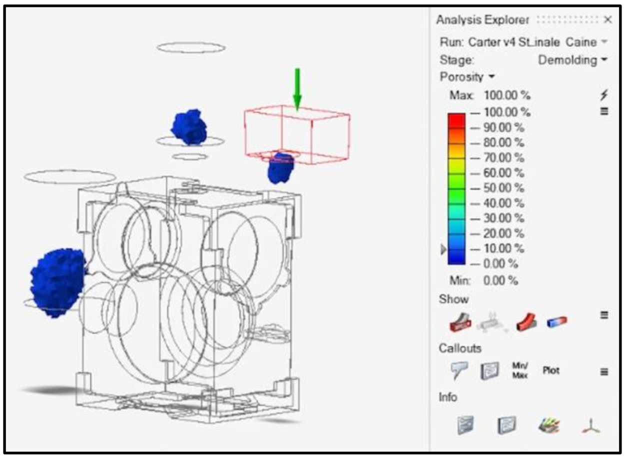

Figure 34 – Analysis of porosity

The predicted porosity is concentrated in the risers and sprue channels; none is found in the component.

2.13 Design of pattern plates

Having created the complete model, we can proceed with the selection of the brackets and pattern plates.

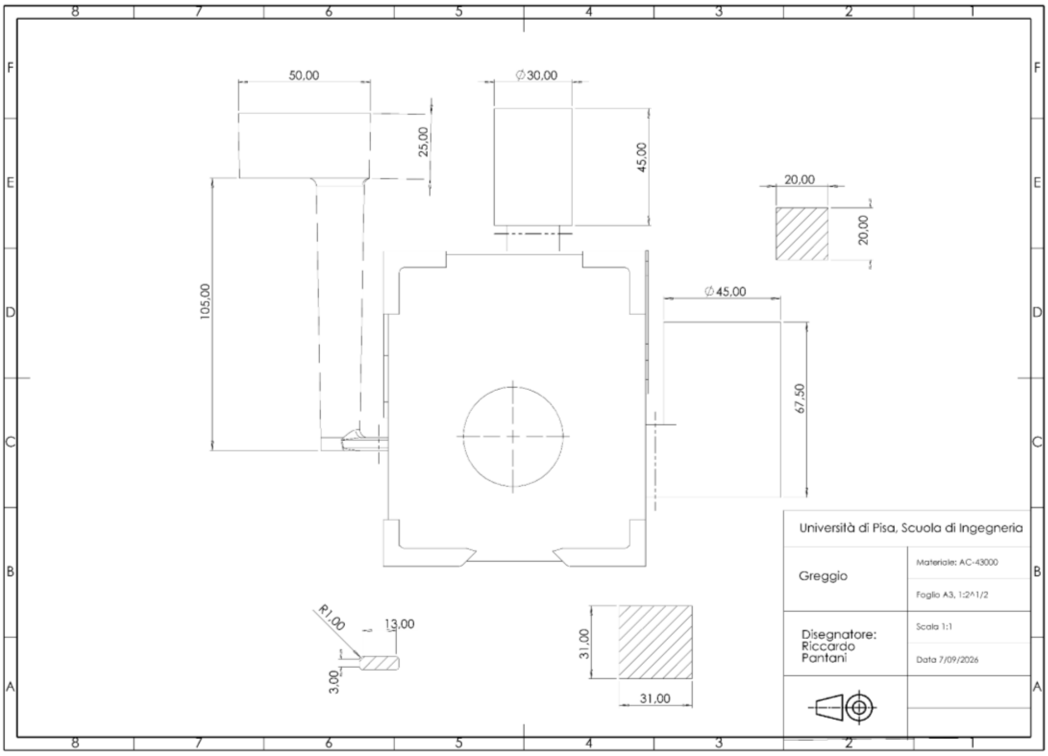

Figure 35 – Inspire Cast rough technical drawing

2.13.1 Pattern plates

As stated in the text, in the shell moulding process, sand that has been preheated and mixed with thermosetting resin is injected – via a special universal cover not dedicated to a single casting – onto the heated metal pattern plate, where it sets to form the shell.

As the pattern plate is subject to the same conditions as the core box, the same material, X40CrMoV5-1, is used for its manufacture.

As indicated in the literature, the plate also features special centring pins, which are necessary to ensure correct alignment between the two half-plates.

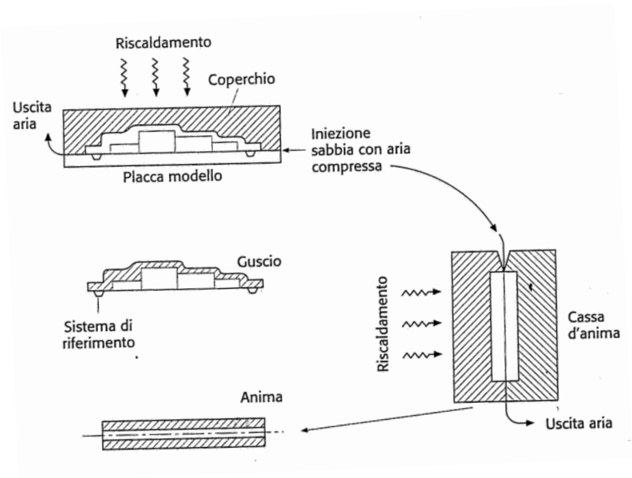

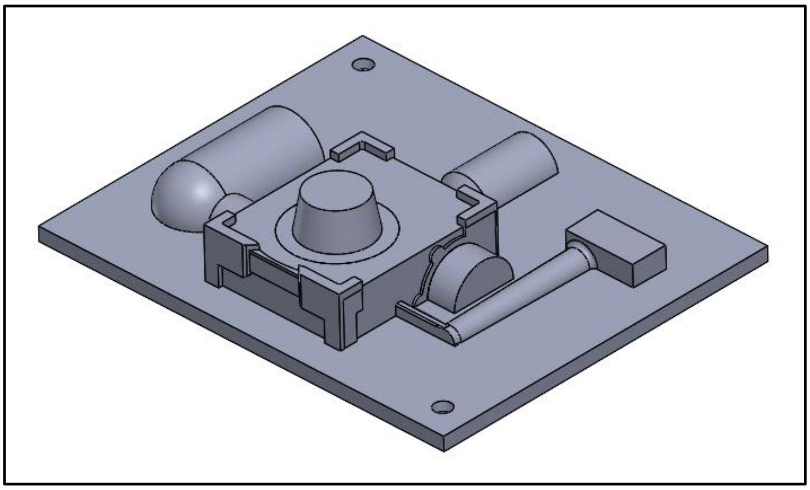

Figure 36 – Upper pattern plate

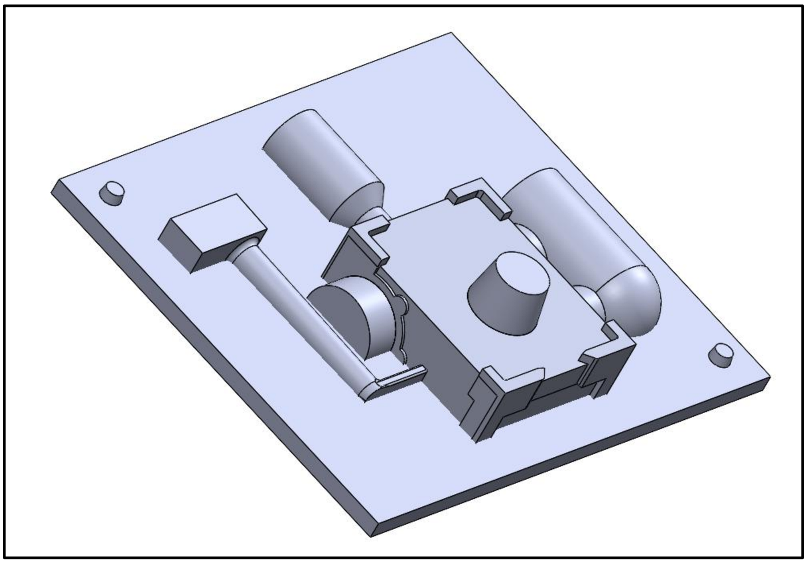

Figure 37 – Lower mould plate

2.14 Assessment of production times and costs

The assumptions underlying the economic and time-based assessment of the production process are set out below. Some data are derived from the analytical calculations and simulations described previously, whilst others are technical estimates (such as department cycle times and unit prices), adopted in the absence of specific guidelines.

2.14.1 Basic assumptions

Data	Value	Source / rationale
Net casting weight (crankcase)	1.23 kg	-
Weight of sprue A	0.254 kg	-
Weight of sprue B	0.075 kg	-
Weight of the casting system	≈ 0.080 kg	-
Total weight cast per cluster (G)	≈ 1.639 kg	sum of the above

Data	Value	Source / rationale
AC-43000 alloy price	3.0 €/kg	Indicative price of primary alloy for die-casting/gravity casting
Price of pre-coated silica sand	€1.0/kg	Indicative price of sand + phenolic resin for shell moulding
Operator's hourly rate	22 €/h	Approximate gross hourly cost of a foundry operator
Castings per furnace charge	25	Approximate sizing of departmental induction furnace

2.14.2 Casting times

The pouring time was calculated in section 2.12.
Substituting the net weight of the casting (G = 1.23 kg), the filling time is given by:

$$T = 3.2\sqrt{G} = 3.2\sqrt{1.23} \approx 3.55 \text{ s}$$

As regards non-operational times, these include all the set-up, preparation and handling activities typical of a foundry department.

Stage	Type	Time (s)
Oven loading (5 mins per load ÷ 25 items)	Not in operation	12.0
Alloy melting (45 mins/batch ÷ 25 pcs)		108.0
Shell moulding preparation		300.0

Stage	Type	Time (s)
Direct assembly without bracket		120.0
Pouring	Operational	3.55
Solidification		55.3 (estimate)
Extraction of casting from sacrificial mould	Not in operation	150.0
TOTAL cycle time per part		**≈ 748.85 s**

2.14.3 Economic assessment

The economic assessment comprises two main components: material costs and labour costs.

- **Material:** foundry processes typically involve the full recovery of ingots and casting systems through remelting; therefore, for the purposes of the economic calculation, the cost of the metal is attributed exclusively to the net weight of the casting (1.23 kg).
  Multiplying this value by the price of the alloy (€3.0/kg) gives a net cost of €3.69 per piece.
  To this amount must be added the cost of the pre-coated sand mould, which is a disposable component: estimating a consumption of approximately 2.1 kg of sand per cluster (including mould and cores) at a price of 1.0 €/kg, this adds 2.10 €.
  The total cost of materials therefore amounts to €5.79 per casing.

- **Labour** costs were assessed by distinguishing between active times – that is, the stages requiring the operator's presence and direct intervention – and passive times, during which the process proceeds autonomously.
  Adding up the various actions gives a total active time of 645.55 seconds, equivalent to approximately 0.1793 working hours.
  Applying the gross hourly rate of €22/h, the labour cost amounts to €3.94 per component.

- Adding the costs for materials (€5.79) and labour (€3.94), the **total cost** of producing a single unfinished casing amounts to **€9.73.**

Multiplying this figure by the required volume, the estimated cost for the entire batch of 500 units is **€4,865.**

Cost item	Quantity / Time	Rate / Unit price	Total Cost
Alloy (net casting weight)	1.23 kg	€3.0/kg	€3.69
Pre-coated sand (shell and cores)	2.1 kg	€1.0/kg	€2.10
		Total materials per piece	**€5.79**
Labour (active time)	0.1793 h (645.55 s)	€22/h	€3.94
		Total cost per housing	**€9.73**
		Estimated cost per batch (500 units)	**€4,865**

3 CHIP REMOVAL

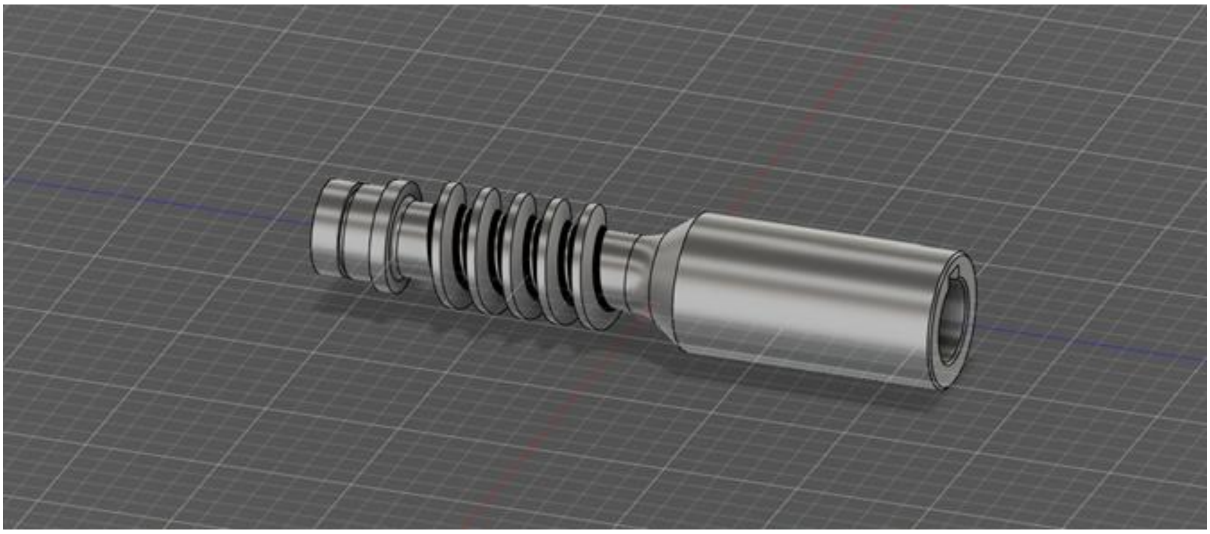

3.1 Component specifications and preliminary choices

3.1.1 Technical drawing

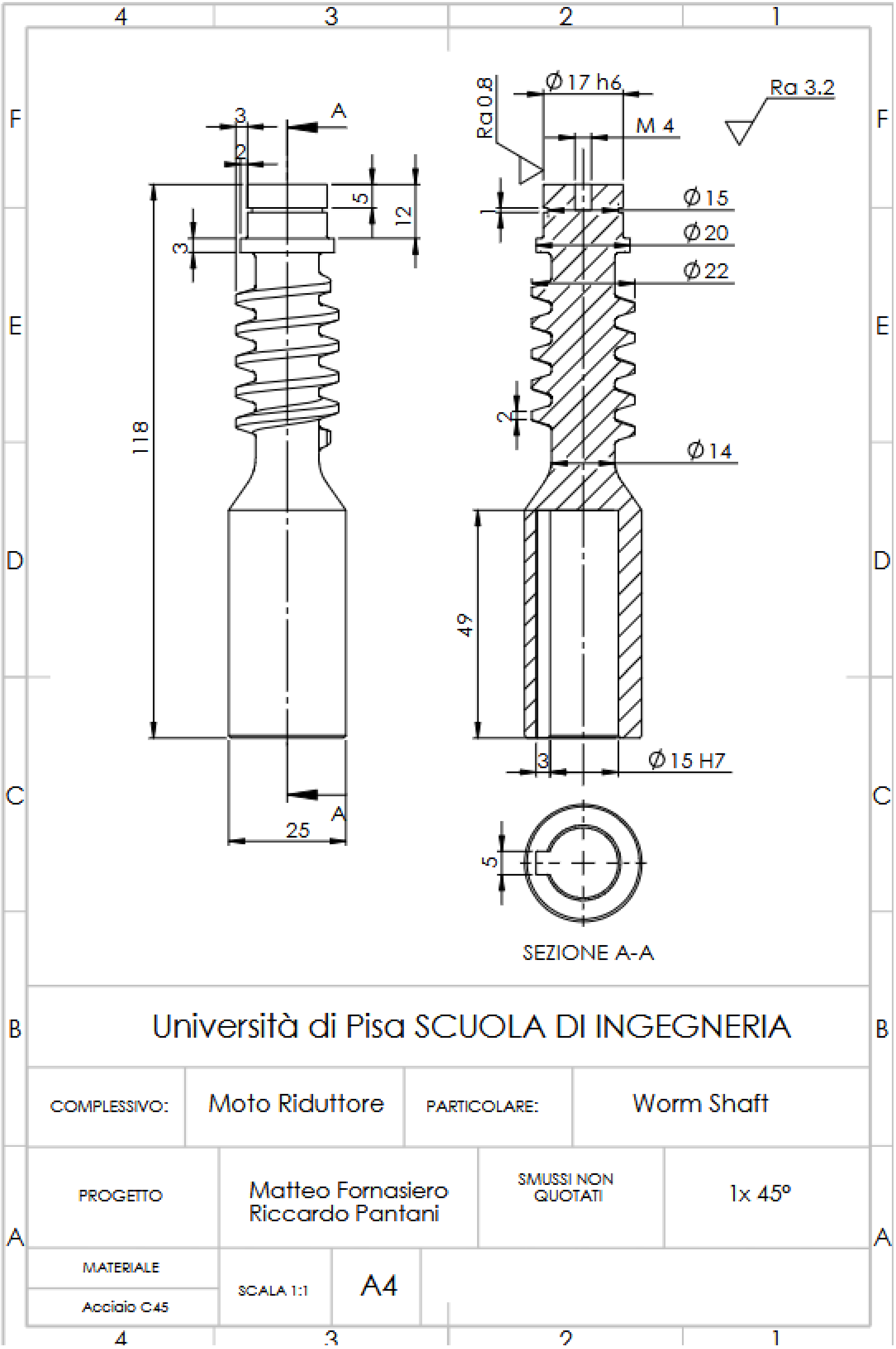

Figure 3.1 – Technical drawing of the worm shaft

The characteristic maximum overall dimensions of the finished part (worm shaft) are:

Total length: L = 118.0 mm.

Cylindrical base: Ø 25.0 mm, length 49.0 mm.

Lower bore: Ø 15 H7, depth 49.0 mm, with a 5 P9 keyway 3.0 mm deep.

Tapered transition: tapering from Ø 25.0 mm to Ø 14.0 mm, with a tapered lead-in section inclined at 30° to the axis (axial length ~9.5 mm).

Milling cutter relief groove: Ø 14.0 mm, width 2.0 mm.

Worm screw (helix): external diameter Ø 22.0 mm, base diameter Ø 14.0 mm.

Bearing shoulder: Ø 20.0 mm, width 3.0 mm.

Bearing seat: Ø 17 h6, length 12.0 mm, with Seeger groove (bottom Ø 15.0 mm, width 1.0 mm at 5.0 mm from the head).

Axial bore in the head: standard 60° centre (DIN 333 Form A) for mounting the rotating tailstock.

3.1.2 Choice of material and semi-finished product

C45 steel (UNI EN 10083-2) was selected for the manufacture of the shaft, as it offers a good balance between mechanical performance, machinability and cost for a production batch of 500 pieces.

During the preliminary phase, **42CrMo4** quenched and tempered steel was also considered; this is widely used for transmission components subjected to high mechanical stresses due to its high fatigue strength and greater toughness. However, such performance would be excessive given the operating conditions of the component under study and would entail increased costs relating to both the material and subsequent machining operations, as well as any heat treatments (estimate: +30–40 per cent). We also ruled out C40 steel, which performs less well than C45 despite a negligible difference in price.
Furthermore, C45 ensures a significantly better response to induction hardening, which is essential for surface hardening the screw flanks and the bearing seat.

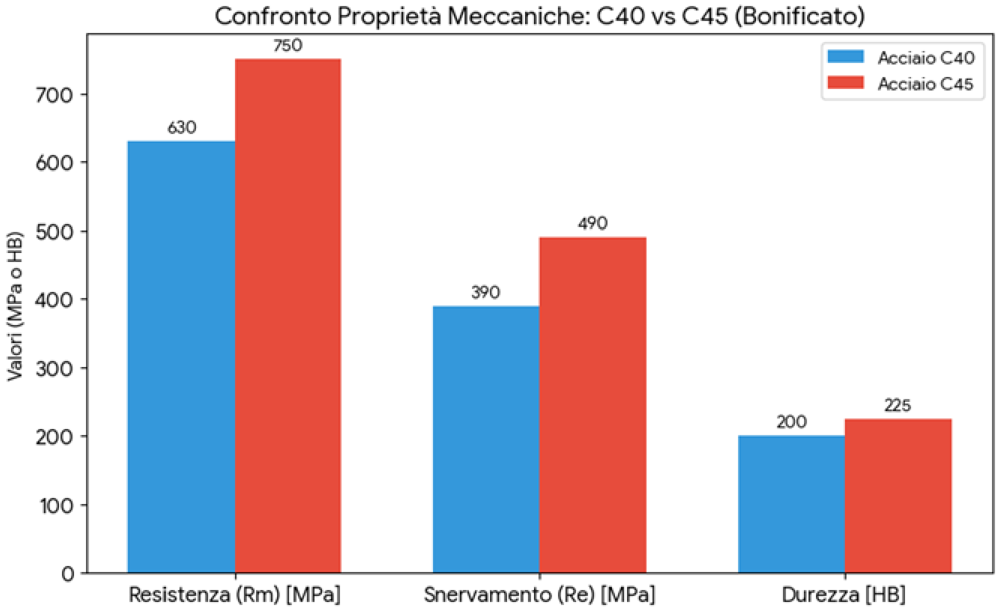

In its normalised as-supplied condition, C45 has:

Tensile strength: Rm = 630–800 MPa (value adopted: Rm = 750 MPa)

Yield strength: Re ≥ 380 MPa

Elongation at break: A% ≥ 14%

Hardness: 190–230 HB (excellent machinability with minimal tool wear)

A solid rolled bar with a diameter of 30 mm and a length of 122 mm was selected as the semi-finished stock. These dimensions provide the necessary stock allowance for facing, parting-off and rough turning operations, enabling the final dimensions of the component to be achieved with precision without unnecessary material waste.

- **Radial stock:** 2.5 mm on the base (Ø 25.0 mm), sufficient to remove the rough surface scale and rolling defects, and 4.0 mm on the screw crest (Ø 22.0 mm) to ensure stable roughing passes.
- **Axial stock allowance:** 4.0 mm in total (122.0 mm rough, 118.0 mm finished), equivalent to 2.0 mm on each of the two faces, which can be easily removed in two facing passes of 1.0 mm each to eliminate cutting imperfections.

3.1.3 Analysis of tolerances and surface finishes

Tolerances and surface roughness values have been assigned by making a clear distinction between functional mating surfaces and free surfaces, in order to keep costs down and avoid unnecessary machining:

Bearing seat (Ø 17 h6, Ra ≤ 0.8 µm): This is the most critical area for the shaft's rotational precision. The h6 class ensures the correct fitting of the inner bearing ring with calibrated clearance. The fine surface roughness of Ra ≤ 0.8 µm is achieved exclusively by external cylindrical grinding (Stage 70) following induction hardening, thereby correcting thermal distortions.

Internal coupling bore (Ø 15 H7, Ra ≤ 1.6 µm): This ensures precise engagement of the drive shaft with coaxial centring and no radial play. It is produced by machine boring with a high-precision reamer.

Internal keyway (5 P9): The tight P9 tolerance provides a light interference fit, essential for transmitting drive torque without torsional play.

Worm gear flanks (Ra ≤ 1.6 µm): As they operate in continuous sliding contact with the bronze wheel, they require low friction to minimise wear and maximise efficiency. The finish is achieved directly by a fine milling pass prior to hardening, followed by post-treatment polishing/lapping.

Non-functional surfaces (ISO 2768-mK, Ra ≤ 3.2 µm): All remaining dimensions (base outer diameter Ø 25 mm, helix crest Ø 22 mm, shoulder Ø 20 mm, cone and grooves) are subject to general tolerances and a standard finish achieved by ordinary turning, thereby reducing cycle times.

3.2 Choice of processes

3.2.1 Identification of surfaces to be machined

Starting with the semi-finished workpiece (cylindrical rolled bar in C45, Ø 30.0 mm, L = 122.0 mm), the surfaces requiring material removal to achieve the final design geometry were identified and numbered.

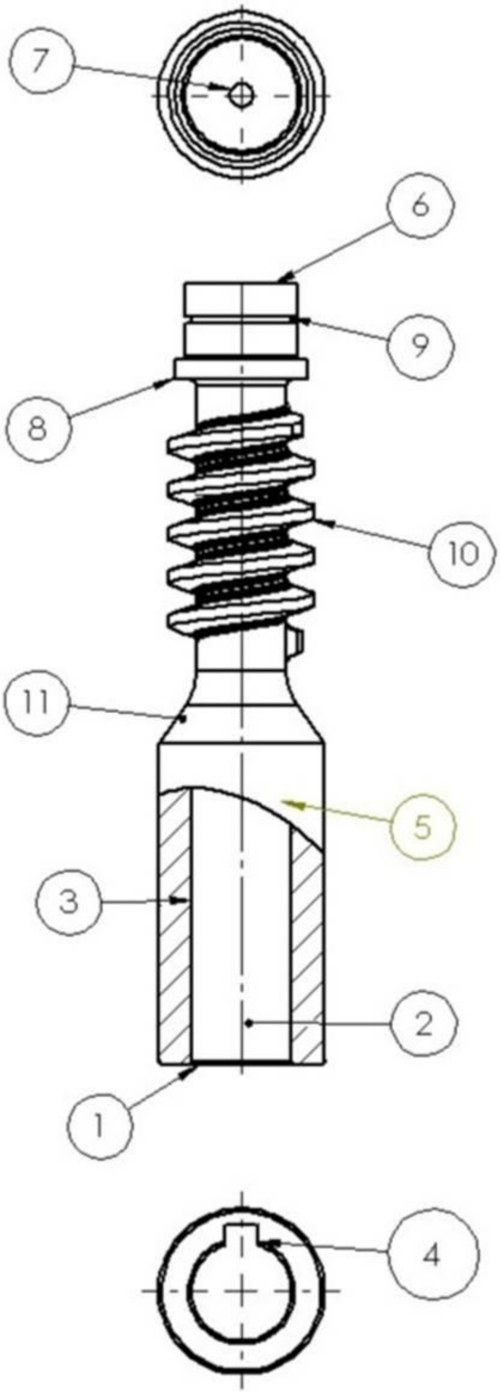

Figure 3.2 – Marking of the surfaces to be machined

The functional analysis shows that the bearing seat (Surface 8b) requires a tight tolerance (h6) and a fine surface roughness (Ra ≤ 1.6 μm), which can only be achieved by post-hardening cylindrical grinding. The lower bore (Surface 3) requires an H7 tolerance for mating with the drive shaft, which can be achieved by boring.

No. Surface	Surface Type	Selected Processes
1	Flat surface perpendicular to the axis (lower face)	Turning (1st face turning)
2	Lower axial pilot hole (Ø 14.5 mm, depth 49 mm)	Deep drilling
3	Internal cylindrical mating bore (Ø 15 H7, depth 49 mm)	Machined bore
4	Internal keyway (5 P9, depth 3 mm, length 30 mm)	Vertical slotting
5	Basic external cylindrical turning (Ø 25 mm, length 49 mm)	Turning (Roughing + Finishing)
6	Flat surface perpendicular to the axis (top face, L = 118 mm)	Turning (Facing, 2nd position)
7	Upper axial centre for tailstock	Centring (DIN 333 centre point)
8a	Axial shoulder machining of bearing ring (Ø 20.0 mm, width 3.0 mm)	Turning (Shoulder face milling, 2nd position)
8b	External cylindrical turning of bearing seat (Ø 17 h6, length 12.0 mm)	Turning + Hardening + Cylindrical grinding
9	Seat for snap ring (Seeger groove, bottom Ø 15 mm, width 1.1 mm)	Turning (groove machining)
10	Helical worm gear profile (ridge Ø 22 mm, root Ø 14 mm)	Milling on a dividing machine + Hardening + Polishing
11	30° truncated cone transition (from Ø 25 mm to Ø 14 mm)	Turning (conical profiling)
12	Milling/grinding relief groove (Ø 14 mm x 2 mm)	Turning (groove machining)

13	External lead chamfer 1 x 45° (on end of Ø 25 mm sleeve)	Turning (Chamfering, 1st position)

Table 3.1 – Selected surfaces and machining processes

3.2.2 Priority and grouping criteria

The operational sequence has been defined to minimise repositioning (ensuring coaxiality) and to comply with the technological constraints:

Rigidity: Drilling (Surface 2) and internal reaming to Ø 15 H7 (Surface 3) precede the external turning of the shaft. Machining at the maximum diameter (Ø 30 mm) eliminates deflection and vibration.

Clamping references: In the first set-up, the Ø 25.0 mm cylindrical base (Fig. 5) is completed, which serves as a secure gripping surface for the spindle jaws in the second set-up.

Slotting operation (Stage 50): The groove for the internal tongue is machined on the intact sleeve once the turning and milling operations are complete, prior to induction hardening.

Tailstock support for the overhang: As the workpiece protrudes approximately 69 mm beyond the chuck jaws in the second setup, the standard 60° centre is immediately set (Surface 7) and the MK3 swivel tailstock is fitted to eliminate deflection during roughing.

Thermal sequence: The cylindrical grinding of the bearing seat (Stage 70) must follow the induction hardening to correct the thermal distortions suffered by the C45 steel.

3.2.3 Choice of machinery

Based on a production batch of 500 parts and to keep the initial investment to a minimum, machine tools from a mechanical workshop with a short estimated service life were selected.

Machine	Femi 784 XL band saw
Cutting capacity	Ø 120 mm
Blade dimensions	1440 × 13 × 0.65 mm
Motor power	1.20 kW
Cutting speed	30 to 80 m/min
Estimated efficiency (η)	0.75
Purchase price	€700.00
	

Machine	PARALLEL LATHE – HBM 330 × 600, complete
Centre distance	600 mm
Centre height	160 mm (max. turnable diameter: 320 mm)
Bar passage (spindle bore)	Ø 38 mm
Spindle speed	60 to 1650 rpm (12 speeds)
Longitudinal feed range	0.05 to 0.35 mm/rev
Main motor power	1.10 kW
Estimated efficiency (η)	0.70
Set-up	160 mm 3-jaw self-centring chuck, MK3 swivel tailstock
Purchase price	€2,700.00

Machine	UNIVERSAL CONSOLE MILLING MACHINE – Grazioli Ludor (Second-hand)
Cross table dimensions	1400 x 325 mm
X / Y / Z axis travel	880 / 280 / 430 mm
Spindle connection	ISO 50
Max. end mill capacity	Ø 25 mm
Spindle speed	25 – 1350 rpm (electronically controlled)
Motor power	4.10 kW
Estimated efficiency (η)	0.70

Equipment	Universal Mechanical Divider, Divider Tailstock
Purchase price	€4,000.00

Machine	VERTICAL SLOTTING MACHINE – CAMS 150 (Second-hand)
Max. slide (tool) stroke	150 mm
Stroke adjustment	35 to 90 strokes/min
Rotary table diameter	250 mm
Motor power	1.50 kW

Estimated efficiency (η)	0.70
Purchase price	€3,500.00

Machine	CYLINDER GRINDING MACHINE – Ribon RUR 500 (Second-hand)
Centre distance	500 mm
Centre height	130 mm (Max. grindable diameter: 200 mm)
Standard grinding wheel dimensions	Ø 300 × 30 × 127 mm
Grinding wheel speed	1750 rpm

Grinding wheel motor power	1.80 kW
Estimated efficiency (η)	0.70
Purchase price	€3,800.00

Table 3.2 – Characteristics of machine tools

3.2.4 Tooling

Equipment:

Grazioli Ludor Universal Milling Machine: fitted with a Universal Mechanical Divider with tailstock mounted on a 1,400 x 325 mm swivel table (inclined at a helix angle $\gamma = 5° 24'$). The dividing head is kinematically connected to the table lead screw via a set of gear wheels (idler gear, ratio i_lira = 36.65) to synchronise the longitudinal feed and rotation of the workpiece, generating a helix with an axial pitch px = 5.498 mm. The horizontal spindle features an ISO 50 mount for the cutter shaft.

HBM 330×600 Parallel Lathe: it is fitted with a Ø 160 mm 3-jaw self-centring chuck, an adjustable tool turret with a holder for tool shanks with a 16 x 16 mm shank, and a rotating tailstock on a Morse MK3 taper for support during overhang turning.

OPERATION	TOOL	INSERT (SPECIFICATION)	CATALOGUE
Facing / Roughing	CoroTurn 107 shank 16x16 mm (SCLCR 1616H 09)	CCMT 09 T3 08-PM 4325 (positive, 2 cutting edges)	Sandvik Coromant
Shank and cone finishing	CoroTurn 107 shank 16x16 mm (SDJCR 1616H 11)	DCMT 11 T3 04-PF 4415 (55°, 2 cutting edges)	Sandvik Coromant
Axial centring	DIN 333 centre drill, Form A, Ø 3.15 mm	Solid HSS	Hoffmann Group
Pilot hole Ø 14.5 mm	CoroDrill 860 drill bit Ø 14.5 mm	Solid carbide (HM)	Sandvik Coromant
Hole reaming Ø 15 H7	CoroReamer 835 machine reamer, Ø 15.00 H7	Solid carbide (HM)	Sandvik Coromant
Seeger groove and relief Ø 14	CoroCut blade, 1–2 flutes, shank 16 × 16 mm (RF123E08-1616B)	N123E2 insert (width 1.0 mm)	Sandvik Coromant
Worm gear milling	Modular shaped disc milling cutter for screws (m=1.75)	Solid HSS-Co body (Df=25 mm, z=10 teeth)	LMT Cutters
5 mm tongue slot slotting	Shank bar for slotting machine (REV UT-05-25)	REV IN-5-P9 sintered insert (width 5.0 mm)	REV Broaching Tools
Bearing seat grinding	Cylindrical grinding wheel Ø 300 x 30 x 127 mm	Specification: Tyrolit 89A 60 K 5 V 217	Tyrolit

Table 3.3 – Tools and inserts used

TOOL	RENDER	DETAIL

CoroTurn 107, shank 16x16 mm (SCLCR 1616H 09)	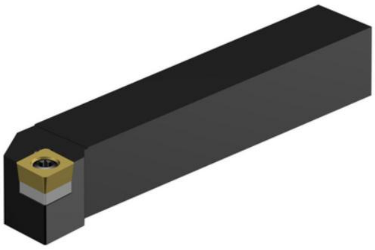	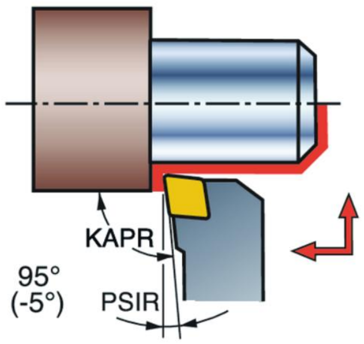
CoroTurn 107 shank 16x16 mm (SDJCR 1616H 11)		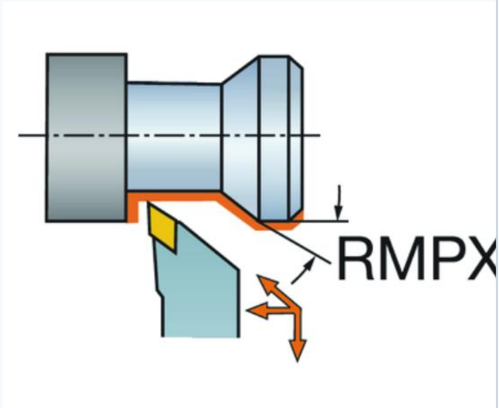
DIN 333 centre drill, Form A, Ø 3.15 mm		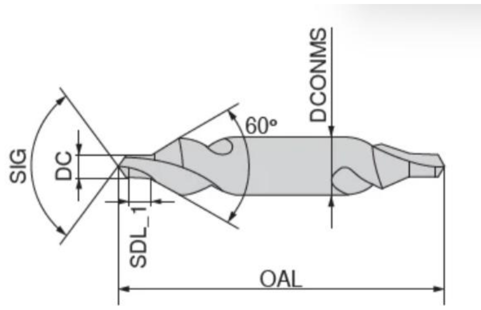
CoroDrill 860 drill, Ø 14.5 mm		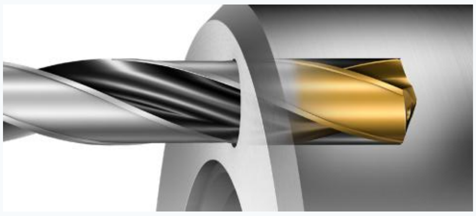
CoroReamer 835 machine reamer Ø 15.00 H7		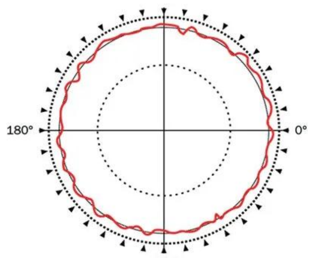

CoroCut 1-2 insert, shank 16x16 mm (RF123E08-1616B)	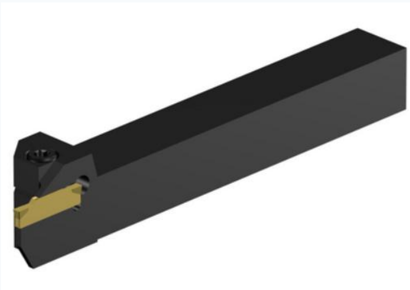	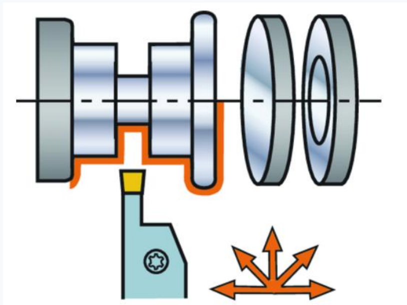
Modular shaped disc cutter for screws (m=1.75)		
Shank bar for slotting machine (REV UT-05-25)		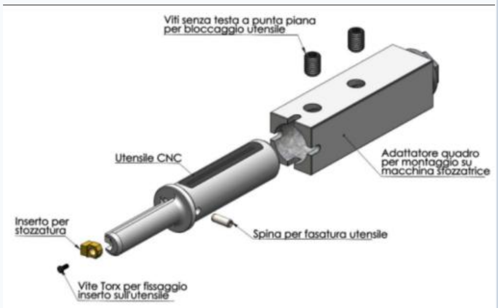
Cylindrical grinding wheel, Ø 300 x 30 x 127 mm		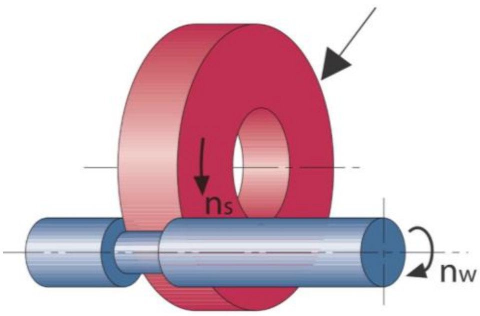

3.2.5 Definition of the logical cycle (machining stages)

The machining sequence, divided into stages and set-ups, follows a logical sequence designed to maximise clamping rigidity, minimise repositioning and group machining operations by machine type:

STAGE 10: Cutting (Femi 784 XL band saw)

Cutting the raw rolled bar Ø 30.0 mm to length into sections of length L = 122.0 mm

STAGE 20: Turning, 1st Set-up – Base Side (HBM 330 parallel lathe)

Clamping of the raw bar with reduced overhang; facing of the lower face (Surface 1), drilling of the blind pilot hole Ø 14.5 mm (Surface 2), precision boring to Ø 15 H7 (Item 3), roughing and finishing of the base sleeve to Ø 25.0 mm (Item 5) with machining of the 1 x 45° front lead-in chamfer (Item 13).

STAGE 30: Turning, 2nd Set-up: Screw Side, Bearing (HBM 330 parallel lathe)

Clamping of the finished sleeve Ø 25.0 mm with soft jaws and support on a tailstock rotated to 60° (Fig. 7); end facing to finished nominal length L = 118.0 mm (Fig. 6), step-by-step roughing of the shank (screw Ø 22.4 mm, shoulder and bearing seat Ø 17.4 mm), finishing of the profile and the 30° taper (Fig. 11), machining of the Ø 14.0 x 2.0 mm grinding relief groove (Fig. 12) and the groove for the Seeger spring ring (Fig. 9).

STAGE 40: Milling of the worm screw (Grazioli Ludor Universal Milling Machine)

Mounting between the centres of the mechanical divider with an inclined table at a helix angle γ = 5° 24’ and synchronised with the table screw via a pulley block (ratio i = 36.65); generation of the modular helical profile m = 1.75 mm (crest Ø 22.0 mm, groove bottom Ø 14.0 mm) using a shaped disc cutter in 5 progressive passes (Fig. 10).

STAGE 50: Slotting for the Tongue (CAMS 150 Vertical Slotting Machine)

Vertical clamping in a precision vice on the Ø 25.0 mm sleeve and machining of the standard internal slot 5 P9 x 3.0 mm with a working length of 30.0 mm (Fig. 4), utilising the end of the blind pilot hole as a free clearance zone for the stroke of the REV slotting insert.

STAGE 60: Heat Treatment (HF Induction System – External Supplier)

Selective high-frequency induction surface hardening on the flanks of the worm screw and the bearing seat (hardness achieved: 52–56 HRC, effective depth 1.0–1.5 mm), followed by stress-relief tempering at 180 °C to eliminate internal hardening stresses.

STAGE 70: Cylindrical Grinding (Ribon RUR 500 Cylindrical Grinding Machine)

Clamping between centres using a centre-point and a calibrated mandrel; cylindrical grinding of the bearing seat using a white corundum grinding wheel to a precision tolerance of Ø 17 h6 with a surface roughness of $Ra \leq 0.8$ μm (Surface 8b), followed by polishing/lapping of the flanks of the hardened helix using a felt disc to reduce meshing friction.

3.3 Turning engineering

The determination of cutting forces and power consumption for machining on the HBM 330 lathe strictly follows Kronenberg's classical model:

Specific unit cutting pressure: $Ps = 2.4 \cdot Rm^{0.454} \cdot \beta^{0.666}$ [N/mm²]

Cross-sectional area of the undeformed chip: $S = ap \cdot f$ [mm²]

Effective specific pressure: $Pt = Ps \cdot S^{(-1/n)} = Ps \cdot S^{(-0.197)}$ [N/mm²]

Principal cutting force: $Ft = Pt \cdot S$ [N]

Cutting power: $Pc = (Ft \cdot Vc) / (60 \cdot 1000)$ [kW]

Power absorbed by the machine: $Pm = Pc / \eta$ [kW] (where $\eta = 0.70$)

Theoretical turning surface roughness: $Rt = (f^2 / (8 \cdot r\varepsilon)) \cdot 1000$ [μm] → $Ra \approx Rt / 4$

For normalised C45 steel (Rm = 750 MPa) and a CCMT rhombic insert (β = 80°):
$Ps = 2.4 \cdot (750)^{0.454} \cdot (80)^{0.666} = 898$ N/mm²

Technological Advantage of the CCMT Positive Insert over the CNMG Negative Insert

The use of a traditional negative CNMG insert (lower rake angle 0° and upper negative rake angle $\gamma o \approx -6°$) would cause severe chip re-cutting with a very high specific pressure Pt, pushing the power consumption Pm to over 1.05 kW, i.e. close to the maximum limit of the 1.10 kW motor on the HBM 330 lathe (residual margin < 5%).

The use of the positive rhombic insert CCMT 09 T3 08 on the SCLCR 1616H 09 tool holder facilitates chip flow, reducing cutting force and power consumption. This ensures a safety margin for the lathe's motor, preventing the risk of jamming or vibrations.

Operation	ap [mm]	f [mm/g]	S [mm²]	Vc [m/min]	n [rpm]	Pt [N/mm²]	Ft [N]	Pc [kW]	Pm [kW]	Ra [µm]
First-stage facing (Surface 1)	1.00	0.15	0.150	113.1	1200	1305	196	0.369	0.527	0.88
Roughing of base Ø25.4 (Surface 5)	1.15	0.15	0.173	104.4	1200	1268	219	0.381	0.544	0.88
Base finish Ø25.0 (Surface 5)	0.20	0.10	0.020	130.6	1650	1937	39	0.084	0.120	0.78
Pilot hole Ø14.5 (Surface 2)	7.25	0.08	0.580	20.5	450	1,000	580	0.198	0.283	—
Bore Ø15 H7 (Surface 3)	0.25	0.12	0.030	11.6	250	1,780	53	0.010	0.015	0.80
Second-stage facing (Surface 6)	1.00	0.15	0.150	113.1	1200	1305	196	0.369	0.527	0.88
DIN 333 centring (Surface 7)	1.57	0.05	0.079	11.9	1200	1,400	110	0.022	0.031	—
Roughing of screw crest (Surface 10)	1.25	0.15	0.188	98.8	1200	1247	234	0.385	0.550	0.88
Rough machining of bearing seat (Fig. 8b)	1.25	0.15	0.188	75.0	1200	1247	234	0.293	0.418	0.88
Barrel and cone finish (Sup. 11)	0.20	0.10	0.020	103.7	1650	1937	39	0.067	0.096	0.78
Seat finish, Ø17.2 (Surface 8b)	0.10	0.10	0.010	89.7	1650	2221	22	0.033	0.047	0.78

Exhaust port Ø14x2 (Sup. 12)	1.50	0.05	0.100	39.2	800	1412	141	0.092	0.131	—
Seeger groove Ø15x1.1 (Sup. 9)	1.00	0.04	0.044	40.5	800	1662	73	0.049	0.070	—

Table 3.4 – Turning cutting parameters (Kronenberg)

3.3.1 STAGE 20: turning, 1st set-up

The starting blank (Ø 30.0 mm rolled bar) is clamped in the 3-jaw self-centring chuck with an overhang limited to approximately 55 mm to ensure maximum flexural rigidity during the internal and external machining of the base sleeve.

A) Facing of the lower face (Surface 1) — Pilot Calculation Example

Facing of the rough end to remove 2.0 mm of axial stock and eliminate the saw cutting error, carried out in 2 passes at ap = 1.0 mm using a Sandvik CoroTurn 107 tool holder (SCLCR 1616H 09) and a positive rhombic insert CCMT 09 T3 08-PM 4325 (rε = 0.8 mm):

Cutting parameters: n = 1200 rpm, f = 0.15 mm/rev, Vc = 113.1 m/min, Vf = 180 mm/min.

Kronenberg pilot calculation: S = ap · f = 0.150 mm² → Pt = 898 · (0.150)^(-0.197) = 1305 N/mm².

Forces and power: Ft = 1305 · 0.150 = 196 N, Pc = 0.369 kW, Pm = 0.527 kW < 1.10 kW (available power margin: 52%).

Active time: Ta = 2 · [(15 + 2) / 180] = 0.19 min.

B) Roughing of the outer diameter of the sleeve Ø 25.4 mm (Surface 5)

Reduction of the outer diameter from Ø 30.0 mm to Ø 25.4 mm (L = 49.0 mm, finishing stock +0.20 mm radial) in 2 passes of ap = 1.15 mm using the same CCMT tool holder (n = 1200 rpm, f = 0.15 mm/rev, Vc = 104.4 m/min).

Kronenberg calculation: S = 0.173 mm² → Pt = 1268 N/mm², Ft = 219 N, Pm = 0.544 kW < 1.10 kW (margin: 51%).

Active time: Ta = 2 · [(49 + 2) / 180] = 0.57 min.

C) Finishing of external diameter Ø 25.0 mm and lead-in chamfer (Sup. 5 and Sup. 13)

Calibrated finishing pass from ap = 0.20 mm at increased speed (n = 1650 rpm, f = 0.10 mm/rev, Vc = 130.6 m/min) using a Sandvik SDJCR 1616H 11 tool holder and a 55° DCMT 11 T3 04-PF insert (rε = 0.4 mm, κr = 93°):

Verification of theoretical kinematic roughness: $Ra \approx f^2 / (32 \cdot r\varepsilon) = 0.10^2 / (32 \cdot 0.4) = 0.78$ μm (fully compliant with Ra ≤ 3.2 μm).

Front chamfering: at the end of the pass, the tool directly performs the 1 x 45° lead-in chamfer (Fig. 13) using the 93° setting.

Dynamics: Ft = 39 N, Pm = 0.120 kW; active time Ta = 0.36 min (including chamfering).

D) Axial pilot hole drilling, Ø 14.5 mm (Fig. 2)

Execution of the axial roughing pilot hole to a blind depth of 49.0 mm using the lathe's tailstock with a Sandvik CoroDrill 860 solid carbide drill (drill angle 140°).

Cutting parameters: D = 14.5 mm, n = 450 rpm, f = 0.08 mm/rev, Vf = 36 mm/min (Vc = 20.5 m/min).

Axial thrust and torque: Fa ≈ 1850 N, Mt ≈ 4.2 N·m, Pm = 0.283 kW < 1.10 kW (power margin: 74%).

Active time: Ta = (49 + 2) / 36 = 1.42 min.

E) Precision boring Ø 15 H7 (Sup. 3)

Calibration of the internal bore to ensure an H7 geometric fit (+0.018 / 0 mm) and a surface roughness of Ra ≤ 1.6 μm for the fitting of the crankshaft, advancing to a working depth of 45.0 mm (leaving 4.0 mm of clearance at the bottom of the blind pilot hole for fine chips).

Tool: Sandvik CoroReamer 835 multi-flute solid carbide reamer, Ø 15.00 H7, mounted on a floating shank.

Parameters: n = 250 rpm, f = 0.12 mm/rev, ap = 0.25 mm radial, Vf = 30 mm/min.

Dynamics: Ft = 53 N, Pm = 0.015 kW << 1.10 kW (margin: 98%).

Active time: Ta = (45 + 2) / 30 = 1.57 min.

3.3.2 STAGE 30: turning, 2nd set-up (head/screw side)

The component is turned over and clamped onto the finished Ø 25.0 mm sleeve using a self-centring chuck fitted with soft, custom-turned jaws, thus preventing any damage to the surface. Given the overhang (~70 mm), after the first face milling of the head, conical centring to DIN 333 is carried out and the MK3 conical rotating tailstock is immediately brought into position, creating a rigid support-beam constraint that eliminates deflection and vibration under shear stress.

A) Facing of the upper face to final dimension L = 118.0 mm (Fig. 6)

Cantilever face milling of the end to remove the remaining 2.0 mm of axial stock and bring the shaft to the nominal length L = 118.0 mm, in 2 passes of ap = 1.0 mm using a CCMT tool holder (n = 1200 rpm, f = 0.15 mm/rev, Vc = 113.1 m/min).

Dynamics: Ft = 196 N, Pm = 0.527 kW < 1.10 kW.

Active time: Ta = 2 · [(15 + 2) / 180] = 0.19 min.

B) Centre drilling for DIN 333 standard tailstock, Form A, 60° (Fig. 7)

Execution of the 60° conical geometric centre on the tailstock using an HSS-E centre point to DIN 333 Form A, Ø 3.15 / 8.0 mm (n = 1200 rpm, f = 0.05 mm/rev, Vc = 11.9 m/min).

• Creates the 60° guide seat for the rotating tailstock (the M4 axial thread is omitted per design specification to ensure a non-deformable guide).

Dynamics: Ft = 110 N, Fa ≈ 450 N, Pm = 0.031 kW. Positioning and clamping of the

MK3 conical rotating tailstock.

Active time: Ta = (4 + 1) / 60 = 0.08 min.

C) Cylindrical roughing of the shaft and screw crest (Sup. 10 and Sup. 8b)

Removal of the main stock from the workpiece clamped between the self-centring chuck and the tailstock using a CCMT tool holder (n = 1200 rpm, f = 0.15 mm/rev, ap = 1.25 mm, Vc = 98.8 m/min):

3 longitudinal passes over a stroke of 62.0 mm to reduce the rough shaft from Ø 30 to Ø 22.4 mm (screw crest with a finishing allowance of +0.40 mm).

2 stepped longitudinal passes over a stroke of 17.0 mm to bring the bearing seat to Ø 17.4 mm.

Dynamics: Ft = 234 N, Pm = 0.550 kW < 1.10 kW (available power margin: 50%).

Active time: Ta = [3 · (62 + 2) + 2 · (17 + 2)] / 180 = 1.28 min.

D) Shaft finishing, 30° conical profiling and bearing seat calibration (Fig. 11 and Figs. 8a–8b)

Continuous calibrated pass from ap = 0.20 mm for copying (n = 1650 rpm, f = 0.10 mm/rev, Vc = 103.7 m/min) using a Sandvik SDJCR 1616H 11 tool holder and a 55° DCMT 11 T3 04-PF insert:

Calibrates the screw crest to Ø 22.0 mm (general tolerance per ISO 2768-m).

Profile the 30° inclined truncated cone transition (from Ø 25 to Ø 14 mm).

Faces the axial shoulder to Ø 20.0 x 3.0 mm (Surface 8a).

Machine the bearing seat to Ø 17.20 mm (+0.20 mm on the diameter as a radial allowance of 0.10 mm for subsequent cylindrical grinding in Stage 70).

Estimated theoretical roughness: Ra ≈ 0.78 µm; dynamic: Ft = 39 N, Pm = 0.096 kW.

Active time: Ta = (64 + 2) / 165 = 0.40 min.

E) Machining of a relief groove for grinding and milling, Ø 14.0 x 2.0 mm (Fig. 12)

Radial plunge groove on the Ø 14.0 mm diameter, 2.0 mm wide, situated between the cone and the helix to allow the helix cutter to disengage and the grinding wheel to overrun during grinding.

Tool: Sandvik CoroCut 1-2 cutting blade for parting off and grooving, shank 16x16 mm with insert w = 2.0 mm (n = 800 rpm, f = 0.05 mm/rev, ap = 1.60 mm, Vc = 39.2 m/min).

Dynamics: Ft = 141 N, Pm = 0.131 kW.

Active time: Ta = [(1.6 + 1.0) / 40] + 0.03 (bottom calibration pause) = 0.10 min.

F) Machining a groove for a Seeger safety ring, Ø 15.0 x 1.10 mm (Fig. 9)

DIN 471 standard plunge-cut groove on a Ø 17 mm shaft: groove bottom diameter d3 = 15.0 mm (tolerance h11: 0 / -0.11 mm), width s = 1.10 mm (tolerance H13: +0.14 / 0 mm) positioned 5.0 mm from the end face.

Tool: CoroCut 1-2 blade with shaped insert w = 1.10 mm (n = 800 rpm, f = 0.04 mm/rev, ap = 1.10 mm, Vc = 40.5 m/min).

Dynamics: Ft = 73 N, Pm = 0.070 kW.

Active time: Ta = [(1.1 + 0.5) / 32] + 0.02 (bottom calibration pause) = 0.07 min.

3.3.3 STAGE 40: production of the worm gear (helical milling)

The generation of the worm screw (Fig. 10) is carried out on the Grazioli universal milling machine by clamping the workpiece between the centres of the mechanical divider.

To follow the pitch of the helical groove, the table is rotated by the helix angle γ = 5° 24'. Via a gear-driven pulley connected to the table lead screw (pv = 6.0 mm), the rotation of the workpiece is synchronised with the axial feed to generate the helix pitch (px = 5.50 mm).

Geometric Parameter of the Lead Screw	Symbol	Formula / Reference	Value
Normal axial modulus	m	Geometric specification from drawing (h = 4.0 mm, standardised)	1.75 mm
Number of threads	z1	Gear ratio (single-start screw)	1
Normal pressure angle	αn	Standard profile DIN 3975	20°
Reference pitch diameter	d1	d1 = da1 – 2·m = 22.00 – 3.50	18.50 mm
Crest diameter (external turned)	da1	Nominal dimension as per technical drawing	22.00 mm
Core diameter (bottom of recess)	df1	Nominal dimension from technical drawing (df1 = da1 - 2·h = 22.0 - 8.0)	14.00 mm
Total tooth/slot height	h	h = 2.25 · m = 3.938 mm ≈ 4.00 mm (clearance at the bottom c = 0.25·m)	4.00 mm
Axial thickness of the tooth at the crest	sa	Nominal dimension as per technical drawing	2.00 mm
Axial pitch of the propeller	px	px = π · m · z1 = π · 1.75 · 1	5.498 mm

Primitive pitch angle	γ	tan γ = px / (π · d1) = 5.498 / (π · 18.50) = 0.09459	5° 24'
Useful threaded length	L_screw	Nominal axial dimension as per drawing	36.0 mm

Table 3.5 – Geometric data for the worm screw

Calculation of the divider's return pulley

With an internal ratio of the divider R = 40:1 and a lead of the table screw pv = 6.0 mm, the transmission ratio of the lead screw to generate the helical pitch (px = 5.50 mm) is:

i_lira = (R · px) / pv = (40 · 5.498) / 6.0 = 36.65

TOOL SELECTION AND CUTTING STRATEGY

Tool:

HSS-Co modular disc cutter (m = 1.75 mm, α = 20°, Df = 25 mm, z = 10 teeth).

Strategy:

the thread height (h = 4.0 mm, from Ø 22 to Ø 14 mm) is machined in 5 passes (4 roughing passes at ap = 0.90 mm and 1 finishing pass at ap = 0.40 mm), with clearance at the end of the stroke in the Ø 14 x 2 mm chip groove (Fig. 12).

CUTTING PARAMETERS, DYNAMICS AND TIMES

Speeds and feed rates:

At N = 230 rpm, the cutting speed Vc is 18.1 m/min. With a feed per tooth fz = 0.03 mm/tooth, the table feed rate is:

Vf = fz · z · N = 0.03 · 10 · 230 = 69.0 mm/min

Forces and power:

with a specific pressure kc ≈ 2800 N/mm², the average tangential force is Fc ≈ 170 N, with power consumption Pm ≈ 0.073 kW (well within the capacity of the milling machine's 4.1 kW motor).

Active time:

total stroke L = 36 + 8 = 44 mm (including approach and withdrawal from the groove). The time per pass is tp = 44 / 69 = 0.64 min. The total active time for the 5 passes is:

Ta = 5 × 0.64 = 3.19 min (roughing: 2.55 min, finishing: 0.64 min).

3.4 Engineering of the slotting operation (PHASE 50)

3.4.1 Machining the Tongue Seat (Fig. 4)

This operation creates the internal slot for a standardised tongue in accordance with UNI 6604 / DIN 6885 (width 5 P9, depth t2 = 3.0 mm, effective length 30.0 mm) within the bored hole Ø 15 H7 (Fig. 3) of the base sleeve. The operation is carried out on the CAMS 150 vertical slotting machine (1.50 kW motor, adjustable slide stroke 0 to 150 mm). The workpiece is clamped vertically in a precision self-centring vice with prismatic jaws on the external diameter Ø 25.0 mm (Surface 5), ensuring that the machined lower face (Surface 1) rests perfectly on the reference surface to guarantee the perpendicularity of the workpiece axis relative to the slide. As the reamed hole has a blind depth of 45.0 mm (with a pilot hole at the bottom at 49.0 mm), there remains a clear space of over 15.0 mm at the bottom of the working slot (30.0 mm), which acts as a natural clearance zone for the insert to exit and for the stroke to reverse without any risk of impact.

Vertical slotting of the keyway for a 5 P9 x 3.0 mm key (Fig. 4):

Machining of the internal keyway for the reciprocating linear motion of the slide, with controlled radial increments to a total radial depth of 3.0 mm in the hub, ensuring a precise, play-free fit with the drive shaft key.

Tool:

REV Broaching Tools slotting system: REV UT-05-25 tool holder (cylindrical shank Ø 16 mm) fitted with a calibrated REV IN-5-P9 sintered insert (cutting edge width w = 5.00 mm, ISO P9 tolerance: -0.012 / -0.042 mm, corner radius $r\varepsilon$ = 0.2 mm).

Cutting parameters:

slide stroke L = 55.0 mm, cutting rate nc = 90 strokes/min, radial feed per stroke fc = 0.05 mm/stroke (60 passes in total for a depth of cut t2 = 3.0 mm).

KINEMATICS AND DYNAMICS:

Slide stroke:

L = 30 mm (useful slot length) + 15 mm (approach) + 10 mm (clearance

) = 55.0 mm.

Slide operating rate:

$nc = 90$ strokes/min.

Average cutting speed: $Vc = (2 \times L \times nc) / 1000 = (2 \times 55 \times 90) / 1000 = 9.9$ m/min (maximum instantaneous downward speed $V_{max} \approx 13.5$ m/min).

Average radial feed rate: $Vf = fc \cdot nc = 0.05 \cdot 90 = 4.5$ mm/min.

Cross-sectional area of the undeformed chip per cut:
$S = w \cdot fc = 5.0 \cdot 0.05 = 0.250$ mm².

Effective specific pressure (orthogonal cut): $kc \approx 2600$ N/mm² (conservative value for C45 steel with neutral rake).
Main cutting force at the slide: $Ft = kc \cdot S = 2600 \cdot 0.250 = 650$ N.
Net cutting power:

$Pc = (Ft \cdot Vc) / 60{,}000 = (650 \cdot 9.9) / 60{,}000 = 0.107$ kW.

Power absorbed by the machine: $Pm = Pc / 0.70 = 0.153 \text{ kW} \ll 1.50$ kW (CAMS 150 motor power margin: 90 per cent).

Active time: $Ta = n\_passes / nc = 60 / 90 = 0.667 \text{ min} \approx 0.67$ min (for a depth reduced to 2.3 mm: $46 / 90 = 0.51$ min).

The use of the CAMS 150 vertical slotting machine with REV modular tooling represents the optimal choice from both a technical and economic perspective:

Geometric constraint: Conventional broaching under tension or compression necessarily requires through-holes for the withdrawal of the stepped broach; in our workpiece, the Ø 15 H7 hole is blind, making it physically impossible for the broach to exit without a radial discharge chamber of increased diameter.

Economic analysis for a batch of 500 parts: A special shaped broach has a procurement cost exceeding €1,200, resulting in an unsustainable unit cost of €2.40 per part. In contrast, the REV system requires a reusable ST-16 shank and an interchangeable IN-5-P9 insert for a total investment of just €150 (a cost of merely €0.30 per piece, amortised over the batch), with re-sharpenable or replaceable inserts at low cost (€18 each) having a guaranteed service life of over 600 grooves.

3.5 Final machining operations

3.5.1 Heat Treatment (Stage 60)

The operational requirements demand high surface hardness and resistance to sliding contact wear on the flanks of the worm screw (Surface 10) and on the bearing raceways (Surface 8), whilst preserving a tough and resilient core capable of absorbing torsional stresses and impact loads without brittle fracture.

Process selection: Full-volume hardening is categorically ruled out as it would embrittle the entire shaft, as is case hardening, which would require long furnace times and the use of low-carbon alloy steels (e.g. 18NiCrMo5). The steel used is normalised C45 (carbon content C ≈ 0.43–0.50%), ideal for direct high-frequency induction hardening (HF 150–250 kHz).

Kinematics and process parameters: Using a water-cooled, shaped copper inductor, the high-frequency electromagnetic field heats, via the skin effect, only the surface layer to the austenitising temperature (840–860 °C) in a very short time (approximately 3–4 seconds). This is immediately followed by quenching using a pressurised annular spray of an anti-decarburisation polymer-water mixture.

Properties achieved: Surface hardness of 52–56 HRC over an effective hardened depth DS = 1.0–1.5 mm. The core and sleeve retain their original tough pearlitic-ferritic microstructure (Rm ≈ 750 MPa, elongation A5 > 16%).

Stress-relief treatment: Following hardening, a stress-relief tempering is carried out in a static furnace at 180–200 °C for 60 minutes to release the peaks of autogenous elastic stress resulting from martensitic transformation without causing any reduction in hardness.

Estimated cycle time: Approximately 0.50 min/piece.

3.5.2 Cylindrical grinding (Stage 70)

External cylindrical grinding is carried out on the Ribon RUR 500 cylindrical grinding machine to bring the individual bearing seat (Surface 8b) to the precision tolerance class Ø 17 h6 (deviations: 0 / -0.011 mm) and to the surface roughness Ra ≤ 0.8 μm specified in the drawing for the assembly of the inner ring of the rolling bearing.

The workpiece is clamped between the centres using a centre-drill and a driver, utilising the 60° centre (DIN 333) machined on the head (Surface 7) and a self-centring pin inserted into the lower bore Ø 15 H7, ensuring perfect geometric coaxiality of the shaft.

Grinding wheel: Cylindrical cup/disc wheel made of high-purity white corundum, Tyrolit 89A 60 K 5V 217 (medium grit 60, porous vitrified bond for hardened steels, diameter Dm = 300 mm, thickness b = 30 mm).

OPERATING PARAMETERS:

Peripheral speed of the grinding wheel: Vm = 27.5 m/s (grinding wheel rotational speed: Nm = 1750 rpm).

Workpiece peripheral speed: Vw = 15.0 m/min (workpiece rotational speed: Nw = 280 rpm on Ø 17 mm).

Speed ratio: q = Vm / Vw = 27.5 / (15.0 / 60) = 110.

Radial feed per pass (increment): ap = 0.005 mm/pass
(roughing) and 0.002 mm per pass (finishing).
Radial stock to be removed: 0.10 mm on the radius (equivalent to 0.20 mm on the

diameter, from a turned Ø 17.20 mm to a finished Ø 17.00 mm).

Number of passes: 16 passes (12 roughing passes + 4 calibrated finishing passes)

followed by 3 spark-out passes with zero feed to eliminate elastic deflection and

ensure Ra ≤ 0.8 µm.

KINEMATICS AND POWER:

Axial table feed: fa = 0.30 · b = 0.30 · 30 = 9.0 mm/workpiece revolution → Vf

= fa · Nw = 9.0 · 280 = 2520 mm/min.

Specific grinding power: us ≈ 35 J/mm³ = 35 W·s/mm³.

Average chip removal rate: Q = π · dw · ap · Vf = π · 17 · 0.005 · (2520 / 60)

= 11.2 mm³/s.

Net cutting power: Pc = us · Q / 1000 = 35 · 11.2 / 1000 = 0.392 kW.

Power absorbed by the machine: Pm = Pc / 0.70 = 0.560 kW << 1.80 kW (grinding wheel motor thoroughly tested).

Active time per bearing seat: Ta = 16 passes · [(12 + 4) / 2520] + t_sparkout = 16 · 0.00635 min + 0.04 min ≈ 0.09 min.

Polishing of the hardened propeller flanks: carried out on the same machine using a felt pad/disc and fine diamond paste (Ra ≤ 0.8 μm; estimated passive time included in the finishing time).

3.6 Assessment of processing times

The calculation of production times plays a key role in cost analysis and industrial planning. The active machining times (Ta), detailed in Table 8, have been rigorously calculated on the basis of the cutting parameters engineered in the previous chapters, taking into account the kinematic and power limitations of the machines used (in particular the 1.10 kW HBM 330 lathe, which necessitated conservative feed rates for roughing and deep drilling, and the 5 passes required to machine the 4.0 mm worm gear tooth). The total active time is 10.22 minutes per workpiece.

Stage	Operation	f [mm/g]	N [rpm]	Vf [mm/min]	No. of passes	e [mm]	L [mm]	Ta [min]
20	Face milling (lower face) (Surface 1)	0.15	1200	180.0	2	2.0	15.0	0.19
20	Basic roughing, Ø 25.4 (Surface 5)	0.15	1200	180.0	2	2.0	49.0	0.57
20	Basic finish Ø 25.0 + chamfer (Surface 5)	0.10	1650	165.0	1	2.0	49.0	0.36
20	Pilot hole Ø 14.5 (Surface 2)	0.08	450	36.0	1	2.0	49.0	1.42
20	Bore reaming Ø 15 H7 (Surface 3)	0.12	250	30.0	1	2.0	45.0	1.57
30	Top face L=118 mm (Face 6)	0.15	1200	180.0	2	2.0	15.0	0.19

30	DIN 333-A 60° centring (Surface 7)	0.05	1200	60.0	1	1.0	4.0	0.08
30	Rough machining of barrel and screw (Sup. 10, 8b)	0.15	1200	180.0	5	2.0	62.0	1.28
30	Finish of barrel, cone and pad seat (Sup. 11, 8b)	0.10	1650	165.0	1	2.0	64.0	0.40
30	Grinding discharge groove Ø 14x2 (Surface 12)	0.05	800	40.0	1	1.0	1.6	0.10
30	Seeger groove Ø 15x1.1 (Sup. 9)	0.04	800	32.0	1	0.5	1.1	0.07
40	Screw milling (4 roughing passes)	0.03	230	69.0	4	8.0	36.0	2.55
40	Screw milling (1 finishing pass)	0.03	230	69.0	1	8.0	36.0	0.64
50	Slotted tongue joint 5 P9 (Fig. 4)	0.05	90	4.5	60	15.0	30.0	0.67
70	Grinding of bearing seat Ø 17 h6 (Surface 8b)	—	280	2520.0	16	4.0	12.0	0.09
70	Polishing/lapping of screw flanks (Sup. 10)	—	500	7500.0	4	8.0	36.0	0.04
							TOTAL	10.22

Table 3.6 – Active processing times (Ta)

Estimate of Passive Times:

The non-machining times (Tp), quantified in Table 9 by analysing the individual basic operations of workpiece loading/unloading, tool change, zeroing, clamping and dimensional inspection on each of the machine tools used, amount to 17.60 minutes per workpiece. Added to this is the proportion of the initial machine set-up time for the entire batch (estimated at a total of 120 minutes spread across the 500 units), amounting to 0.24 minutes per part.

The estimated total cycle time per component is therefore:

Unit cycle time = Ta + Tp + Tsetup = 10.22 + 17.60 + 0.24 = 28.06 min ≈ **28.1 min**

Activity / Phase (10 – 30)	Time (min)	Activity / Phase (40 – 70)	Time (min)
PHASE 10 – Truncation		STEP 40 – Milling a worm gear	
Positioning the bar and clamping it in the vice	0.30	Mounting the workpiece on the indexing table	0.80
Cutting to size	0.50	Fitting of tailstock to dividing head	0.40
Deburring and inspection	0.20	Fitting the milling cutter to the spindle	0.80
Subtotal for Stage 10	1.00	Alignment and light contact between workpiece and milling cutter	0.50
STAGE 20 – Turning, 1st Set-up		Selection of speed and feed rate	0.20
Mounting the workpiece on the self-centring chuck and centring	0.50	Start/stop per pass (0.05 × 8)	0.40
Selection of speed and feed rate	0.20	Removal of workpiece from indexing table	0.60
Tool change (3 changes: 0.50 × 3)	1.50	Inspection with gear gauge	0.20
Tool positioning (4 positions: 0.30 × 4)	1.20	Subtotal Stage 40	3.90
Machine start/stop (8 cycles: 0.05 × 8)	0.40	STAGE 50 – Slotting	
Check with gauge / plug (2 checks: 0.20 × 2)	0.40	Mounting the workpiece on the slotting table	0.60
Removing the workpiece	0.30	Aligning the slot	0.40
Subtotal for Stage 20	4.50	Selection of stride and cadence	0.20
STAGE 30 – Turning, 2nd Positioning		Dismantling and inspection of P9 plug	0.40
Turning the workpiece over and refitting it on Ø25	0.60	Subtotal for Stage 50	1.60

Fitting and clamping of MK3 tailstock	0.40	STAGE 70 – Grinding	
Selection of parameters (speed and feed rate)	0.20	Clamping the workpiece between the centres using a tailstock	0.40
Tool change (3 changes: 0.50 × 3)	1.50	Grinding wheel approach and skimming	0.30
Tool positioning (4 positions: 0.30 × 4)	1.20	Selection of working parameters	0.20
Machine start/stop (8 cycles: 0.05 × 8)	0.40	Dismantling and inspection with h6 micrometre	0.40
Check of gauge/micrometer (3 checks: 0.20 × 3)	0.60	Subtotal Stage 70	1.30
Removal of workpiece and tailstock	0.40	—	—
Subtotal for Stage 30	5.30	TOTAL PASSIVE TIME (Tp)	17.60

Table 3.7 – Passive processing times (Tp)

3.7 Economic assessment (costs)

A) Raw Material Cost:

The volume of the raw rolled cylindrical bar (Ø 30.0 mm, L = 122.0 mm) is:

$V = \pi \cdot (15)^2 \cdot 122 = 86{,}237\ mm^3 = 8.62 \cdot 10^{-5}\ m^3$

Taking into account the density of C45 steel (ρ = 7,850 kg/m³):

$Mass = 8.62 \times 10^{-5} \times 7850 = 0.677$ kg

At a commercial supply price of 1.20 €/kg for bars:

$C_{mat} = 0.677 \times 1.20 = 0.81$ €/piece

B) Cost of in-house machining:

With a total cycle time per unit of 28.06 minutes, to calculate the machining cost we use a workshop hourly rate of 40.00 €/h (i.e. 0.6667 €/min):

$C_{mach} = 28.06$ mins $\times$ 0.6667 €/min = 18.71 €/unit

The hourly rate of 40.00 €/h covers: the company's cost of skilled labour (~25.00 €/h), the machines' electricity consumption, routine maintenance and a contribution towards the plant's overheads (heating, lighting, miscellaneous expenses).

C) Heat Treatment Cost (Subcontractor):

High-frequency selective induction hardening of the screw threads and bearing seat, including stress-relief tempering, carried out in batches by a specialist supplier, amounts to:

C_{tratt} = 2.50 €/pc

D) Cost of Tooling and Inserts (Cutting Tool Depreciation):

Calculated analytically based on Taylor's useful life and the active cutting engagement per piece:

Positive rhombic inserts CCMT 09 T3 08 (rough turning, 2 cutting edges): 10 inserts required per batch (**€172.00,** at €17.20 each)

55° DCMT 11 T3 04 inserts (finishing turning, 2 cutting edges): 5 inserts required (**€74.75**, at €14.95 each)

CoroDrill 860 solid carbide drill, Ø 14.5 mm: 1 amortised drill per batch (**€140.00**)

CoroReamer 835 solid machine reamer, Ø 15 H7: 1 reamer included in the batch (**€206.40**)

DIN 333 standard centre drill, Form A 60°, Ø 3.15 mm: 1 centre drill for the entire batch (**€16.60**)

CoroCut 1-2 grooving inserts (Seeger groove and relief): 2 inserts (**€76.00**, at €38.00 each)

HSS-Co shaped modular disc cutters, m = 1.75 mm: 3 cutters included **in the batch** (**€375.00**, at €125.00 each)

REV IN-5-P9 sintered grooving insert: 1 insert (**€28.00**)

Tyrolit 89A corundum grinding wheel: 1 cushioned grinding wheel (**€62.80**)

Total tooling cost for a batch of 500 pieces:

€1,151.55 → Unit cost: C_{ut} = **€2.30/pc**

E) Machinery Depreciation Charge (Table 10):

Ten-year depreciation (annual rate of 10% based on 2,000 working hours per year = 120,000 minutes per year) for the entire machine fleet:

C_amm = €0.07 per unit

Machine tool	Purchase price [€]	Annual depreciation (10%) [€/year]	Cost per Minute [€/min]	Time per unit [min]	Cost per piece [€/piece]
Femi 784 XL band saw	700	70	0.0006	1.00 min	€0.0006
HBM 330–600 parallel lathe	2,700	270	0.0023	16.03 min	€0.0369
Grazioli Ludor Universal Milling Machine	4,000	400	0.0033	7.09 min	€0.0234
CAMS 150 slotting machine	3,500	350	0.0029	2.27 mins	€0.0066
Ribon RUR 500 grinding machine	3,800	380	0.0032	1.43 min	€0.0046
TOTAL INVESTMENT IN MACHINERY	€14,700	€1,470 per year	€0.0123/ min	27.82 mins	€0.0721 ≈ 0.07

Table 3.8 – Depreciation of machine tools

Total Industrial Unit Cost (Workshop Standard):

C_tot = C_mat + C_labour + C_handling + C_ut + C_depreciation = 0.81 + 18.71 + 2.50 + 2.30 + 0.07 = **24.39 €/unit**

Total Job Cost (Batch of 500 pieces):

C_order = 500 × 24.39 € = **12,195.00 €**

3.8 Final technical documentation

3.8.1 Metrological Control

Metrological testing and quality control ensure that the *Worm Shaft* complies with the design specifications in terms of geometry, dimensions and surface finish:

Digital slide gauge (resolution 0.01 mm):

used to verify the overall axial lengths (total length L = 118.0 mm, sleeve L = 49.0 mm, bearing seat L = 12.0 mm, shoulder L = 3.0 mm) and external diameters, with general tolerance in accordance with ISO 2768-m.

Millesimal external micrometre 0 – 25 mm (resolution 0.001 mm):

used to certify the tight ISO h6 tolerance (0 / -0.011 mm, from 17.000 to 16.989 mm) on the ground bearing seat (Surface 8b).

Smooth cylindrical Pass/Fail (P/NP) plug gauge, Ø 15 H7:

used for the rapid inspection of the reamed internal bore (+0.018 / 0 mm) for the fitting of the crankshaft.

Flat plug gauge for keyways P/NP 5 P9:

used to verify the width of the keyway (5.00 mm with tolerances of -0.012 / -0.042 mm) and its radial depth (3.0 mm).

Depth gauge for grooves:

used to check the axial positioning at 5.0 mm from the head and the bottom diameter Ø 15.0 mm of the Seeger groove (Fig. 9).

Micrometer for gear wheels / three-wire calibration method:

used to verify the axial thickness (sa = 2.0 mm at the crest) and the correctness of the helical profile of the worm screw (m = 1.75 mm).

Precision stylus roughness tester:

used to verify surface roughness Ra ≤ 0.8 μm on the ground bearing seat and Ra ≤ 1.6 μm on the flanks of the hardened helical section and on the turned functional surfaces.

3.8.2 Cycle Sheets (Summary Machining Sheet)

The chronological sequence of machining operations is summarised in Table 11 in order to provide the workshop with an immediate overview of the operations, machine tools, clamping equipment and tooling involved in each stage of the manufacturing cycle.

Stage	Process Description	Machine Tool	Fixturing / Tooling	Tools Used	Inspection Tools
10	Cutting raw bar stock into lengths of L=122 mm	Femi 784 XL band saw	Mechanical screw vice	Bimetallic blade 1440 × 13 × 0.65 mm	Sliding caliper
20	First turning operation (base side: facing, drilling Ø14.5, boring Ø15 H7, shank Ø25, chamfer 1x45°)	HBM 330–600 parallel lathe	Self-centring 3-jaw chuck Ø 160 mm	Tool holders SCLCR 1616 (CCMT 09T3), SDJCR 1616 (DCMT 11T3), CoroDrill 860 twist drill Ø 14.5 mm, CoroReamer 835 reamer Ø 15.00 H7	Digital calliper, smooth cylindrical plug gauge P/NP Ø 15 H7
30	Second-set turning (head/screw side: facing L=118, centring 60°, roughing and finishing of shank, taper, bearing seats, Ø14x2 groove, Seeger groove)	HBM 330–600 parallel lathe	Clamping on finished Ø 25 with soft jaws + MK3 conical rotating tailstock	Tool holders SCLCR 1616 (CCMT 09T3), SDJCR 1616 (DCMT 11T3), DIN 333-A 60° centre drill Ø 3.15, CoroCut 1-2 grooving insert 16x16	Digital calliper, outside micrometer, Seeger depth gauge
40	Helical worm gear profile milling (m=1.75, z1=1, px=5.50 mm, crest Ø22, root Ø14)	Grazioli Ludor Universal Milling Machine	Universal mechanical dividing head + tailstock (table oriented at γ = 5° 24', return gear i=36.65)	Modular HSS-Co shaped disc milling cutter, m = 1.75 mm (Df = 25 mm, z = 10 teeth) on ISO 50 shaft	Gear tooth gauge, micrometre with calibrated plates / wires
50	Internal slotting for standardised 5 P9 x 3.0 mm tongue	CAMS 150 vertical slotting machine	Precision self-centring vice with prismatic jaws on Ø 25	REV Broaching Tools system: REV UT-05-25 shank + REV IN-5-P9 calibrated sintered insert	P/NP plug gauge for 5 P9 slots, Depth gauge

60	Selective induction hardening (screw flanks and bearing seat: 52–56 HRC) + stress relief	High-frequency (HF) induction system	Vertical rotating support with automatic positioning	Water-cooled shaped copper inductor + polymer shower quenching ring	Portable Rockwell hardness tester (HRC)
70	Single-station round grinding of bearing seat Ø 17 h6 and polishing of screw flanks	Ribon RUR 500 cylindrical grinding machine	Rigid centre-point clamping with keyway driver (self-centring pin on Ø 15 H7 bore + 60° centre)	Tyrolit 89A 60 K 5 V 217 white corundum cylindrical grinding wheel (Ø 300 · 30 mm)	Millesimal micrometre for external surfaces (h6), stylus-type roughness tester
80	Metrological inspection and final conformity testing	Test bench and quality control	V-block reference prisms, granite reference surface	Thousandth-inch micrometer, roughness tester, P/NP test blocks Ø 15 H7 and 5 P9, height gauge	Test report and certificate of dimensional conformity

Table 3.9 – Summary processing sheet

4. PLASTIC DEFORMATION PROCESSING

4.1 Function of the component and technical drawing

The output flange (component no. 2 of the worm gearbox) acts as a lateral closure element for the housing, a housing for the ball bearing and oil seal of the hollow output shaft, and a mounting flange for securing the unit to the operating machine. It is a structural component subject to bending and torsional loads and vibrations resulting from the transmission of motion.

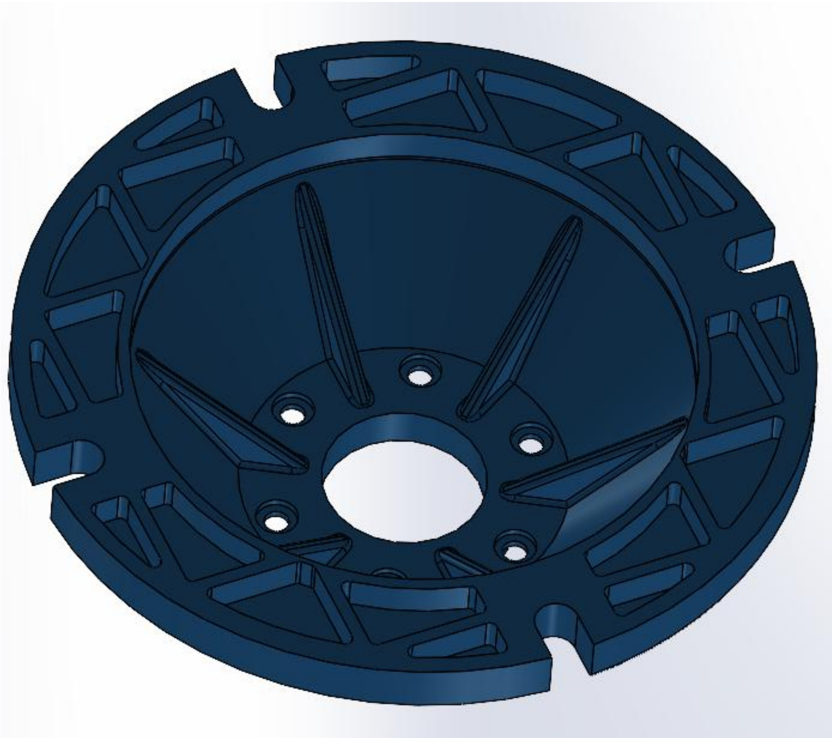

Figure 4.1 – Three-dimensional model of the gearbox output flange

The finished part has the following nominal geometric characteristics:

- Maximum external diameter: 160 mm
- Total height: 47.25 mm
- Central bearing seat diameter: Ø 33 mm
- Hub shoulder diameter: Ø 45 mm
- Circular rim thickness: 7.16 mm
- Mounting: 6 M5 x 1.0 threaded holes (on a circumference of Ø 55 mm) and 4 open slots on the outer edge (width 8.12 mm)
- Stiffening: 6 internal conical radial ribs

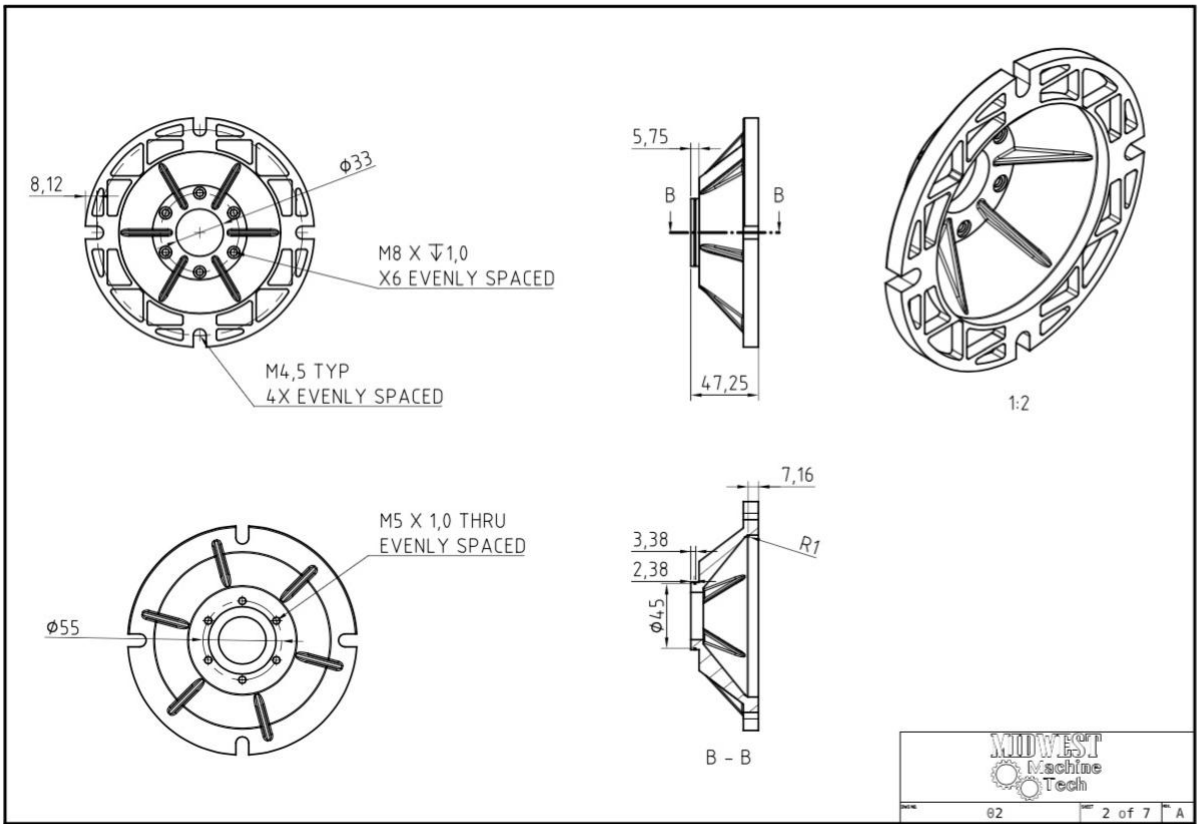

Figure 4.2 – Two-dimensional construction drawing of the finished flange

4.2 Selection of the plastic deformation process

Given the three-dimensional geometry of the component, with significant variations in thickness between the central hub and the outer ring and the presence of radial stiffening ribs, the most suitable process is hot forming in a closed die with flash. The process involves heating a cylindrical aluminium billet to the plasticity temperature (420–480 °C), and then compressing it between two steel die halves using a hydraulic press.

Compared with the alternatives assessed:

Cold forging: ruled out because the resistance to deformation of EN AW-6082 at room temperature, combined with the required thicknesses, would necessitate excessive forces and entail a high risk of cracking.
Open die forging: ruled out as it does not allow the flange geometry (ribs, bearing seat, bell profile) to be achieved easily.
Impact extrusion: not applicable to the component's asymmetrical three-dimensional geometry.

Die-casting: ruled out due to the inevitable presence of shrinkage porosity and the unfavourable orientation of the crystalline grain, which are incompatible with the component's fatigue strength requirements.
Hot forming, on the other hand, ensures a favourable orientation of the material fibres along the part's profile and refinement of the crystalline grain, whilst being fully compatible with the required geometric complexity.

It should be noted that certain geometries of the finished part cannot be produced directly by moulding: the central hole (Ø 33 mm), the 6 M5 fixing holes and the 4 slots on the edge will be solid in the raw moulded part and will be machined in the subsequent stage of material removal (turning, drilling and milling).

4.3 Choice of material

The **EN AW-6082 (AlSi1MgMn) aluminium alloy**, belonging to the 6000 series, was selected for the production of the flange by hot forging.
This is a heat-treatable alloy, the most widely used amongst structural aluminium alloys for stressed mechanical components.

The reasons for this choice are:

Excellent hot formability: forming temperature range 420–480 °C, with high deformability and low flow loads, which allow the mould cavities to be completely filled even in the presence of ribs and variations in thickness.
High mechanical properties in the T6 condition: following solution treatment and artificial ageing, the alloy achieves Rm = 310–340 MPa, Rp0.2 = 260–290 MPa and elongation A = 8–10 %.
Good corrosion resistance: essential for a component in contact with the gearbox's lubricating oil.
Low density: 2.71 g/cm³ (approximately one-third that of steel), resulting in a reduction in the overall weight of the assembly.
During the preliminary phase, the EN AW-2014 (AlCu4SiMg) alloy was also evaluated; whilst it offers superior mechanical strength (Rm up to 485 MPa), it has significantly lower corrosion resistance and a higher cost, neither of which are justified for this application.

Properties	Value
Tensile strength (R_m)	310–340 MPa
Yield strength ($R_{p0.2}$)	260–290 MPa
Elongation at break (A)	8–10 %
Brinell hardness (HB)	90–100
Density (ρ)	2.71 g/cm³
Modulus of elasticity (E)	70 GPa
Hot-forming range	420–480 °C
Melting point	555–650 °C

Table 4.1 – Properties of the EN AW-6082 T6 alloy

Standards: EN 573-3 (chemical designation), EN 755-2 (extruded and forged products).

4.4 Design of the die blank

4.4.1 Flash plane, draft angles and fillet radii

FLASH PLANE

The mould parting line (flange plane) has been positioned at the lower flat face of the outer circular rim, i.e. on the plane of maximum transverse extent of the component. This choice:

divides the part into an upper half-mould (which forms the conical bell and the hub) and a lower half-mould (which forms the flat bearing surface);
coincides with the section of maximum projected area, reducing the risk of lateral displacement of the mould halves during closure;
allows the blank to be ejected without undercuts on either side.

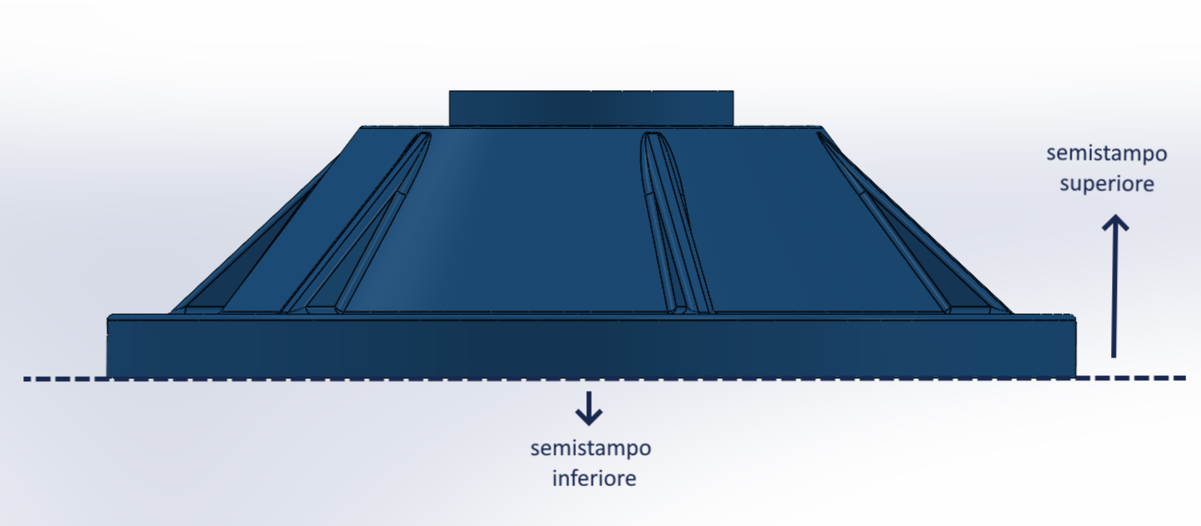

Figure 4.3 – Definition of the mould parting line (flash line)

DRAFT ANGLES

To allow the blank to be easily removed from the mould without damaging the surfaces or causing sticking, all walls not parallel to the flash plane must have an adequate draft angle. In accordance with the guidelines in the technical literature on hot forming of aluminium alloys (Santochi-Giusti), the following values are adopted depending on the depths involved:

Part area	Depth / height	Draft angle
Conical outer surface (bell and hub)	~41.5 mm	3°
Internal walls of central hub	~15 mm	5th
Side faces of the 6 radial ribs	~30 mm (h = 29.93 mm)	3°

Table 4.2 – Draft angles used

The inner walls of the hub require a greater draft angle (5°) than the outer walls, as the thermal shrinkage of the material during cooling tends to clamp the blank onto the mould's core/punch, making extraction more difficult.

ROUNDING RADIUS

The fillet radii of the die cuts are calculated using Table 5-5 by Santochi-Giusti, based on the h/b ratio between the height and width of the cut, and standard workshop values are then adopted.

Radial flanges ($h = 29.93$ mm, $b = 6.61$ mm):

$h/b = 29.93 / 6.61 = 4.53 \rightarrow h/b > 4$

- Inner radius of the groove (bottom of the cavity in the mould, corresponding to the crest of the tab):

  $r_i = 0.08 \times h + 0.75 = 0.08 \times 29.93 + 0.75 = 2.39 + 0.75 = 3.14$ mm → r_i is set to 3.5 mm

- Outer radius of the cut (mould fillet, base of the tab on the bell body):

  Applying the equation in Table 5-5 with the standardised value adopted ($r_i = 3.5$ mm):

  $r_e = 3.5 \times r_i + 0.75 = 3.5 \times 3.5 + 0.75 = 12.25 + 0.75 = 13.00$ mm → r_e is taken as 13.0 mm

The large value of r_e at the base of the ribs is essential to facilitate the plastic flow of the material within the deep, narrow grooves, preventing filling defects and reducing stress concentrations on the mould.

Hub ($h = 10.50$ mm, $b = 47$ mm):

$h/b = 10.50 / 47 = 0.22 \rightarrow h/b$ ratio ≤ 2

- Internal radius of the groove:

  $r_i = 0.06 \times h + 0.5 = 0.06 \times 10.50 + 0.5 = 0.63 + 0.5 = 1.13$ mm → r_i is set to 1.5 mm

- Outer radius of the notch:

  Applying the formula with the standardised value adopted ($r_i = 1.5$ mm):

  $r_e = 2.5 \times r_i + 0.75 = 2.5 \times 1.5 + 0.75 = 3.75 + 0.75 = 4.50$ mm → r_e is taken as 4.5 mm

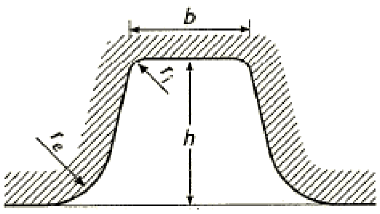

Tab. 5-5 Valori minimi di raggi di raccordo interni ed esterni delle incisioni degli stampi.

h/b	r_i (mm)	r_e (mm)
≤ 2	0,06h + 0,5	$2{,}5r_i + 0{,}75$
2 ÷ 4	0,07h + 0,6	$3r_i + 0{,}75$
> 4	0,08h + 0,75	$3{,}5r_i + 0{,}75$

Table 4.3 – Formulas for calculating the fillet radii of notches (Santochi-Giusti, Table 5-5)

4.4.2 Allowances and geometric simplifications

The functional surfaces of the flange that require tight tolerances (bearing seat, flange-casing mating surface, hub shoulder) cannot be obtained directly by stamping with the necessary precision. A machining allowance is provided on these surfaces, to be removed subsequently on a CNC lathe.

According to the Santochi-Giusti table (machining allowances on forged blanks), for nominal dimensions of 100–400 mm and a workpiece length ≤ 100 mm, the prescribed value is 3 mm per side. This value compensates for:

the inevitable dimensional inaccuracies of the process (IT13–IT14 typical of hot forging);
the thermal shrinkage of EN AW-6082 aluminium during cooling (shrinkage coefficient ≈ 1.2 per cent);
surface losses due to hot oxidation.

Dimensioni nominali (mm)	Lunghezza del pezzo (mm)			
	≤ 100	100 ÷ 300	300 ÷ 500	500 ÷ 1000
≤ 50	1,8 ÷ 2,3	1,8 ÷ 2,3	2,3 ÷ 3,1	3 ÷ 3,4
50 ÷ 75	2 ÷ 3	2 ÷ 3	2,5 ÷ 3	3,5 ÷ 4
75 ÷ 100	2 ÷ 3,5	2 ÷ 3,5	3 ÷ 3,5	3,5 ÷ 4,5
100 ÷ 400	3 ÷ 3,5	3 ÷ 4	3,5 ÷ 4,5	4,5 ÷ 5
400 ÷ 800	4 ÷ 4,5	4 ÷ 5	4,5 ÷ 5	5 ÷ 5,5
800 ÷ 1000	4 ÷ 5	4,5 ÷ 5,5	5,5 ÷ 6	5 ÷ 6,5

Tab. 5-4 Valori medi indicativi (in mm) dei sovrametalli di lavorazione sui greggi di stampaggio a caldo.

Table 4.4 – Standardised values for machining allowances (Santochi-Giusti, Table 5-4)

In particular:
Central bore Ø 33 mm: the blank is solid; this is achieved by turning/boring in the subsequent stage.

Shoulder Ø 45 mm: radial stock allowance of 3 mm → rough diameter Ø 51 mm to be turned.

Flat bearing surface (crown): 3 mm axial stock allowance → facing on the lathe.

Geometric simplifications

The following geometries of the finished part cannot be achieved by stamping and are therefore omitted from the blank:

Geometry of the finished part	In the blank	Subsequent machining
Central bore Ø 33 mm	Solid	Turning / boring
6 M5 threaded holes on the hub	Solid	Drilling + tapping
4 open slots on the edge	Solid continuous rim	Milling
Lattice-pattern pockets on the crown	Smooth, solid crown	Milling
Stop step Ø 45 mm	Solid flat surface	Turning

Table 4.5 – Geometric simplifications of the blank

The volume and mass of the blank, calculated using CAD software (SolidWorks) on the simplified model, are as follows:

Raw blank volume: V_{raw} = 200 087 mm³ (200.1 cm³)
Mass of the blank: M_{blank} = 200 087 × 0.00271 = 542 g (0.542 kg)

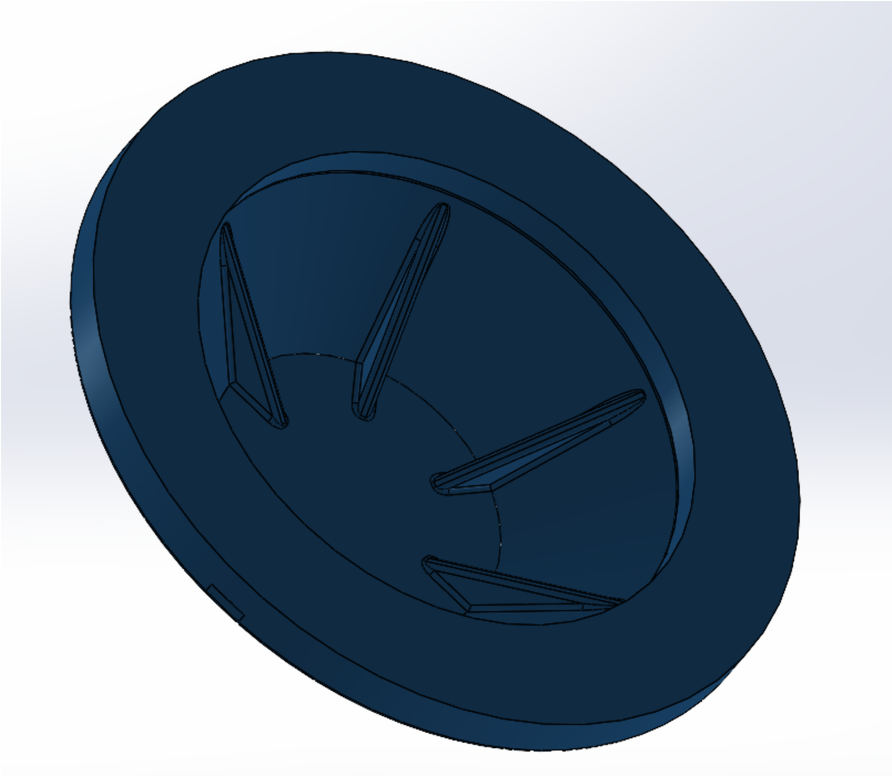

Figure 4.4 – 3D model of the blank

4.5 Dimensioning of the sprue

The sprue channel serves to accommodate the excess material volume of the billet and, via the sprue bridge, to generate the hydraulic resistance to flow necessary to ensure the complete filling of the deep cavities of the die (radial ribs and central hub).

The geometric dimensions are calculated using the standardised Santochi-Giusti equations:

Thickness of the sprue bridge (l): $l = 0.0175 \times \sqrt{A}$

where A is the area of the part's impression projected onto the parting line ($A = 20\,106$ mm²):

$l = 0.0175 \times \sqrt{20\ 10^6} = 0.0175 \times 141.8 = 2.48$ mm

The calculated value (2.48 mm) does not correspond to any entry in Table 24 of Santochi-Giusti. The closest standardised values are l = 2 mm and l = 3 mm. Since the flash bridge must be at least as thick as indicated by the calculation (a smaller value would reduce the hydraulic resistance, preventing the filling of deep cavities), the next higher entry is adopted: l = 3 mm.

The geometric parameters can be read directly from the l = 3 mm row in Table 24:

l (mm)	*h* (mm)	*r* (mm)	*m* (mm)	*n* (mm)
0,6	3,3	1	6	18
0,8	3,4	1	6	20
1	3,5	1	7	22
1,6	4,3	1	8	22
2	5	1,5	9	25
3	6,5	1,5	10	28
4	8	2	11	30
5	9,5	2	12	32
6	11	2,5	13	35
8	14	3	14	38
10	17	3	15	40

Table 4.6 – Standardised dimensions of the well-type sprue (Santochi-Giusti, Table 24)

Parameter	Symbol	Value (Table 24)
Thickness of the sprue bridge	l	3 mm
Cockpit height	h	6.5 mm
Radius of connection to the deck	r	1.5 mm
Inlet width	m	10 mm
Total well width	n	28 mm
Radius of the well base (R = 2.5 × r + 0.5)	R	4.25 mm

Table 4.7 – Dimensions of the burr channel

4.6 Dimensioning of the starting billet

The billet is the cylindrical aluminium blank from which the final part is formed by die-casting. It must contain sufficient volume to fill the entire die cavity plus the material that will flow into the sprue.

Total volume required:

The volume of the sprue is estimated at 20 per cent of the blank's volume, a standard value for circular parts with a sprue dimensioned according to Santochi-Giusti:

$V\_sprue = 0.20 \times V\_blank = 0.20 \times 200\,087 = 40\,017\ mm^3$

$V\_billetta = V\_green = 200\,087 + 40\,017 = 240\,104\ mm^3$

Selection of commercial diameter:

A commercially available extruded bar in EN AW-6082 with a diameter of Ø 80 mm is used, as listed in standard catalogues (e.g. EN 755-2). The diameter is chosen to be significantly smaller than the external diameter of the billet (160 mm) to allow for an initial phase of free radial expansion before the die halves are fully closed.

Billet cutting length:

$H\_billetta = V\_billetta / (\pi/4 \times D^2) = 240\,104 / (\pi/4 \times 80^2) = 240\,104 / 5\,027 = 47.8\ mm$

$\rightarrow H = 48\ mm$

Verification of the H/D ratio:

$H/D = 48/80 = 0.60$

This value is below the maximum limit of 2.5, above which a cylindrical billet would tend to become laterally unstable during the initial flattening stage. There is no risk of the material buckling.

The starting billet is therefore a cylinder with a diameter of 80 × 48 mm, cut from a commercially available extruded bar made of EN AW-6082 using a band saw.

Mass of the billet:

$M\_billetta = V\_billetta \times \rho = 240\,104 \times 0.00271 = 651\ g\ (0.651\ kg)$

For verification purposes, the burr scrap mass is: M_burr = M_billetta - M_greggio = 651 - 542 = 109 g → 16.7% of the total mass (consistent with the 20% estimate)

4.7 Calculation of the forming force and selection of the press

4.7.1 Calculation of the forming force

The maximum force required at the end of the stroke for closed-die forging with flash is determined using the classic semi-empirical model:

$P = K \times \sigma_f \times A_b$

Area projected onto the flash plane (A_b):

$A_b = (\pi / 4) \times 160^2 = 20\,106\ mm^2$

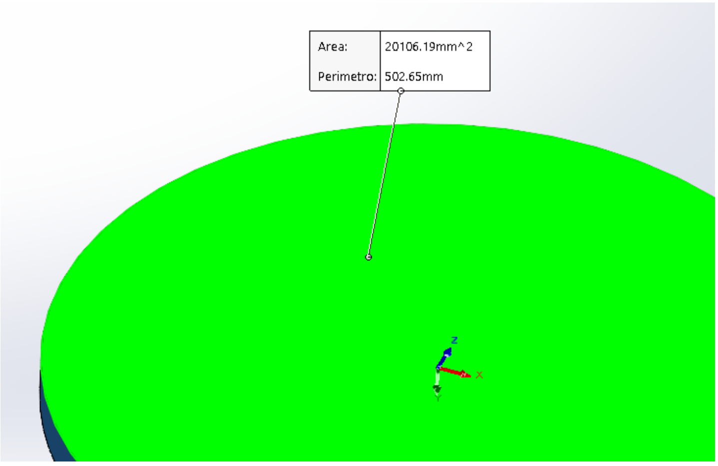

Figure 4.5 – Area projected onto the flash plane

Average height of the blank (h_m):

$h_m = V_{blank} / A_b = 200\,087 / 20\,106 = 9.95\ mm \approx 10\ mm$

Working speed of the press (v):

For hydraulic presses, the typical range is 0.05–0.30 m/s. A value of v = 0.05 m/s = 50 mm/s is adopted to ensure uniform plastic flow without cracking in the hot aluminium.

Average strain rate ($\dot{\varepsilon}$):

$\dot{\varepsilon} = v / h_m = 50 / 9.95 = 5.0\ s^{-1}$

Hot yield stress (σ_f) — Table 5-2:

For hot plastic deformation processes, the yield stress of the material is described by the constitutive law:

$\sigma_f = C \times (\dot{\varepsilon})^m$

where:
- C is the hot yield strength [MPa]
- $\dot{\varepsilon}$ is the average rate of plastic deformation [s^{-1}]
- m is the strain rate sensitivity exponent

Materiale	Temperatura (°C)	C (Mpa)	*m*
Leghe di Al	200-500	300-40	0,05-0,02
Leghe di Cu	200-800	400-20	0,02-0,3
Acciai			
• bassa % C	900-1200	170-50	0,08-0,20
• media % C	900-1200	180-55	0,07-0,25
• inossidabili	600-1200	420-40	0,02-0,4

Tab. 5-2 Valori indicativi dei parametri *C* e *m* per alcuni materiali per valori di ε compresi tra 0,2 e 1.

Table 4.8 – Parameters C and m for hot deformation (Santochi-Giusti, Table 5-2)

The parameters C and m are obtained by linear interpolation from Table 5-2 in Santochi-Giusti (row 'Al alloys', temperature range T = 200–500 °C) at the selected forming temperature T = 450 °C:

$C(450\ °C) = 300 + [(450 - 200) / (500 - 200)] \times (40 - 300) = 83.3\ MPa \approx 83\ MPa$

$m(450\ °C) = 0.05 + [(450 - 200) / (500 - 200)] \times (0.02 - 0.05) = 0.025$

Table 5-2 defines the parameters C and m for a strain rate range of $\dot{\varepsilon} = 0.2$ to $1.0\ s^{-1}$. The value calculated during the final stage of the press closure ($\dot{\varepsilon} = 5.0\ s^{-1}$) exceeds the upper limit given in the table. In order to avoid arbitrary extrapolation of the mathematical model beyond the certified experimental domain, the saturation value at the upper limit of the validity range is adopted as a precaution:
$\dot{\varepsilon} = 1.0\ s^{-1}$

Substituting the values:
$\sigma_f = 83 \times (1.0)^{0.025} = 83\ MPa$

Geometric complexity factor (K):
A dimensionless coefficient which takes into account, with considerable approximation, the shape of the component and the material's resistance to flow. According to the Santochi-Giusti classification, the reference values are:
- K = 3 to 5 for simple shapes without a flash groove;
- K = 5 to 8 for simple shapes with a sprue;
- K = 8 to 12 for complex shapes.

The geometry of our blank features a peripheral sprue and a configuration characterised by six deep, thin radial ribs (steep aspect ratio h/b = 4.53), a central hub and a hollow conical body. These characteristics significantly increase the contact surfaces, friction and the pressure required to fully fill the cavities at the end of the stroke, placing the component in the category of complex shapes (range 8 to 12).

K=8 is adopted as a representative value for the geometry under consideration, as it is a moderately complex shape.

Moulding force:

$P = K \times \sigma\_f \times A\_b = 8 \times 83\ MPa \times 20\ 10^6\ mm^2 = 13\ 350\ 384\ N \approx 13\ 350\ kN$ (equivalent to approximately 1 360 tonnes).

4.7.2 Selection of the hydraulic press

Based on the force required at the end of the stroke (13,350 kN) and the technical characteristics of the EN AW-6082 light aluminium alloy, a 4-column hydraulic press is selected.

Compared with a mechanical eccentric press, the hydraulic press offers:

Maximum rated force available throughout the entire stroke of the ram;
Controlled and adjustable descent speed, ideal for aluminium;
The ability to pause at the end of the stroke (contact time under pressure) to ensure perfect filling and calibration of the 6 radial ribs.
The **MOSSINI industrial press**, **model PO 1500** (manufactured by the Italian company Mossini S.p.A.), has been selected for the process; its technical specifications as per the catalogue are summarised in the table below:

Technical specification	Symbol / Unit	Catalogue value
Machine model	-	**MOSSINI PO 1500**
Type	-	4-column hydraulic press
Nominal closing force	F_nom	15,000 kN (1,500 t)
Slider return force	F_ret	1,200 kN
Maximum slide stroke	C	800 mm
Maximum distance between tables	H_max	1,400 mm

Worktop dimensions (table)	L × D	1,600 × 1,400 mm
Working speed (moulding)	v_working	10 – 50 mm/s
Rapid approach speed	v_rapid	300 mm/s
Maximum hydraulic circuit pressure	p_max	280 bar
Installed power of hydraulic unit	P_motor	90 kW

Table 4.9 – Technical specifications of the MOSSINI press

Figure 4.6 – MOSSINI 4-column hydraulic press, model PO 1500 (15 000 kN)

Load verification:
P_calculated = 13,350 kN < P_nominal = 15,000 kN
The machine's load factor is:
Utilisation rate = (13,350 / 15,000) × 100 = 89.0 %
This verification unequivocally confirms the need to select the 15,000 kN (1,500 t) industrial size. A smaller commercial size (e.g. 12,500 kN / 1,250 t) would be undersized, causing the press to be continuously overloaded (beyond 106 per cent of the nominal force) and risking failure to fully fill the thin ribs at the end of the stroke. The residual margin of 11 per cent ensures the process can be carried out safely and successfully.

4.8 Work cycle and economic analysis

4.8.1 Work cycle and time analysis

The hot forging process for the flange is carried out at a billet temperature of between 420 °C and 480 °C. The operating cycle for a single part consists of the following basic stages:

Billet retrieval and positioning: the billet, preheated in an induction furnace, is retrieved by the operator (or a robotic arm) and positioned in the cavity of the lower die half.
Press cycle: descent of the ram, progressive plastic deformation, a brief pause at the end of the stroke to ensure the 6 ribs are filled, and ascent of the ram.
Ejection and visual inspection: mechanical ejection of the part using ejectors and a preliminary visual check of the component's integrity.
Hot deburring: shearing of the peripheral burr ring on an auxiliary deburring press using a cutting die.
In accordance with the industry reference data for the forging of light alloys, the duration of the individual stages is summarised in the table below:

Operational stage	Estimated time [min]	Estimated time [s]
Positioning of the hot billet in the die	0.10	6
Press cycle (descent, stroke, pause, ascent)	1.50	90
Part removal and visual inspection	0.15	9
Hot trimming of the weld bead	0.50	30
Total cycle time for a single piece (T_piece)	**2.25 min**	**135 s**

Table 4.10 – Moulding cycle times

For the production batch in question, amounting to N = 500 pieces, the total processing time on the press is:

T_batch = N × T_piece = 500 × 2.25 min = 1 125 min (18.75 hours)

Assuming standard 8-hour working shifts, the batch is completed in approximately 2.3 shifts.

4.8.2 Mould sizing

To estimate the cost of the mould, it is first necessary to determine its main geometric dimensions: the length L, width B and height H of the two mould halves.
As the component has an axially symmetric geometry, the cavity on the parting line is circular in shape. The characteristic dimensions of the cavity are:
- Diameter of the cavity on the flash plane: D_inc = b = l = 160 mm
- Maximum depth of the cut in the upper mould half: h = 41.50 mm (bell housing, radial fins and hub: 47.25 mm – 5.75 mm)

In accordance with the methodology set out in the Santochi-Giusti text (Fig. 5-40: ‘Charts for calculating indicative mould dimensions’), the block dimensions are derived using allowance factors:
L = l × f_l
B = b × f_b
H = h × f_h

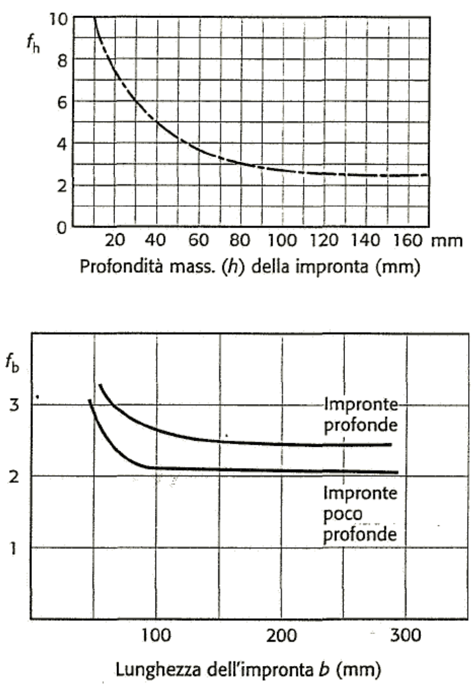

Fig. 5-40 Grafici per il calcolo dei valori indicativi delle dimensioni degli stampi.

Figure 4.7 – Charts for mould dimensions (Santochi-Giusti, Fig. 5-40)

From the charts in Fig. 5-40, the following are derived:
- Plan factors (f_l, f_b): based on the cavity width b = 160 mm, $f_l = f_b = 2.0$ is obtained from the curve for shallow cavities.
- Height factor (f_h): based on the maximum cavity depth h = 41.50 mm, $f_h = 4.8$ is obtained from the upper curve.
The characteristic dimensions are therefore:
- L = 160 mm × 2.0 = 320 mm
- B = 160 mm × 2.0 = 320 mm
- H = 41.50 mm × 4.8 = 199.2 mm ≈ 200 mm (height of a single mould half)

The total height of the paired mould halves is:
$H_{tot} = 2 \times H = 400$ mm
The total volume of the pair of rough blocks is:
$V_{mould} = L \times B \times H_{tot} = 320 \times 320 \times 400 = 40{,}960{,}000\ mm^3 \approx 0.041\ m^3$ ($41.0\ dm^3$)

Assuming a density $\rho = 7{,}850\ kg/m^3$ for hot-working die steel (UNI EN ISO 4957 X37CrMoV5-1 / AISI H13), the total mass of the die is:

$M_{die} = V_{die} \times \rho = 0.041\ m^3 \times 7\,850\ kg/m^3 \approx 321.5$ kg (equivalent to approximately 160 kg for each die half).

4.8.3 Analysis of production costs

The calculation of the unit cost of the hot-forged part takes into account four main cost items: the cost of raw materials, depreciation of the forging press, labour costs including related overheads, and depreciation of the dedicated equipment (die).

A) Material cost (Aluminium EN AW-6082 T6)

The initial cylindrical billet (Ø80 × 48 mm) has a nominal mass of:
$M_{billetta} = 0.651$ kg (651 g)
Assuming a unit supply cost for commercial extruded bars of 4.50 €/kg:
$C_{material} = M_{billetta} \times Price_{kg} = 0.651\ kg \times 4.50$ €/kg $= 2.93$ €/piece
For the entire production batch (N = 500 pieces):
$C_{material\_batch}$ = 2.93 € × 500 = **1 465.00 €**
(Note: the scrap from the hot-cut flash, amounting to 109 g per piece or a total of 54.5 kg for the batch, constitutes clean primary aluminium scrap that is recyclable or resalable; however, for the sake of economic certainty, it is not deducted from the calculation).

B) Machinery cost (MOSSINI PO 1500 hydraulic press)

For the 15,000 kN (1,500 t) hydraulic press and the auxiliary induction furnace, the following industrial depreciation parameters are applied:
- Purchase cost of the plant: €120,000

- Depreciation period: 20 years
- Average utilisation: 250 working days/year, based on one 8-hour shift per day = 120,000 minutes/year
- Annual depreciation charge = €120,000 / 20 years = €6,000 per year
- Depreciation cost per minute = €6,000 / 120,000 minutes = €0.050 per minute

Adding an hourly rate for routine maintenance and auxiliary energy consumption (€0.030 per minute, equivalent to €1.80 per hour), the machine cost per minute amounts to €0.080 per minute (€4.80 per hour).

The machine cost allocated to each individual part (cycle time T_part = 2.25 min) is:

C_machine = T_piece × Cost_per_minute = 2.25 min × 0.080 €/min = 0.18 €/piece

For a batch of 500 pieces:

Machine_cost_batch = 0.18 € × 500 = **90.00 €**

C) Labour and departmental overheads

The estimated hourly cost for skilled labour for a press operator is 25.00 €/h (0.417 €/min). This figure, when added to the costs for routine maintenance, electricity consumption for maintaining the oven temperature and general factory overheads (lighting, heating, ancillary costs), results in a total hourly rate for the workstation of approximately 40.00 €/h.

Taking into account the direct labour cost:

C_labour = T_piece × 0.417 €/min = 2.25 min × 0.417 €/min = 0.94 €/piece

For a batch of 500 pieces:

C_labour_batch = 0.94 € × 500 = **470.00 €**

D) Mould cost

Based on the geometric sizing carried out in section 4.8.2 using the Santochi-Giusti charts (Fig. 5-40), the pair of mould halves has a total mass of raw steel equal to M_mould = 321.5 kg (2 blocks measuring 320 × 320 × 200 mm).

The total cost of manufacturing the die comprises:
- Cost of the forged and heat-treated raw material (6.00 €/kg):
  C_mat_stamp = 321.5 kg × 6.00 €/kg = **1 929.00 €**
- Precision machining (CNC roughing, 5-axis HSC finishing of the cavities, die-sinking EDM for the 6 radial ribs, heat treatment involving hardening and tempering to 48–50 HRC, manual surface polishing): 2 500.00 €

Total cost of the mould:

C_mould = €1,929.00 + €2,500.00 = **€4,429.00**

As the mould is manufactured specifically for this order, the depreciation of the equipment is allocated in full across the entire production batch (N = 500 pieces):

C_depreciation_mould = C_mould / N = 4,429.00 € / 500 = **8.86 €/unit**

4.8.4 Overall economic summary

The total unit cost for producing the hot-stamped blank flange is given by the sum of the individual costs analysed:

C_tot_piece = C_material + C_machine + C_labour + C_mould_maintenance
C_tot_piece = 2.93 € + 0.18 € + 0.94 € + 8.86 € = 12.91 €/piece
The following table summarises the cost structure per piece and for the entire batch of 500 pieces:

Cost item	Unit cost [€/piece]	Incidence [%]	Batch cost (500 pcs) [€]
Raw material (Aluminium EN AW-6082)	2.93	22.7 %	1,465.00
Depreciation of hydraulic press (1,500 t)	0.18	1.4 %	90.00
Skilled labour and department management	0.94	7.3 %	470.00
Depreciation of forging die (AISI H13)	8.86	68.6 %	4,429.00
TOTAL	**€12.91**	**100.0 %**	**€6,454.00**

Table 4.11 – Summary of the production cost structure per unit and for the entire batch

As is typical of plastic forming processes for small to medium-sized batches (N = 500 units), the predominant cost item is the depreciation of the tooling (approximately 69 per cent of the total). As the batch size increases (for example, for mass production runs exceeding 5,000–10,000 pieces), the proportion accounted for by the mould would fall to negligible levels, bringing the unit cost of the semi-finished product down to the cost of materials and labour alone (approximately €4.05 per piece).

5. WELDING

5.1 Component installation and choice of material

The reaction arm is an accessory, fitted with an anti-vibration bushing, used to laterally secure the worm gear motor to the supporting structure, with the function of compensating for misalignments of the output shaft and absorbing the reaction torque generated during operation.

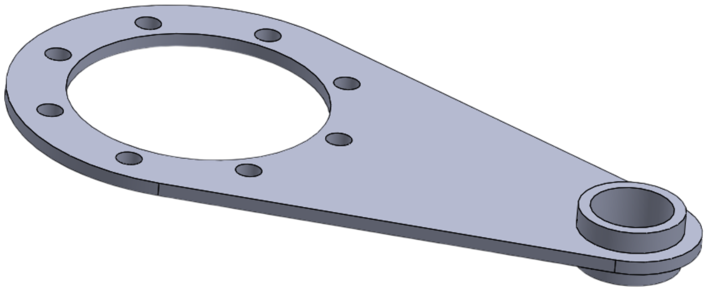

S235JR steel was chosen as the material for manufacturing the reaction arm.

It has good ductility and its moderate hardness makes it easy to machine and manufacture, characteristics consistent with the 4 mm thickness of the plate and the simple plate-cylinder geometry of the component in question.

S235JR steel ensures cost-effectiveness for a production batch of 500 units, as well as adequate fatigue strength.

Commercial reaction arms available on the market for NMRV gearboxes are typically made from this type of structural steel.

BETTINELLI ACCIAI
HOT ROLLED | FORGED | COLD DRAWN | PEELED | STAINLESS STEEL | TUBES

S235JR
Norma di riferimento EN 10025-2 : 2004
Numero 1.0038

ACCIAI NON LEGATI STRUTTURALI

CORRISPONDENZE								
EN	UNI	GB	DIN	AFNOR	BS	GOST	AISI	-
S235JR	FE360BFN	Q2358	RSt 37-2	-	40 B	St3SP		-

COMPOSIZIONE CHIMICA									
C% max	Mn% max	Si%	Cr%	Ni%	Mo%	Cu% max	Nb%	V%	
0,17*	1,40	-	-	-	-	0,40	-	-	colata
0,19*	1,50	-	-	-	-	0,45	-	-	prodotto
Al%	P% max	S% max	N% max	-	-	-	-	-	
-	0,035	0,035	0,012**						colata
-	0,045	0,045	0,014***						prodotto

S235JR n° 1.0122 P% - S% max 0,040 in colata
* = per spessori > 40 mm fino a mm 100 max 0,20 in colata/0,23 su prodotto; per spessori >100 da concordare
** = valore max di N non si applica se la composizione chimica mostra contenuto di Al (tot.) > 0,020%
*** = valore max di N non si applica se la composizione chimica mostra contenuto di Al (tot.) > 0,015%

CARATTERISTICHE MECCANICHE					
stato	**TRAFILATO A FREDDO + C** EN 10277-2:2008				
sezione [mm]		Prova di trazione in longitudinale a + 20°C			
		R	Rp 0,2	A%	HB
oltre	fino a	N/mm^2	N/mm^2 min	min	*per informaz.*
5	10	470-840	355	8	*141-250*
10	16	420-770	300	9	*125-231*
16	40	390-730	260	10	*114-224*
40	63	380-670	235	11	*110-203*
63	100	360-640	215	11	*104-198*

per piatti e profili speciali il carico Rp 0,2 può differire del - 10% e R del +/- 10%
i valori sopra esposti valgono anche per +C + SL

table

5.2 Weld bead geometry

The cylinder to be welded has a diameter of 25 mm and a height of 14 mm, whilst the plate thickness is 4 mm. Given this geometric configuration, the resulting joint is a T-joint, with a continuous fillet weld along the entire circumference of contact between the plate and the cylinder, carried out in a single pass.

The length of the weld bead is determined by the following equation:

$L = \pi \times D = \pi \times 25 \text{ mm} \approx 78.5 \text{ mm}$

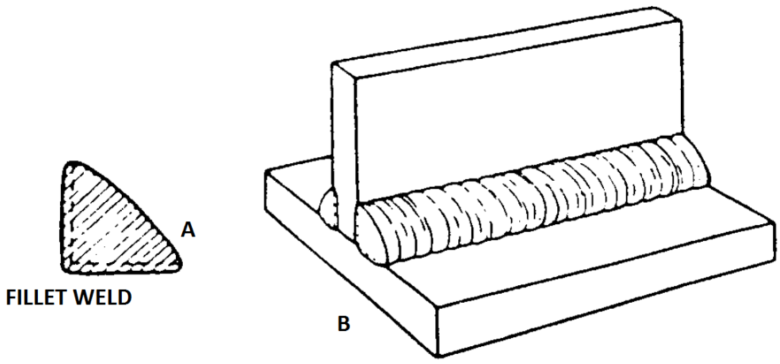

Figure 1: Tee joint - single pass fillet weld.

5.3 Welding process

The MIG/MAG (GMAW) process was selected as the welding method.

As the component is not subject to aesthetic quality requirements for the weld bead, priority can be given to process productivity over the precision typically associated with other welding techniques, such as TIG

MIG/MAG therefore represents the best compromise between deposition rate, cost per part and repeatability in mass production.

As regards the joint geometry, the choice of a T-joint is dictated directly by the assembly configuration, as the cylinder is positioned orthogonally to the plate.

5.4 Welding parameters

The estimated MIG/MAG welding parameters for the T-joint under consideration are given below; these were obtained by interpolation from technical reference tables for fillet welds on carbon steel with thicknesses ranging from 3 to 5 mm. These are indicative values, to be validated on a test specimen.

Parameter	Estimated value
Process	GMAW (MIG/MAG) – EN ISO 4063, procedure 135
Filler wire	ER70S-6, Ø 1.0 mm
Shielding gas	Ar/CO_2 80/20 (M21), 12–15 l/min
Current	≈ 195–210 A
Arc voltage	≈ 23–25 V
Wire feed speed	≈ 7.5–8.5 m/min
Welding speed (travel speed)	≈ 35–40 cm/min
Number of passes	1 (single weld bead)
Polarity	DCEP (positive electrode)

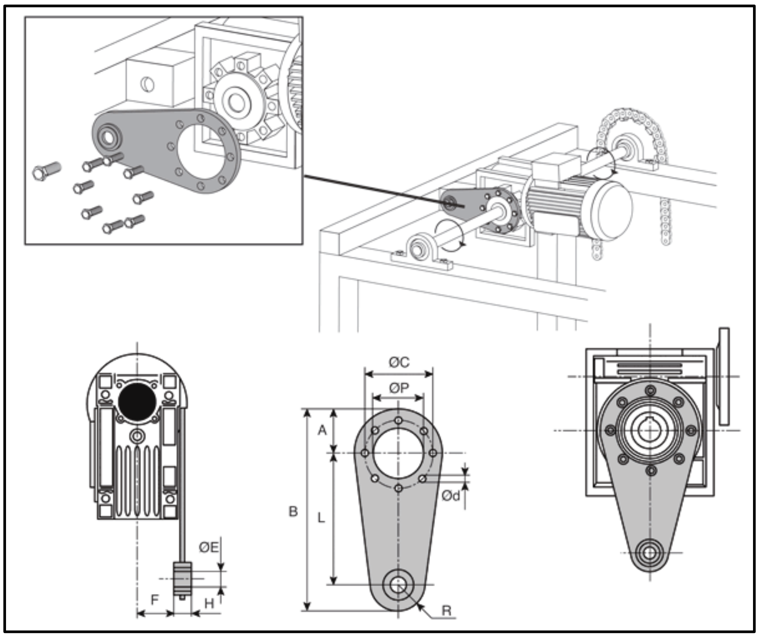

5.4.1 Typical use and positioning of the reaction arm

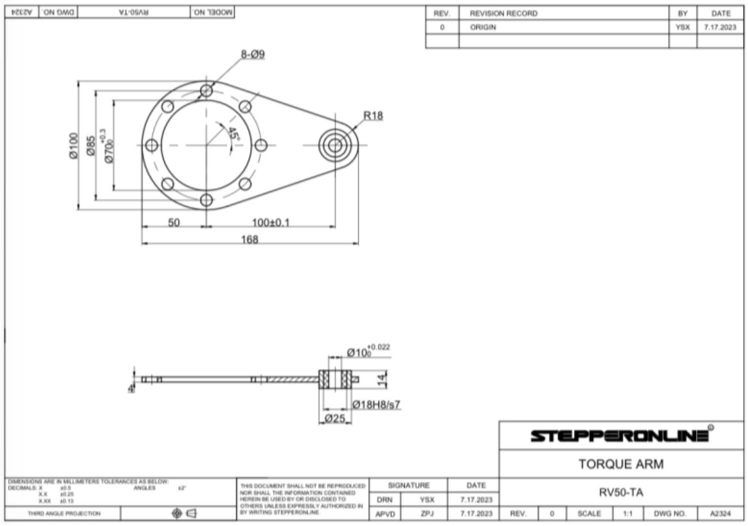

5.4.2 Technical drawing of the reaction arm for the gear motor

6. 3D PRINTING

6.1 The Sealing Cap: Function and Material

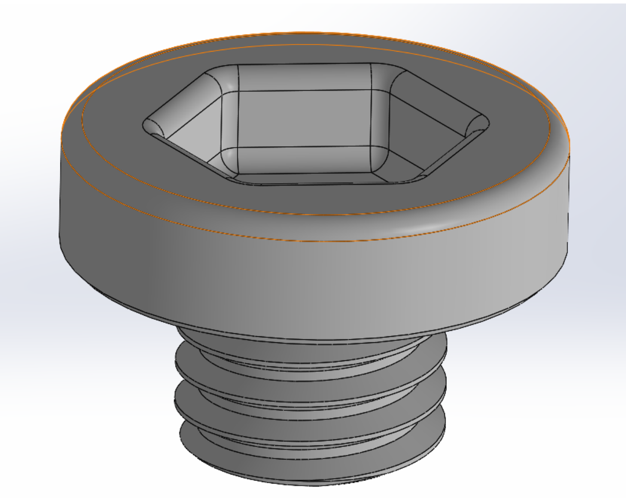

The component selected for additive manufacturing is the upper sealing cap (part no. 18), located at the threaded lubricating oil filler hole on the gearmotor housing. The part has a compact geometry characterised by a flanged head with a diameter of 15.00 mm, a total height of 10.00 mm and a net geometric volume of 792.27 mm³.

From a functional point of view, the component operates under low continuous mechanical stresses but must meet specific operational requirements:

Chemical and thermal resistance: prolonged contact with the lubricating oil in the housing and gearbox operating temperatures of up to 60°C;

Mechanical resistance to handling: integrity of the threaded connection (metric pitch M10 x 1.5 mm) when the tightening torque is applied using a hex key (Allen key), and sufficient mechanical properties to withstand repeated unscrewing operations for oil top-ups;

Leak-tightness: minimisation of the porosity typical of filament deposition, aided by a flat shoulder to accommodate a rubber seal in contact with the housing.

To meet these requirements, the choice of material fell on Nanovia PETG Natural filament (Polyethylene Terephthalate Glycol, diameter 1.75 mm), ruling out the alternatives commonly used in FDM technology for the following technical reasons:

PLA: ruled out from the outset due to its poor mechanical properties and low thermal threshold (softening temperature around 55–60 °C, incompatible with the thermal conditions of the casing).

ABS / Nylon (PA): Nylon, in particular, would have offered high performance but at almost double the filament cost, with high hygroscopicity and greater printing difficulties; ABS has lower chemical resistance to oils than PETG and a strong tendency to shrinkage/warping, which is critical for the precision of a metric thread.

PETG, on the other hand, offers excellent chemical inertness towards hydrocarbons and mineral oils, a glass transition temperature of approximately 80 °C (well above the casing's operating temperatures) and superior inter-layer adhesion compared to ABS, ensuring high yield strength and resistance to the shear stresses generated during thread tightening.

Property / Parameter	Value
Density	1.27 g/cm³
Glass transition temperature (T_g)	80 °C
Tensile strength	approximately 44 MPa
Modulus of elasticity	2260 MPa
Elongation at break	3.2 %
Recommended extruder temperature	220–240 °C

Print bed temperature	80–90 °C
Supply cost	€34.05/kg

Table 1 – Technical data and properties of Nanovia PETG filament

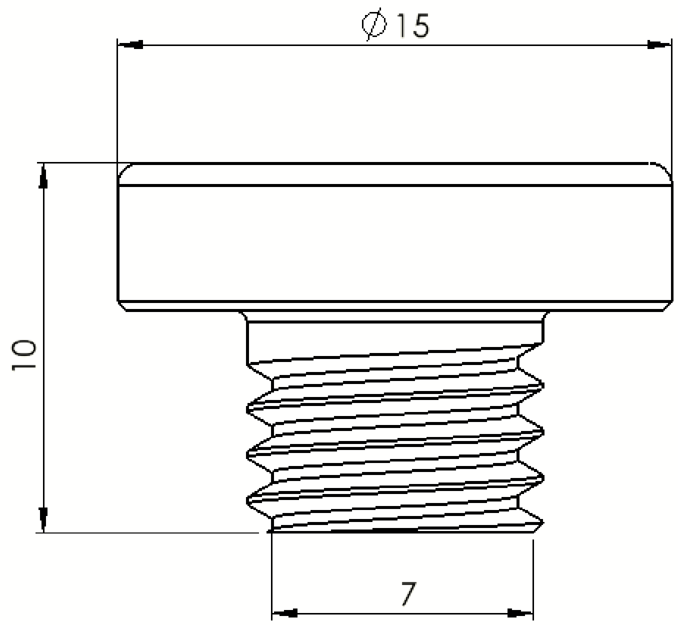

Figure 1 – Drawing with overall dimensions

6.2 Choice of 3D printer

The Bambu Lab P1S printer was selected for the production of the batch of caps; this is an FDM printer with a closed build chamber and a single extruder.

This choice was based on specific technological and economic considerations:

Enclosed print chamber:

to ensure the mechanical integrity and airtightness of the PETG, it is essential to prevent temperature fluctuations and draughts during deposition. The enclosed chamber maintains a warm and stable microclimate (approximately 35–40 °C without active heating), improving inter-layer adhesion and reducing residual stresses along the thread;

All-metal direct-drive extruder unit:

allows the nozzle to be heated up to 300 °C and the bed up to 100 °C, comfortably covering the temperatures required by Nanovia PETG (240 °C at the nozzle and 80–90 °C on the bed);

Build plate dimensions and build volume:

the total volume of 256 x 256 x 256 mm (usable volume of 230 x 230 mm) comfortably accommodates a 10 x 10 matrix, equivalent to 100 parts simultaneously per print cycle, minimising operator intervention and the total number of print processes.

Optimisation of depreciation costs:

with a list price of €379.00, the machine costs approximately one-third as much to purchase as industrial printers of the same volume, drastically reducing the impact of depreciation on the unit cost of the component;

Feature / Specification	Specification value
Model	Bambu Lab P1S
Purchase cost	€379.00
Process technology	FDM (CoreXY architecture)
Build volume	256 × 256 × 256 mm
Supplied nozzle diameter	0.4 mm (hardened steel / brass)
Maximum nozzle temperature	300 °C
Maximum heated bed temperature	100 °C

Table 2 – Technical and cost data for the selected printer

Power consumption: peak of 350 W during heating, approximately 130 W during continuous printing

Useful life for industrial depreciation: 5 years (equivalent to 10,000 conventional working hours calculated at 2,000 hours per year)

Figure 2 – Bambu Lab P1S 3D printer

6.3 Part orientation, process parameters and slicing

6.3.1 Orientation and support management

The quality and functionality of an FDM-printed component depend critically on its orientation on the build plate, due to the anisotropy of the process (the mechanical properties along the Z-axis are inferior to those in the X-Y plane because of the resistance at the interface between layers).

For the sealing cap, a vertical orientation was chosen, with the flanged head in direct contact with the build plate and the threaded shank extending upwards along the Z-axis. This arrangement represents the optimal configuration for specific engineering reasons:

Maximum stability and adhesion: the flanged head provides the maximum contact surface with the build plate (diameter 15 mm, area approximately 176 mm²), ensuring a solid anchorage of the part and eliminating the risk of accidental detachment during the printing of multiple moulds;

Self-supporting geometry (no supports): the transition from the flange (15 mm) to the threaded shank (10 mm) results in a gradual reduction in cross-section towards the top. The overhang angle is zero, allowing the component to be printed without any support structures and ensuring a perfectly flat finish at the edge;

Compromise regarding axial tension in the Z direction: the Z direction of growth coincides with the direction of tensile stress during thread clamping. This critical issue was overcome by combining the high heat seal strength of PETG (extruded at 235 °C with controlled ventilation at 30 per cent), a substantial wall thickness (4 solid perimeters) and the fact that the oil seal requires a low tightening torque, well below the component's delamination load.

6.3.2 Compensation for volumetric shrinkage

PETG exhibits isotropic linear thermal shrinkage estimated to be in the order of 0.3 per cent. To ensure the correct thread tolerance class and avoid forcing or seizing during screwing into the tapped hole in the casing, the model was compensated for in the slicer by setting a horizontal wall expansion parameter of –0.06 mm.

6.3.3 Definition of slicing parameters

The machine code (G-code) was generated using slicing software (Kiri:Moto, Bambu Lab P1S profile).

A key technical consideration concerned the extrusion factor (Shell Factor set to 1.2): by extruding 20 per cent more material, the hot nozzle presses and compresses the molten filaments laterally against the adjacent ones. This slight over-extrusion seals all the microscopic air gaps between the adjacent perimeters through plastic deformation, eliminating porosity and making the fillet wall airtight and impervious to hot oil leaks.

The final process parameters are summarised in the following table:

Process parameter	Set value	Technical rationale
Nozzle diameter	0.4 mm	Optimal resolution of the metric filament and flow stability
Layer height	0.20 mm	Balance between filament definition and cycle times

Number of walls	4 lines	High resistance to shear stress on the thread flanks
Upper/lower layers	4 solid layers	Hermetic seal at the head to prevent oil leakage
Fill density (Infill)	35%	Structural rigidity with low material consumption
Filling pattern	Hexagonal	Closed-cell structure with excellent torsional strength
Flow factor (Shell Factor)	1.2 (+20% flow rate)	Filling of micro-voids for a watertight seal
Nozzle temperature	235 °C	Maximum fusion between layers to withstand clamping
Bed temperature	80 °C	Optimal adhesion to the bed with no lifting
Part ventilation (Fan Speed)	30%	Controlled cooling to maintain adhesion in the Z-axis
Support structures	None	Self-supporting pyramid geometry

Table 3 – Process parameters (FDM printing)

Data obtained from the final CAM simulation (single component):

- **Estimated deposition time:** 12 mins and 38 s (00:12:38 = **0.2106 h**)
- **Length of extruded filament: 362 mm**
- **Mass of filament used: 1.09 g**

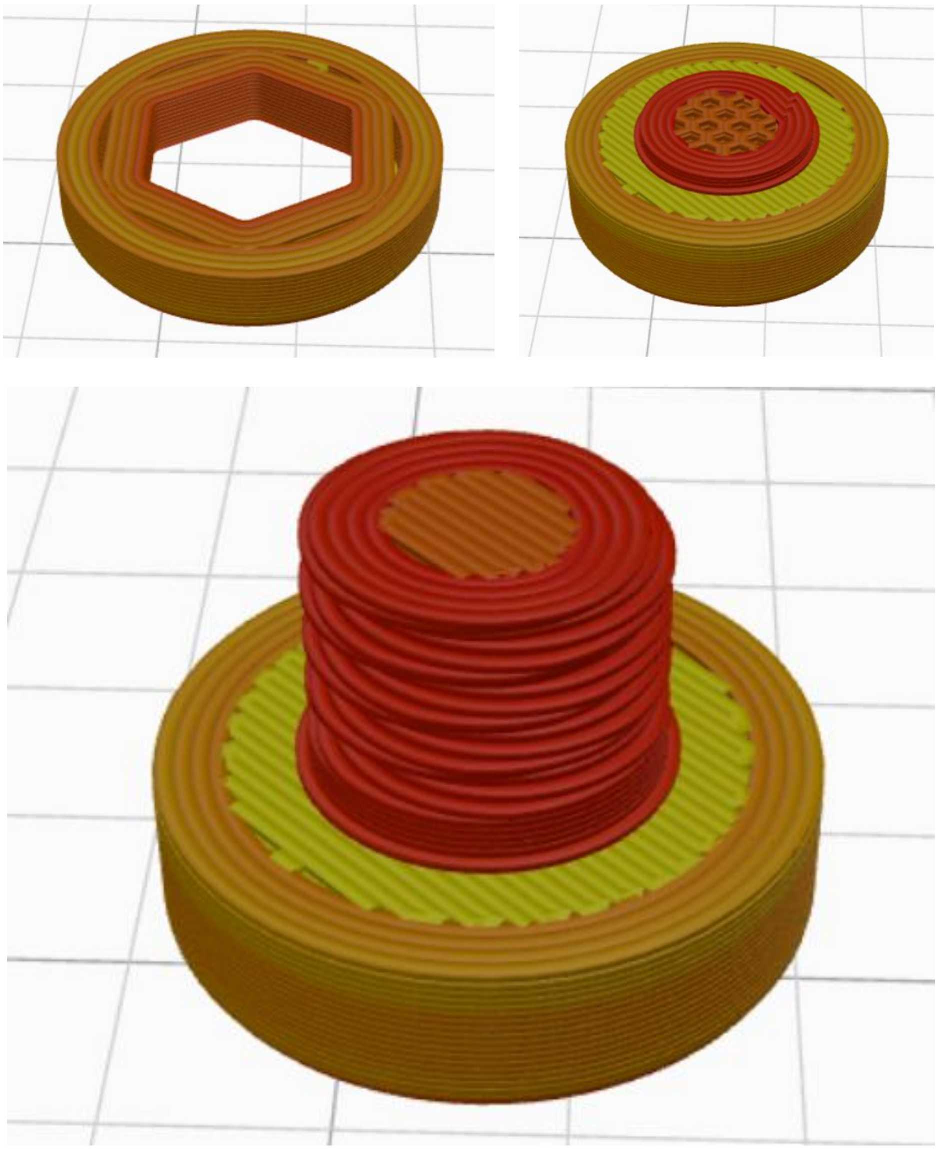

Figure 3 – Simulation of slicing and toolpaths in Kiri:Moto

6.4 Production planning and machine utilisation

6.4.1 Plate layout (nesting)

To optimise productivity and eliminate downtime, the components are arranged in a matrix on the printer's build plate.

Given that the flange diameter is 15.00 mm, a centre-to-centre distance between the parts of 23.00 mm was set, ensuring a clearance of 8.00 mm between adjacent edges. This spacing prevents thermal interference, ensures even cooling of the PETG and allows for easy manual removal.

On the build area of the Bambu Lab P1S (230 x 230 mm, with a 13 mm safety margin around the perimeter), the overall dimensions of the mould are: Overall dimensions = (10 – 1) x 23.00 mm + 15.00 mm = 222.00 mm ≤ 230.00 mm

The tray capacity is:

Capacity per tray: 10 x 10 matrix = 100 pieces per cycle

6.4.2 Printing strategy and timing

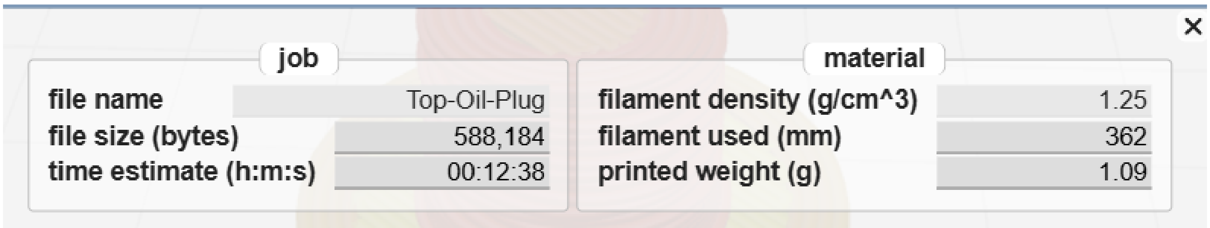

job		material	
file name	Top-Oil-Plug	filament density (g/cm^3)	1.25
file size (bytes)	588,184	filament used (mm)	362
time estimate (h:m:s)	00:12:38	printed weight (g)	1.09

Figure 4 – parameters extracted from the print simulation on Kiri:Moto

Based on the CAM simulation data (unit time of 12 mins and 38 s), the simultaneous printing of a full tray of 100 pieces, including rapid empty-run movements between profiles, takes an estimated total time of approximately 22 hours (equivalent to an average of 13.2 minutes per piece), with a total filament consumption of 109 g per batch.

A 22-hour cycle fits perfectly into a 24-hour continuous daily operation: the machine is started at the beginning of the work shift, operates completely autonomously throughout the day and night without any supervision, and makes the finished and cooled batch of 100 parts available the following morning for rapid unloading.

The full-capacity productivity of a single printer is 100 pieces per day.

6.4.3 Sizing of the machine fleet and duration of the contract

To ensure the supply of 500 compliant components, a precautionary scrap margin of 4 per cent is factored in:

Total number of parts to be produced: 500 + 20 = 520 parts

The total quantity is made up as follows:

5 full plates of 100 pieces each + 1 extra plate of 20 pieces (total of 6 print cycles).

With a single Bambu Lab P1S continuous-cycle printer (100 parts per day), the entire production run of 520 parts requires a total machine time of approximately 115 hours, equivalent to:

Actual duration of the order: 5.5 working days

This result confirms that a single, cost-effective machine tool is more than sufficient to fulfil the order without causing any delays in the assembly of the gearbox.

6.5 Profit and loss account and analysis of manufacturing costs

The manufacturing cost of the sealing cap was determined by analysing the four main cost items: direct material and component costs, direct labour costs, depreciation of the machine tool and energy consumption.

6.5.1 Direct material and component costs

Based on data obtained from the CAM simulation on Kiri:Moto, the manufacture of a single component requires a net quantity of filament equal to 1.09 g (362 mm). Applying a conservative scrap allowance of +8% to compensate for initial nozzle purging and priming lines on the build plate:

Gross mass of PETG per part: 1.09 g × 1.08 = 1.18 g

Taking into account the supply cost of Nanovia PETG filament at 34.05 €/kg (0.03405 €/g):

Material cost per piece: 1.18 g × 0.03405 €/g = **0.040 €/piece**

6.5.2 Direct labour cost

In line with the other machining operations in the project, the hourly rate for skilled labour is assumed to be 25.00 €/h (0.417 €/minute). Staff time is divided between the preparatory phase for the build plate and the handling of the parts at the end of the cycle:

Fixed initial set-up time: preparation of the G-code file, cleaning of the PEI magnetic plate with isopropyl alcohol, automatic calibration of the Z-axis and checking the adhesion of the first layer: 15 minutes per plate (equivalent to 15 min / 100 pcs = 0.15 min/piece);

Variable time per part: removal from the flexible spring steel build plate, visual inspection of the thread and removal of any burrs: 1.00 minute per part.

Total operator time per piece: 0.15 + 1.00 = 1.15 minutes (0.0192 hours)

Labour cost per piece: €25.00/h × 0.0192 h = **€0.479 per piece**

6.5.3 Depreciation charge for the printer

The hourly cost of the Bambu Lab P1S (purchase price €379.00) is determined in accordance with standard industrial practice over a depreciation period of 5 years at 2,000 working hours per year (10,000 hours in total):

Hourly depreciation cost: €379.00 / 10,000 h = €0.0379/h

As a print run of 100 parts requires 22 hours of continuous machine operation, the hourly machine cost attributable to each component is:

Machine time per piece: 22 h / 100 = 0.22 hours/piece (13.2 minutes)

Machine depreciation cost per piece: €0.0379/h × 0.22 h = **€0.008/piece**

6.5.4 Electricity costs

With an average power consumption at continuous operation of 130 W (0.130 kW) and an assumed industrial electricity tariff of 0.250 €/kWh:

Energy consumed per unit: 0.130 kW × 0.22 h = 0.0286 kWh/unit

Energy cost per unit: 0.0286 kWh × 0.250 €/kWh = **0.007 €/unit**

6.5.5 Summary of costs and overall balance sheet for the contract

Adding up the individual components, the unit manufacturing cost for producing the closure cap is:

Unit cost = $C_{material} + C_{labour} + C_{depreciation} + C_{energy}$

Unit cost = 0.040 € + 0.479 € + 0.008 € + 0.007 € = 0.534 € per unit.

Cost item	Unit cost (€/piece)	Percentage share (%)
Direct materials (Nanovia PETG)	€0.040	7.5 %
Direct labour (Set-up + Inspection/Finishing)	€0.479	89.7%
Depreciation of 3D printer	€0.008	1.5 %
Electricity	€0.007	1.3%
TOTAL UNIT COST	**€0.53**	**100.0 %**

Table 4 – Breakdown of unit cost

Total budget for the supply batch (500 compliant items): Taking into account the planned production of 520 unfinished items to account for the 4% natural wastage:

Total cost of the order: 520 units × 0.534 €/unit = 277.68 €

Cost per finished gearmotor: €277.68 / 500 = €0.56 per gearmotor

7. ASSEMBLY CYCLE

As assembly cycles and production data are strictly confidential to the company, the analysis of timings, deadlines and the allocation of operators for the order of 500 gearmotors is based on assumptions.

7.1 Determination of the Assembly Cycle

The assembly cycle is a list of operations to be carried out, each accompanied by the relevant technical information.

It sets out a sequence of operations that identifies the optimal sequence achievable given the available equipment and the chosen assembly method. In this case, it is assumed that the operators have all the necessary equipment at their disposal and that there is a single operator dedicated to processing the entire batch.

Op.	Operation Description	Technical Details	Priority	Duration
10	Pre-assembly of the high-speed shaft	Press-fitting of bearings (14, 16) onto screw (5)	None	0.30 min
20	Pre-assembly of the slow-speed shaft	Press-fitting of bearings (13, 15) onto the ring gear (4)	None	0.30 min
30	Insertion of the fast shaft	Horizontal insertion of screw assembly into housing (1)	Op. 10	0.20 min
40	Sealing of the high-speed shaft	Fitting of plug (8) and inlet oil seal (7)	Step 30	0.30 min
50	Insertion of slow shaft	Lower the slow shaft vertically into the housing and check that it meshes correctly	Op. 20, 30	0.20 min
60	Preparation of closures	Insertion of O-rings (9, 10) and alignment of flanges (2, 3)	Step 50	0.40 min
70	Tightening the flanges	Tightening of M5 screws (11, 12) to a controlled torque	Op. 60	0.50 min
80	Slow-speed shaft seals	Fitting of outlet oil seals (6) onto through shaft	Step 70	0.20 min
			Total cycle time:	**2.40 min**

7.1.1 Assembly cycle

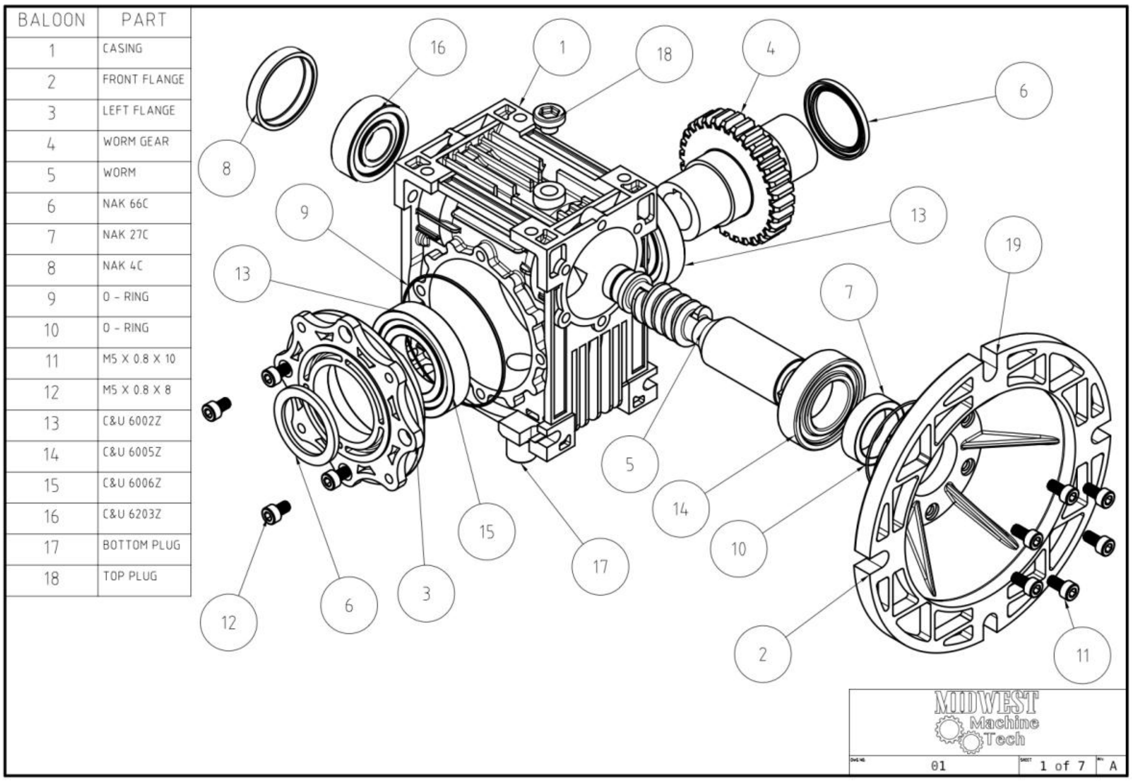

7.1.2 Exploded view of the assembly

7.2 Assembly Graph

The assembly network diagram provides an intuitive and schematic representation of the sequence of operations and the topological constraints of the assembly.

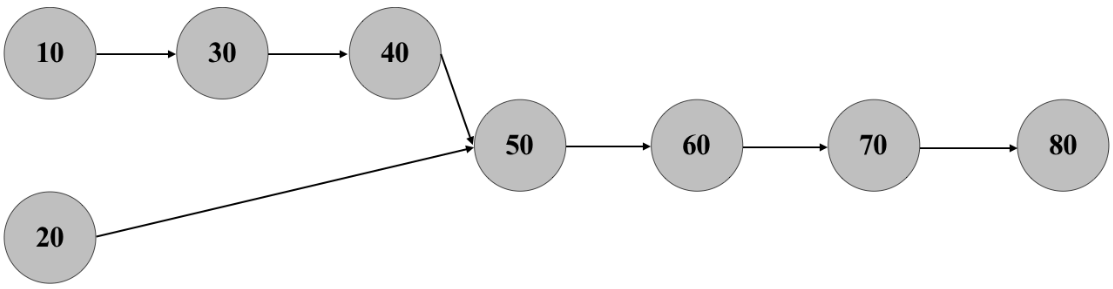

Figure 7.2 - Graph

7.3 Technical Assembly Precautions

As stipulated in the official installation, operation and maintenance manual for the gearmotor, assembly and subsequent commissioning require strict adherence to specific guidelines to ensure the integrity and efficiency of the system.

During the assembly phase, it is essential to clean the surfaces and shafts to remove all traces of dirt, and then to lubricate them to prevent oxidation and dangerous seizure.

The gearbox, electric motor and transmission components must be coupled without applying excessive force. To this end, the use of unsuitable tools such as hammers is strictly prohibited; instead, the operations must make use of the appropriate threaded holes to prevent irreversible damage to the bearings and the housing seats. The operator must also ensure in advance that the tolerances of the motor shaft and flange correspond to at least a ‘normal’ quality class.

8 BIBLIOGRAPHY AND SOURCES

University textbooks and reference manuals

- Marco Santochi, Francesco Giusti, MECHANICAL TECHNOLOGY and Manufacturing Studies, 2000
- Sandro Barone, Alessandro Paoli, Armando V. Razionale, Maurizio Berretta, Industrial Technical Drawing, 2020

Industrial technical catalogues and product data sheets

- Sandvik Coromant: Technical Guide to Machining: Turning, Drilling and Milling, and general tool catalogues (CoroTurn 107 toolholders, CoroDrill 860 drills, CoroReamer 835 reamers).
- REV Broaching Tools: Technical manual for slotting and internal broaching on machine tools, REV IN-P9 series standardised inserts.
- Tyrolit Schleifmittel: General handbook on abrasive wheels and cylindrical grinding parameters for hardened steels, Corundum 89A specification.
- Mossini S.p.A.: Technical catalogue and dimensional data sheets for PO series 4-column industrial hydraulic presses (PO 1500).
- Nanovia S.A.S.: Technical Data Sheet – Nanovia PETG Natural 3D Printing Filament (Thermal, mechanical and chemical specifications).
- Bambu Lab: P1S 3D Printer User Manual & Technical Specifications, Shenzhen Tuozhu Technology Co., Ltd.

Technical documentation for gearboxes and publications

- Motovario S.p.A.: General Technical Catalogue – NMRV and NMRV-P series worm gearmotors, Formigine (MO).
- Gearmotor and Motovario brochure – NMRV
- Operating and maintenance manual – NMRV
- Assembly manual – NMRV
- Analysis of an automated approach to identifying assembly sequences – Alessio Giannotti

9 SOFTWARE USED

- SolidWorks Student Edition 2024
- Altair Inspire Cast 2026
- Kiri:Moto
- Google Workspace